

Medical University of South Carolina

MEDICA

MUSC Theses and Dissertations

Spring 4-5-2023

Role of Macrophages in Regression of Myocardial Fibrosis Following Alleviation of Left Ventricular Pressure Overload

Lily Neff

Medical University of South Carolina

Follow this and additional works at: <https://medica-musc.researchcommons.org/theses>



Part of the [Cardiovascular Diseases Commons](#)

Recommended Citation

Neff, Lily, "Role of Macrophages in Regression of Myocardial Fibrosis Following Alleviation of Left Ventricular Pressure Overload" (2023). *MUSC Theses and Dissertations*. 787.

<https://medica-musc.researchcommons.org/theses/787>

This Dissertation is brought to you for free and open access by MEDICA. It has been accepted for inclusion in MUSC Theses and Dissertations by an authorized administrator of MEDICA. For more information, please contact medica@musc.edu.

Role of Macrophages in Regression of Myocardial Fibrosis Following Alleviation of Left
Ventricular Pressure Overload

Lily Soon Neff

A dissertation submitted to the faculty of the Medical University of South Carolina in
partial fulfillment of the requirements for the degree of Doctor of Philosophy in the
College of Graduate Studies.

Department of Molecular Cellular and Pathobiology

April 5, 2023

Approved by:
Chairman, Advisory Committee

Amy D. Bradshaw

Jeffrey Jones

Carol Feghali-Bostwick

David Long

Donald Menick

LILY SOON NEFF. Macrophages Promote Regression of Myocardial Fibrosis Following Alleviation of Pressure Overload. (Under the direction of AMY BRADSHAW).

Dedication

This study is wholeheartedly dedicated to my beloved parents and fiancé who continually provide their support and encouragement through this journey.

LILY SOON NEFF. Macrophages Promote Regression of Myocardial Fibrosis Following Alleviation of Pressure Overload. (Under the direction of AMY BRADSHAW).

Acknowledgements

I would like to acknowledge the guidance and help from my mentor, Amy Bradshaw, and my dissertation committee; Jeffrey Jones, Donald Menick, Carol Feghali-Bostwick, and David Long. I would like to acknowledge the support from Kristine DeLeon-Pennell and Carsten Krieg in learning new techniques to help understand the macrophage-dependent mechanisms regulating collagen turnover. Furthermore, I would like to acknowledge grant support from T32GM132055 and the FA9550-21-F-0003 through the National Defense Science and Engineering Graduate (NDSEG) Fellowship Program, sponsored by the Air Force Research Laboratory (AFRL), the Office of Naval Research (ONR) and the Army Research Office (ARO).

LILY SOON NEFF. Macrophages Promote Regression of Myocardial Fibrosis Following Alleviation of Pressure Overload. (Under the direction of AMY BRADSHAW).

Dedication	ii
Acknowledgements	iii
Table of Contents	v
List of Tables	viii
List of Figures	ix
Key to Abbreviations	xi
Abstract	xii

LILY SOON NEFF. Macrophages Promote Regression of Myocardial Fibrosis Following Alleviation of Pressure Overload. (Under the direction of AMY BRADSHAW).

Table of Contents:

Chapter 1: Background	2
1.1 Extracellular Matrix (ECM) of the Heart	3
1.2 Collagen Turnover in Homeostasis and Disease	4
1.3 Heart Failure	9
1.4 Left Ventricular Pressure Overload	10
1.5 Preclinical Models of Unloading the Myocardium	12
1.6 Myocardial Macrophages in Homeostasis	13
1.7 Myocardial Macrophages in LVPO	13
Chapter 2: Characterization of TAC/unTAC Preclinical Murine Model	17
2.1 Effects of TAC and unTAC on Myocardial Hypertrophy	18
2.2 Effects of TAC and unTAC on Fibrillar Collagen Content	21
2.3 Effects of TAC and unTAC on Collagen Crosslinking Protein Production	23
2.4 Effects of TAC and unTAC on Initiation of Collagen Degradation	25
2.5 Effects of TAC and unTAC on Myocardial Stiffness	30
2.6 Clinical Relevance	30
2.7 Limitations	32
Chapter 3: Macrophage Dependent Mechanisms of Collagen Turnover in the TAC/unTAC Preclinical Murine Model	33
3.1 Introduction	34
3.2 Effects of TAC and unTAC on Myocardial Macrophage Number and Morphology	35
3.3 Effects of TAC and unTAC on the Myocardial Cytokine Profile	37

LILY SOON NEFF. Macrophages Promote Regression of Myocardial Fibrosis Following Alleviation of Pressure Overload. (Under the direction of AMY BRADSHAW).	
3.4 Macrophage Association with Collagen Turnover	39
3.5 Effects of TAC and unTAC on Myocardial Macrophage Phenotype	41
3.6 Defining an Accurate Macrophage Phenotype for the Antifibrotic Subset Observed in 2wk unTAC	44
3.7 Effects of Macrophage Depletion in the unTAC Myocardium	49
3.8 Discussion	56
3.9 Limitations	59
3.10 Clinical Relevance	60
3.11 Conclusion	60
Chapter 4: Future Directions and Conclusions	63
4.1 Introduction	64
4.2 The Complexity of Total Macrophage Markers	64
4.3 Parsing the Causal Role of Recruited Macrophages versus Resident Macrophages	66
4.4 Immune Cell Profiling of the unTAC Myocardium	73
4.4.1 Introduction	73
4.4.2 Neutrophils	74
4.4.3 T-cells	77
4.4.4 Conclusions	77
4.5 Fibroblasts in the TAC/unTAC Myocardium	78
4.6 Targeting the Persistent Fibrosis Observed in the unTAC Myocardium	83
4.6.1 Earlier Alleviation of LVPO	83
4.6.2 Combination Therapy of LOX Inhibition and Unloading the Myocardium for Regression of Myocardial Fibrosis	86

LILY SOON NEFF. Macrophages Promote Regression of Myocardial Fibrosis Following Alleviation of Pressure Overload. (Under the direction of AMY BRADSHAW).	
4.6.3 Combination Therapy of Unloading the Myocardium and Inhibition of TIMP1	88
4.6.4 Combination Therapy of Unloading the Myocardium and Pirfenidone	90
4.7 CHP Reactivity in referent control, LVH, and HFpEF patients	93
4.8 Conclusions	95
Chapter 5: Materials and Methods	99
5.1 Murine Model of LVPO and Alleviation of LVPO	100
5.2 Liposome Mediated Depletion of Macrophages	101
5.3 Echocardiography	102
5.4 Histological Quantification of Cardiomyocyte Cross-Sectional Area (CSA)	102
5.5 Histological Quantification of Collagen Volume Fraction (CVF)	103
5.6 Histological Quantification of Collagen Hybridizing Peptide Reactivity (CHP)	104
5.7 Immunohistochemical Analysis of Macrophages	105
5.8 Immunoblotting to Measure Protein Levels in TAC and unTAC Myocardium	105
5.9 Immunoassay to Measure Cytokine Profiles in TAC and unTAC Myocardium	106
5.10 Fluorescence Activated Cell Sorting (FACS) to Assess Macrophage Phenotype in TAC and unTAC Myocardium	107
5.11 Quantitative real-time polymerase chain reaction (rt-PCR) of Macrophage and Fibroblast Populations in the TAC and unTAC Myocardium	110
5.12 Myocardial Stiffness	112
5.13 Statistical Analysis	112
References	114

LILY SOON NEFF. Macrophages Promote Regression of Myocardial Fibrosis Following Alleviation of Pressure Overload. (Under the direction of AMY BRADSHAW).

List of Tables:

Table 1: Structural and Hemodynamic Characteristics of the TAC/unTAC Myocardium 20

Table 2: Echocardiographic measurements of C57Bl/6 mice treated with PBS Liposome or Clodronate Liposome and harvested at 4wk TAC+2wk unTAC 50

List of Figures:

Figure 1: Types of Myocardial Fibrosis	8
Figure 2: Aortic stenosis/Surgical Aortic Valve Replacement LV Mass and CVF	11
Figure 3: Schematic of Central Hypothesis	16
Figure 4: Characterization of Cardiomyocyte Cross-Sectional Area in TAC and unTAC Myocardium	19
Figure 5: Characterization of Collagen Volume Fraction in TAC and unTAC Myocardium	22
Figure 6: Characterization of Collagen Crosslinking Enzymes in TAC and unTAC Myocardium	24
Figure 7: Characterization of Collagen Hybridizing Reactivity in TAC and unTAC Myocardium	26
Figure 8: Characterization of Enzymes Implicated in Collagen Turnover in TAC and unTAC Myocardium	28
Figure 9: Characterization of Enzymes Implicated in Collagen Degradation in TAC and unTAC Myocardium	29
Figure 10: Comparison of TAC/unTAC Murine Model to AS/SAVR Paradigm	31
Figure 11: Characterization of IBA1+ Macrophage Number and Area in TAC and unTAC Myocardium	36
Figure 12: Differential Myocardial Cytokine Profile in TAC versus unTAC Myocardium	38
Figure 13: Macrophages Associate with Areas of Collagen Hybridizing Peptide in 2wk unTAC Myocardium	40
Figure 14: Macrophage Phenotype in TAC versus unTAC Myocardium	43
Figure 15: Differential mRNA profiles in F4/80+ Macrophages Isolated from TAC and unTAC Myocardium	46
Figure 16: Differential mRNA Profiles in F4/80+ Macrophages Isolated from TAC and unTAC Myocardium	48
Figure 17: Decreased Macrophage Area and CHP Reactivity in unTAC	51

LILY SOON NEFF. Macrophages Promote Regression of Myocardial Fibrosis Following Alleviation of Pressure Overload. (Under the direction of AMY BRADSHAW).

Myocardium treated with Clodronate Liposomes

Figure 18: Reduction in Select ECM Degradatory Enzymes in Response to Clodronate Liposome Injection	53
Figure 19: Differential VCAM and Cytokine Expression in Liposome Depleted Myocardium	55
Figure 20: Depletion of CD11b+ Cells by Diphtheria Toxin in unTAC Myocardium	69
Figure 21: Quantification of Fibrosis in CD11b-DTR TAC mice	72
Figure 22: Differential Expression of Cytokines in TAC/unTAC	76
Figure 23: Differential mRNA Profiles in PDGFRa+ Fibroblasts Isolated from TAC and unTAC Myocardium	82
Figure 24: Characterization of Unloading the Myocardium at 2wk TAC	85
Figure 25: Decreased CHP Reactivity in Biopsies Isolated from HFpEF Patients	94
Figure 26: TAC/unTAC Schematic Summary	98
Supplemental Figure 1: Gating Strategy Used for Macrophage Phenotyping	109

LILY SOON NEFF. Macrophages Promote Regression of Myocardial Fibrosis Following Alleviation of Pressure Overload. (Under the direction of AMY BRADSHAW).

Abbreviations:

AS: Aortic Stenosis

SAVR: Surgical Aortic Valve Replacement

LVPO: Left Ventricular Pressure Overload

TAC: Transverse Aortic Constriction

unTAC: Removal of Transverse Aortic Constriction

ECM: Extracellular Matrix

WGA: Wheat Germ Agglutinin

CSA: Cardiomyocyte Cross-sectional Area

CVF: Collagen Volume Fraction

B-CHP: Biotinylated Collagen Hybridizing Peptide

IBA1: Ionized calcium binding adaptor molecule 1

MMP2: Matrix Metalloproteinase 2

MMP14: Matrix Metalloproteinase 14

TIMP1: Tissue Inhibitor of Metalloproteinases 1

CD206: Cluster of Differentiation 206

CD163: Cluster of Differentiation 163

CD86: Cluster of Differentiation 86

CD11b: Cluster of Differentiation 11b

Ly6C: Lymphocyte Antigen 6 Complex, Locus C1

ICAM1: Intercellular Adhesion Molecule 1

VCAM1: Vascular Cell Adhesion Molecule 1

CCR2: C-C Chemokine Receptor Type 2

F4/80: EMR1, EGF module-containing mucin-like receptor

MHCII: Major Histocompatibility Complex Class II

CytoF: Cytometry by Time of Flight

IFN γ : Interferon gamma

CCL2: C-C motif ligand 2

CCL7: C-C motif ligand 7

Abstract

Antecedent conditions that affect the heart, such as aortic stenosis (AS), can develop into left ventricular pressure overload (LVPO). LVPO is associated with increased myocardial interstitial fibrosis, specifically fibrillar collagen, that leads to increased myocardial stiffness. Patients undergoing surgical aortic valve replacement (SAVR) to correct AS demonstrate significant but incomplete regression of fibrosis. Although current therapies normalize hemodynamic load, treatments that regress collagen content within the myocardium remain a critical need. To elucidate cellular mechanisms of this persistent fibrosis in LVPO, we utilized a transverse aortic constriction (TAC) and removal of the constriction (unTAC) murine model. Outputs were assessed for: Control, 2wk TAC, 4wk TAC, 4wk TAC+2wk unTAC, 4wk TAC+4wk unTAC, and 4wk TAC+6wk unTAC. Collagen volume fraction (CVF), collagen hybridizing peptide (CHP), and macrophage abundance were assessed by immunohistochemistry. Macrophage phenotype was assessed by flow cytometry and rt-qPCR. Cytokine profiles and enzymes implicated in collagen turnover were determined by immunoassay and immunoblots. To determine the role of macrophages in collagen turnover following alleviation of LVPO, macrophages were depleted with clodronate liposomes at time of unTAC surgery and endpoints were measured at 2wk unTAC. CHP reactivity was significantly increased at 2wk unTAC compared to other time points. A significant reduction in CVF was observed at 4wk unTAC compared to 4wk TAC and 2wk unTAC although it remained increased compared to control levels. A defined temporal pattern in myocardial macrophage cell count was observed: increased in 2wk TAC that decreased at 4wk TAC followed by a further increase at 2wk unTAC and then decreased at 4wk and 6wk unTAC. Macrophage counts at all time

LILY SOON NEFF. Macrophages Promote Regression of Myocardial Fibrosis Following Alleviation of Pressure Overload. (Under the direction of AMY BRADSHAW).

points remained higher than control. Macrophage area was significantly increased at 2wk unTAC compared to all other time points. Profibrotic macrophage markers, F4/80⁺CD206⁺, F4/80⁺CD163⁺, and Ly6C^{low}F4/80^{high}, were increased in TAC compared to unTAC. Depletion of macrophages reduced CHP reactivity and decreased Cathepsin K and proMMP2 levels. In conclusion, normalization of hemodynamic load leads to regression of cardiomyocyte hypertrophy but does not result in complete regression of myocardial fibrosis. Temporal changes in macrophage cell count and phenotype play a critical role in the development of fibrosis during TAC and the partial, but incomplete regression of fibrosis in unTAC.

Chapter 1:
Background

1.1 Extracellular Matrix (ECM) of the Heart

The extracellular matrix (ECM) is an active and dynamic tissue component that plays an important role in mechanotransduction and regulating processes such as progenitor cell differentiation and cell migration.¹ The ECM plays a key role in the pathology of cardiovascular diseases. The ECM is comprised of two main components: basal lamina and interstitium. The basal lamina is a two-dimensional, sheetlike structure composed of collagen type IV, laminin, nidogen, and perlecan. The interstitium constitutes approximately 25% of the myocardial space and the primary protein component is fibrillar collagen. The interstitium contains glycoproteins such as fibronectin and matricellular proteins such as thrombospondins and secreted protein acidic and rich in cysteine (SPARC) which help in collagen fibril assembly. Along with this, the ECM stores latent bioactive molecules. For example, transforming growth factor- β (TGF β) is stored in a latent form within the myocardial ECM until needed in response to injury.²

By volume, cardiomyocytes constitute approximately ~70% of the myocardial tissue.² Cardiomyocytes are connected by intercalated discs to coordinate myocardial excitation and contraction. Cardiac fibroblasts are the primary producer of ECM proteins, specifically fibrillar collagen type I and III, and they comprise one of the largest cell population within the myocardium.^{1,2} Fibroblasts lack a basement membrane and are flat, spindle-shaped cells with multiple projecting processes. By cell number, endothelial cells account for approximately two-thirds of the cells in the heart. Along with these cell types, during homeostasis, the heart contains a diverse array of other cell types such as resident macrophages, T cells, and B cells.³

1.2 Collagen Turnover in Homeostasis and Disease

Collagen is the single most abundant protein in the body, and approximately 90% of collagen found in the body is composed of collagen type I, II, and/or III. For example, collagen type II is the primary component of cartilage, and collagen type I is found in skin, tendon, bone, ligaments, muscle, and interstitial tissues. The basic structural unit of collagen is a triple helical structure composed of three *alpha* chains, but the triple helical composition of the alpha chains differs based on the collagen. For example, fibrillar collagen type I is composed of two *a1(I)* chains and one *a2(I)* chain, whereas fibrillar collagen type III and V are composed of three *a1* chains, *a1(III)* and *a1(V)*, respectively. Collagen contains a repeating motif of Gly-Pro-X, where the X can be any amino acid but has a high propensity to be hydroxyproline.⁴ This repeating motif allows for the formation of the triple helical structure of collagen.⁵

Collagen turnover is the process of synthesis, processing, deposition, and degradation of collagen. Beginning with synthesis, the mRNA encoding the alpha chains are translated and transported into the lumen of the rough endoplasmic reticulum (ER). These synthesized peptide chains create procollagen. Within the ER, the procollagen chains are processed prior to forming the triple helical structure. Galactose and glucose residues are added to hydroxylysine residues, and oligosaccharides are added to asparagine residues on the C-terminal propeptide domain. Along with this, specific proline and lysine residues are hydroxylated to form hydroxyproline and hydroxylysine residues. The three chains of procollagen are aligned by intrachain disulfide bonds and the triple helical structure is formed. The procollagen is secreted into the extracellular space via exocytosis. In the

LILY SOON NEFF. Macrophages Promote Regression of Myocardial Fibrosis Following Alleviation of Pressure Overload. (Under the direction of AMY BRADSHAW).

extracellular space, procollagen peptidases remove the N- and C-terminal propeptide domains which allows polymerization into collagen fibrils.⁵

Collagen crosslinking occurs as intramolecular links to stabilize monomeric triple helices and intermolecular links to stabilize neighboring triple helices within collagen fibrils.⁶ Several enzymes within the myocardium play a key role in initiating these crosslinks. Lysyl oxidase (LOX) initiates the formation of crosslinks on lysine and hydroxylysine residues creating dehydro-lysinonorleucine (deH-LNL) and dehydroxylysinonorleucine (deH-HLNL), respectively, that become mature crosslinks by incompletely defined processes. LOX is secreted into the ECM as the inactive zymogen, proLOX, which is activated when the propeptide domain is cleaved off by bone morphogenetic protein 1 (BMP1).⁶ Along with this, transglutaminase catalyzes the formation of cross-links between a lysine and glutamine residue on neighboring proteins in the ECM.⁶

Collagenolysis is the process of degrading collagen. The initiation of interstitial fibrillar collagen degradation begins at a single site, Pro-Gln-Gly⁷⁷⁵~Ile⁷⁷⁶-Ala-Gly, which creates ¼ and ¾ length fragments for additional degradation. This initial cleavage is completed by a collagenase. Collagenases include matrix metalloproteinases (MMPs) such as MMP1, MMP8, MMP12, MMP13, and membrane bound MT1-MMP. Continued degradation of fibrillar collagen is completed by gelatinases, such as MMP2 and MMP9, which laterally diffuse along the fibrils and further proteolyze the *α* chains.⁴

The excessive deposition of fibrillar collagen in parenchymal tissues is termed fibrosis. The development of myocardial fibrosis, in response to injury or disease, is an imbalance of collagen turnover which favors increased synthesis, processing, and deposition of

LILY SOON NEFF. Macrophages Promote Regression of Myocardial Fibrosis Following Alleviation of Pressure Overload. (Under the direction of AMY BRADSHAW).

fibrillar collagen while reducing the amount of collagen degradation. Several types of myocardial fibrosis can develop within the myocardium dependant on the stimulus or antecedent disease (Fig. 1). For example, replacement/scarring fibrosis occurs following a myocardium infarction. Necrosis of cardiomyocytes occurs due a coronary artery block that prevents oxygenation of cardiomyocytes. These dead cardiomyocytes are removed and a collagen scar is deposited to prevent cardiac rupture. In response to pressure overload, such as hypertension or aortic stenosis, where the heart must work harder to overcome an increased afterload, perivascular fibrosis and reactive interstitial fibrosis occurs (Fig. 1). Perivascular fibrosis is the deposition of collagen around the vasculature within the myocardium, and reactive interstitial fibrosis is deposition of collagen around the cardiomyocytes. Overall, replacement fibrosis is localized to an infarct region, whereas reactive interstitial fibrosis is diffuse throughout the myocardium.

The excessive deposition of fibrillar collagen relies on key proteins which facilitate procollagen synthesis and processing and collagen fibril assembly in the ECM. Matricellular proteins, such as Secreted protein acidic and rich in cysteine (SPARC) and periostin, are highly expressed in developing tissues and in response to injury but not in healthy tissue. SPARC binds to collagen at the same motif as discoidin domain receptor 2 (DDR2), so it is hypothesized that SPARC and DDR2 compete for binding to collagen. SPARC^{-/-} murine studies have demonstrated reduced fibrosis and one proposed mechanism is that procollagen remains at the cell surface bound to DDR2.⁷ Furthermore, SPARC^{-/-} mice that received TAC exhibited more soluble collagen but less insoluble collagen.⁸ Taken together, it is proposed that SPARC facilitates the deposition and crosslinking of collagen by forming an extracellular scaffold with other proteins such as BMP-1, periostin,

LILY SOON NEFF. Macrophages Promote Regression of Myocardial Fibrosis Following Alleviation of Pressure Overload. (Under the direction of AMY BRADSHAW).

LOX, and fibromodulin.^{6,9} Periostin^{-/-} mice subjected to myocardial infarction demonstrate reduced levels of total collagen and mature cross-linked collagen, and decreased myocardial stiffness.¹⁰ Periostin^{-/-} mice subjected to LVPO demonstrated reduced interstitial fibrosis and improved fractional shortening.¹⁰ Although periostin is commonly used as a marker of activated fibroblasts, it is thought that a profibrotic, fibroblast-like macrophage subset exists that express periostin.¹¹ Transforming growth factor- β (TGF β) is stored in the ECM bound to latent TGF β binding protein (LTBP) in an inactive form. In the event of disease or injury, such as LVPO, TGF β can be activated to induce ECM synthesis and deposition, enhanced inflammation, and increased cell proliferation.¹² In the context of LVPO induction, membrane type 1-matrix metalloproteinase (MT1-MMP), also known as MMP14, stimulates fibrosis by cleaving LTBP to activate TGF β .¹³ However, previous research has demonstrated that MMP14 promotes collagen degradation in the resolution of fibrosis, specifically macrophage dependent MMP14 expression regresses liver fibrosis.¹⁴

LILY SOON NEFF. Macrophages Promote Regression of Myocardial Fibrosis Following Alleviation of Pressure Overload. (Under the direction of AMY BRADSHAW).

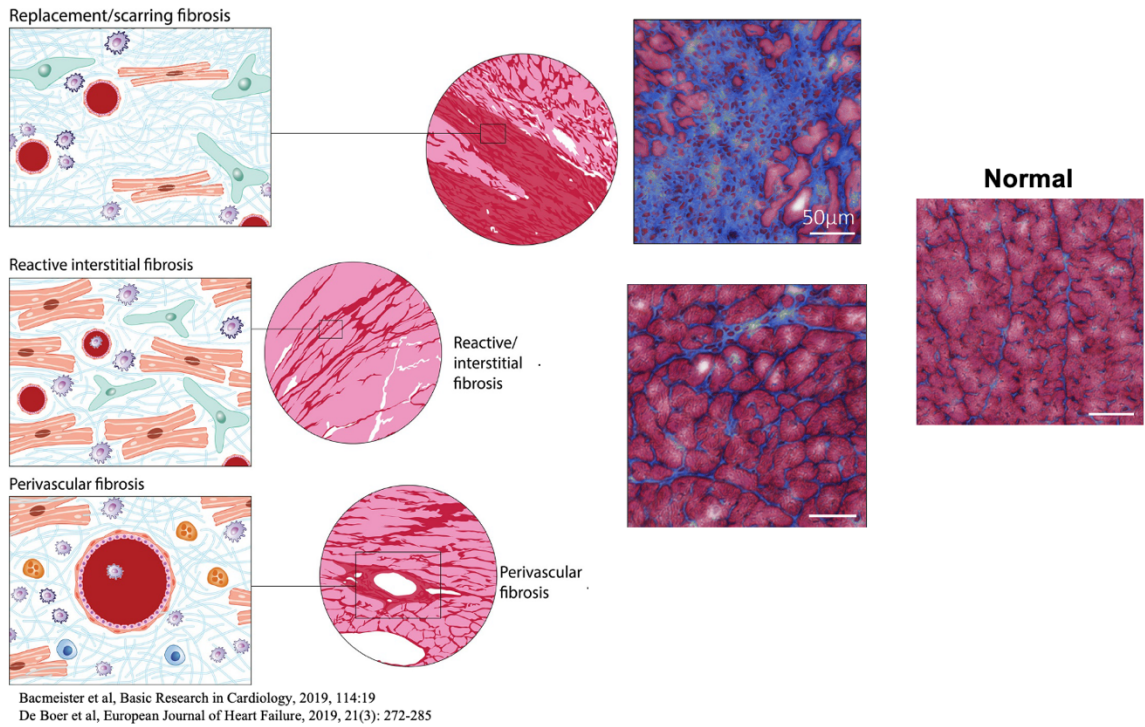


Figure 1: Types of Myocardial Fibrosis. Three main types of fibrosis occur in the myocardium; replacement/scarring fibrosis, reactive interstitial fibrosis, and perivascular fibrosis. Figure obtained from Amy Bradshaw, Ph.D.

1.3 Heart Failure

Heart Failure is when the heart is unable to meet the metabolic demands of the body, both at rest and during exercise. Two main types of Heart Failure are exhibited in the patient population, Heart Failure with Reduced Ejection Fraction (HFrEF) and Heart Failure with Preserved Ejection Fraction (HFpEF).¹⁵ Ejection fraction is the percentage of blood that is pumped from the heart with each beat. Patients with an ejection fraction less than 50% exhibit HFrEF, whereas patients with an ejection fraction greater than 50% are HFpEF.¹⁵ Although our lab conducts mechanistic studies on both HFrEF and HFpEF, this research project focused on a murine model of HFpEF. A patient can develop through key pathophysiological stages to HFpEF. First developing aortic valve stenosis and/or systemic hypertension which further progresses into left ventricular pressure overload (LVPO) characterized by cardiomyocyte hypertrophy. LVPO can further progress into Heart Failure characterized by reactive interstitial fibrosis and myocardial stiffness.^{16,17} Heart Failure is a major public health and economic burden. Approximately 500,000 to 600,000 new cases are diagnosed each year.¹⁸ Along with this, even with our advancements in therapy, the 1-year rehospitalization and 5-year mortality rates still remain 50%.¹⁶ Furthermore, \$108 billion a year is spent globally on heart failure treatments, and the United States accounts for 30% of this expenditure.¹⁸ A reason these statistics remain so high is because we currently do not have direct, targeted antifibrotic therapies available for the treatment of Heart Failure.¹⁵ Understanding the underlying cellular and molecular mechanisms of persistent fibrosis observed in Heart Failure will allow for us to develop direct, antifibrotic therapies that will improve quality of life for patients.¹⁵

1.4 Left Ventricular Pressure Overload

As previously mentioned, left ventricular pressure overload (LVPO) can develop from antecedent conditions such as systemic hypertension and/or aortic valve stenosis. Sustained hemodynamic overload causes the left ventricular chamber to undergo cellular and ECM remodeling that is associated with excess accumulation of fibrillar collagen resulting in myocardial interstitial fibrosis. Whether and to what extent alleviation of LVPO leads to regression of fibrosis is poorly defined as are the cellular and molecular mechanisms that might influence the regression of fibrosis in the heart. Patients who underwent surgical aortic valve replacement (SAVR) for correction of aortic stenosis (AS) demonstrated normalization of hemodynamic load (Fig. 2).¹⁹⁻²¹ However, left ventricular endocardial biopsies obtained from these patients 5-years post-SAVR demonstrated only a 30% reduction in collagen volume fraction (CVF), a measurement of fibrosis within the myocardium (Fig. 2). In conclusion, this clinical data demonstrates current therapies lead to incomplete reduction myocardial interstitial fibrosis and patients still exhibit persistent LV diastolic dysfunction.¹⁹⁻²¹

LILY SOON NEFF. Macrophages Promote Regression of Myocardial Fibrosis Following Alleviation of Pressure Overload. (Under the direction of AMY BRADSHAW).

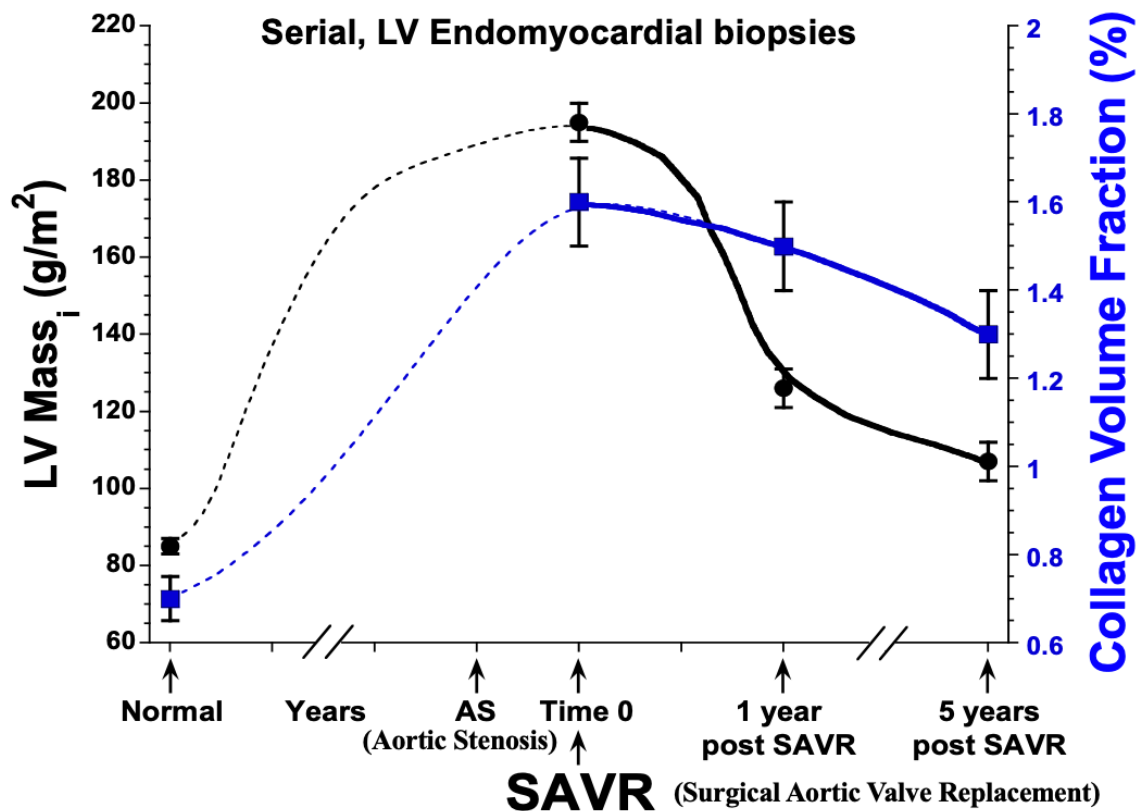


Figure 2: Aortic stenosis/Surgical Aortic Valve Replacement LV Mass and CVF. Serial, left ventricular endomyocardial biopsies were isolated from patients in the 1980's and 1990's by cardiologists in Zurich at the time of SAVR surgery, and 1 year and 5 years post-SAVR surgery. LV mass (g/m²) is demonstrated by the black line. Collagen volume fraction (CVF) was measured and data is displayed as the blue line. Figure created by Michael Zile, M.D. and Catalin Baicu, Ph.D. from published data.¹⁹⁻²¹

LILY SOON NEFF. Macrophages Promote Regression of Myocardial Fibrosis Following Alleviation of Pressure Overload. (Under the direction of AMY BRADSHAW).

1.5 Preclinical Models of Unloading the Myocardium

To mimic this AS/SAVR clinical paradigm, our studies utilize a mechanical induction of LVPO through TAC to induce fibrosis in mice. Previous studies utilizing TAC to induce LVPO and alleviation of LVPO by debanding (unTAC) have been reported. Previous studies and our work demonstrate variations in experimental parameters such as animal age, sex, degree of LVPO (i.e. gauge of TAC needle), and the length of LVPO prior to debanding and endpoints (length of unTAC prior to harvest)²²⁻²⁴. Gao et. al. evaluated male mice, 6-8 weeks of age, that were banded for either 4 or 8 weeks followed by 6 weeks of unbanding. Their study reported a complete reversal of cardiomyocyte hypertrophy after 6 weeks of unbanding. Similar to our data presented herein, their study demonstrated that collagen content did decrease from levels in LVPO hearts but remained elevated compared to control after 6 weeks of unbanding.²² Rodrigues et. al. utilized male mice, 7 weeks of age, and subjected them to LVPO for 7 weeks and evaluated outputs after 2 weeks of debanding. Rodrigues et. al. found that mice demonstrating diastolic dysfunction at debanding had elevated levels of fibrosis.²⁴ To further characterize LV remodeling in heart failure, Weinheimer et. al. combined TAC/unTAC with myocardial infarction and found persistent fibrosis after debanding was associated with continued activation of ECM genes and pathways associated with fibroblast activation and ECM deposition.²⁵ Taken together, findings from other studies are consistent with the data presented herein and further confirm the validity of our murine model for evaluating cellular parameters of persistent fibrosis after alleviation of PO.

1.6 Myocardial Macrophages in Homeostasis

Macrophages have several key functions including tissue development and maintenance, tissue surveillance, pathogen clearing, antigen presentation, inflammation resolution and tissue repair. During embryogenesis, early primitive hematopoiesis on embryonic days E6 to E8 leads to seeding of macrophages in the embryonic yolk sac.¹¹ These macrophages are considered yolk-sac derived macrophages, are F4/80^{hi}, and comprise the resident macrophage population found in the heart during homeostasis. Tissue resident macrophages are mainly maintained by local self-renewal and approximately 2% of resident macrophages are renewed by circulating monocytes. Advanced experimental techniques such as single cell sequencing and cytometry by time of flight (CyTOF) have demonstrated that within the heart, four cardiac resident macrophage subsets exist. All four subsets express MerTK and CD64, but vary in expression of other markers like MHCII, CD206, and CD11c.¹¹ Interestingly, macrophages play a role in facilitating action potential propagation in the conduction system of the murine heart. Using connexin 43 containing gap junctions, macrophages electronically couple to cardiomyocytes. This macrophage-cardiomyocyte coupling allows for a more positive depolarized resting membrane potential and facilitation of higher rates of conduction beats.¹¹

1.7 Myocardial Macrophages in LVPO

Systemic hypertension and aortic stenosis can induce systemic inflammation. In response to this systemic proinflammatory state, endothelial cells within the vasculature of the myocardium demonstrate increased reactive oxygen species, increased secretion of CCL2 and CCL7, and increased expression of adhesion molecules such as VCAM1 and

LILY SOON NEFF. Macrophages Promote Regression of Myocardial Fibrosis Following Alleviation of Pressure Overload. (Under the direction of AMY BRADSHAW).

ICAM1.¹¹ Increased production of pro-inflammatory cytokines, such as IFN γ , activates hematopoiesis and the recruitment of monocytes to the heart. CCL2, CCL7, and adhesion molecules allow for adherence and extravasation of monocytes from the circulation into the myocardium. Monocyte derived macrophages and resident macrophages can affect the extracellular matrix either directly by producing matrix metalloproteinases (MMPs) or indirectly by producing cytokines, such as the anti-inflammatory cytokines IL-10 and TGF β .^{11,26,27} Previous research utilizing murine models of LVPO have demonstrated the detrimental role of monocyte-derived macrophages in promoting fibrosis through the activation of myofibroblasts and T-cells.²⁶ Specifically, previous research from our lab has demonstrated SPARC expression by monocyte-derived macrophages promotes the deposition of interstitial fibrosis, and the cytokine/chemokine profile of the TAC myocardium promotes a profibrotic, alternatively activated (M2) macrophage phenotype.^{28,29,30} Depletion of resident macrophages in TAC, using a macrophage colony-stimulating factor 1 receptor (CD115) blocking antibody results in robust fibrosis demonstrating that resident macrophages are beneficial during LVPO to reduce the extent of fibrosis observed.³¹

To date, macrophage-dependent mechanisms that regulate myocardial collagen turnover following alleviation of LVPO, have not been examined. The objective of this research focused on elucidating macrophage-dependent mechanisms that regulate collagen turnover following alleviation of LVPO. Our central hypothesis was that following alleviation of LVPO (unTAC), macrophages would demonstrate a distinct, but transient, anti-fibrotic phenotype that initiates, but does not completely regress collagen degradation. This unsustained, antifibrotic response contributes to the partial but incomplete regression

LILY SOON NEFF. Macrophages Promote Regression of Myocardial Fibrosis Following Alleviation of Pressure Overload. (Under the direction of AMY BRADSHAW).

of LVPO-induced interstitial fibrosis (Fig. 3). During homeostasis, resident macrophages promote the balanced amount of collagen deposition and degradation that results in low levels of collagen for structural integrity of the myocardium. In response to increased load (LVPO, TAC), a pro-fibrotic macrophage phenotype is observed that promotes enhanced collagen deposition and reduce collagen degradation resulting in robust interstitial fibrosis. In response to unTAC, returning the myocardium to normal load, an early, anti-fibrotic macrophage phenotype is observed that promotes increased collagen degradation and reduce collagen deposition which results in a partial regression of fibrosis. In late unTAC, it is hypothesized that a new pro-fibrotic macrophage phenotype is observed with increased expression of specific profibrotic genes (Fig. 3).

LILY SOON NEFF. Macrophages Promote Regression of Myocardial Fibrosis Following Alleviation of Pressure Overload. (Under the direction of AMY BRADSHAW).

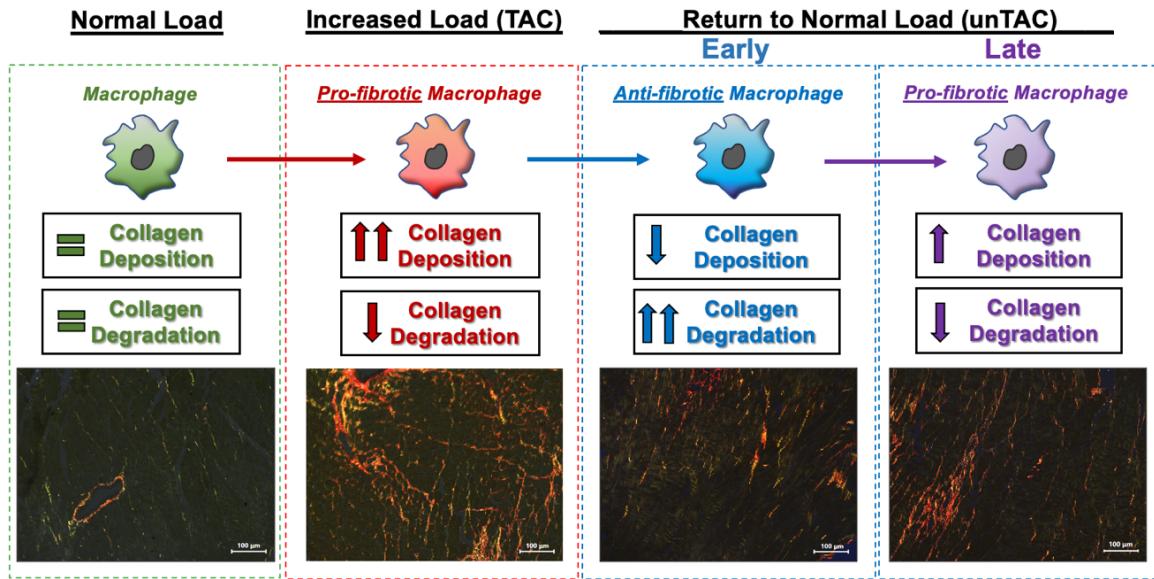


Figure 3: Schematic of Central Hypothesis. Schematic detailing the central hypothesis of the role of macrophages in response to increased load (TAC) and return to normal load (unTAC) with representative picrosirius red (PSR) stained images of fibrillar collagen.

Created with Biorender.com.

LILY SOON NEFF. Macrophages Promote Regression of Myocardial Fibrosis Following Alleviation of Pressure Overload. (Under the direction of AMY BRADSHAW).

Chapter 2:

Characterization of the TAC/unTAC Preclinical Murine Model

2.1 Effects of TAC and unTAC on Myocardial Hypertrophy

To induce LVPO, a transverse aortic constriction (TAC) by tying a suture around the transverse aorta using a 26-gauge needle is completed. To alleviate LVPO, the suture is removed from around the aorta (unTAC). Gravimetric analysis of LV mass/body weight and LV mass/tibia length demonstrated an increase in 2wk and 4wk TAC compared to control (Table 1). To determine cardiomyocyte cross-sectional area (CSA), tissue sections were incubated with Wheat Germ Agglutinin (WGA). WGA is a lectin that binds to glycoproteins in the cell membrane and ECM.³² Histological analysis of cardiomyocyte CSA, by WGA staining, demonstrated an increase at 2wk TAC compared to control (Figure 4A-B, G). A further increase in CSA was observed at 4wk TAC compared to 2wk TAC (Fig. 4B-C, G). TAC myocardium demonstrated increased peak aortic velocity and peak systolic stress compared to control demonstrating a successful pressure gradient (Table 1). After alleviation of LVPO (unTAC), peak aortic velocity and peak systolic stress returned to control levels demonstrating successful and complete removal of the pressure gradient (Table 1). CSA significantly decreased at 2wk and 4wk unTAC compared to 4wk TAC (4C-E, G). CSA remained increased at 2wk and 4wk unTAC compared to control levels (4A, D-E, G). By 6wk unTAC, CSA returned to control levels (4A, F-G). However, LV mass/body weight and LV mass/tibia length remained significantly increased at 6wk unTAC compared to control (Table 1). Interestingly, LV mass/body weight and LV mass/tibia length at 6wk unTAC was significantly decreased compared to 2wk TAC (Table 1). Although complete regression of hypertrophy was not observed at the chamber level, regression of cardiomyocyte hypertrophy to control level was observed at the cellular level.

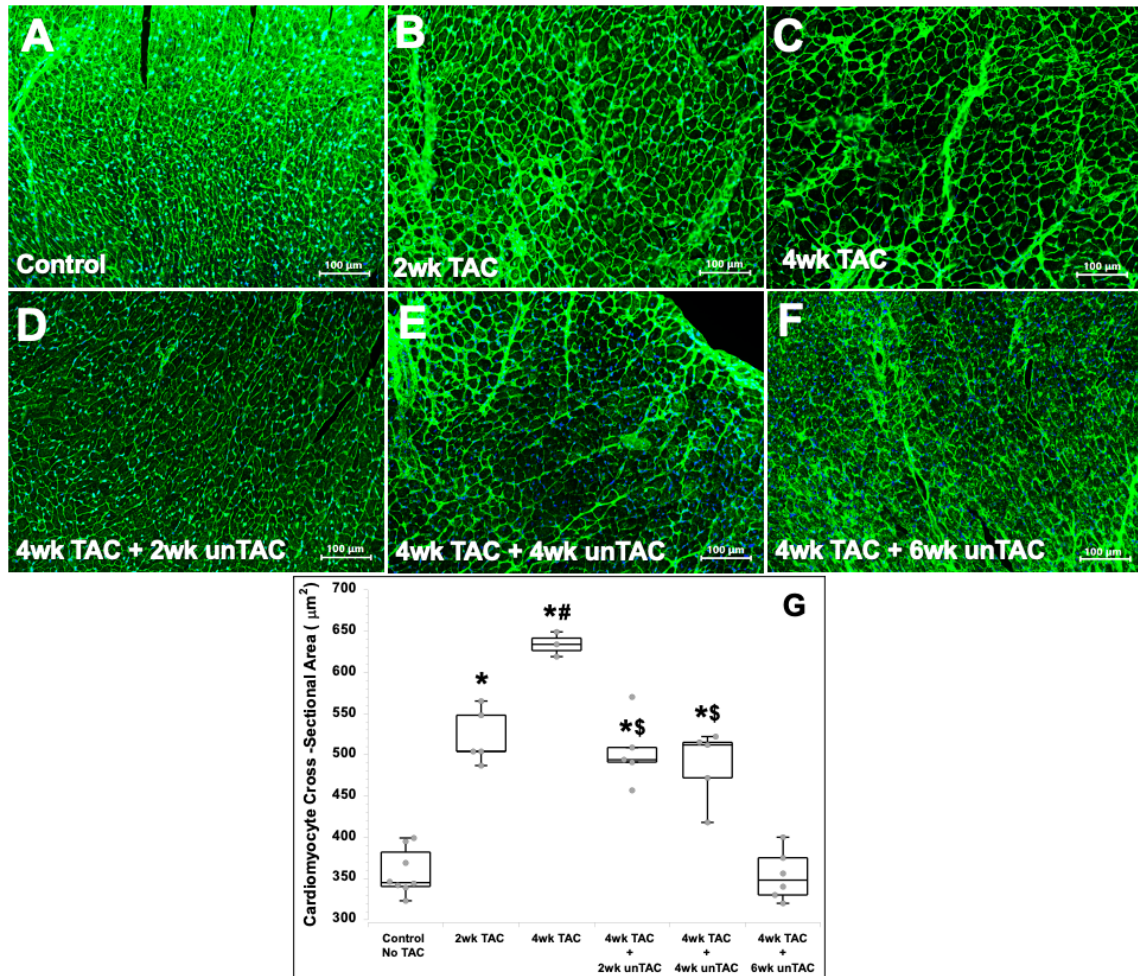


Figure 4: Characterization of Cardiomyocyte cross-sectional area in TAC and unTAC Myocardium. Wheat germ agglutinin (WGA) staining was completed on left ventricular myocardium with transverse aortic constriction (TAC) (B and C) and following unTAC (D-F) versus control (A). Quantification of cardiomyocyte cross-sectional area from WGA images of the TAC/unTAC time points (G). Panels A-F are represented with equivalent magnification (Scale bar = 100um). Animal sample sizes: control (n = 8), 2wk TAC (n = 5), 4wk TAC (n = 3), 2wk unTAC (n = 5), 4wk unTAC (n = 5), and 6wk unTAC (n = 6). *p<0.05 vs. Control; #p<0.05 vs. 2wk TAC; \$p<0.05 vs. 4wk TAC; +p<0.05 vs. 4wk TAC+2wk unTAC.

LILY SOON NEFF. Macrophages Promote Regression of Myocardial Fibrosis Following Alleviation of Pressure Overload. (Under the direction of AMY BRADSHAW).

Table 1: Structural and Hemodynamic Characteristics of the TAC/unTAC Myocardium. LV mass/Body Weight (mg/g), LV mass/Tibia Length (mg/mm), Average LV wall thickness, % LV Ejection Fraction (EF), LV End diastolic volume (mL) (EDV), Lung/BW (mg/g), Peak Aortic Velocity (m/sec), Cardiomyocyte cross-sectional area (CSA), LV Peak Systolic Stress (g/cm²), and Myocardial Stiffness parameters were measured and compared between control, 2wk TAC, 4wk TAC, 4wk TAC+2wk unTAC, 4wk TAC+4wk unTAC, and 4wk TAC+6wk unTAC. *p<0.05 vs. Control; #p<0.05 vs. 2wk TAC; §p<0.05 vs. 4wk TAC.

	Control	2wk TAC	4wk TAC	4wk TAC + 2wk unTAC	4wk TAC + 4wk unTAC	4wk TAC + 6wk unTAC
LVmass/BW (mg/g)	3.5±0.3	6.1±0.2*	6.5±1.2*	4.6±0.3*§	4.3±0.5*§	4.2±0.7*§
LVmass/TL (mg/mm)	4.3±0.8	6.3±0.8*	9.0±1.2*#	6.0±1.0*§	5.9±0.9*§	5.9±1.6*§
Average LV wall thickness	0.72±0.04	0.98±0.04*	1.00±0.04*	0.85±0.04*§	0.83±0.06*§	0.80±0.07*§
LV EF (%)	55±5	52±6	51±5	52±7	51±7	50±14
LV EDV (mL)	55±9	56±11	66±8	64±13	67±18	71±12
Lung/ BW (mg/g)	6.6±1.1	9.0±3.7*	17.5±3.8*#	10.6±2.0*§	7.6±2.2 [§]	7.9±2.9 [§]
Peak Aortic Velocity (m/sec)	0.64 ± 0.07	3.59 ± 0.39*	3.58 ± 0.42*	0.64 ± 0.31 [§]	0.67 ± 0.24 [§]	0.57±0.14
CSA (µm²)	357±27	522±33*	625±21*#	504±41*§	488±14*§	354±30 [§]
LV Peak Systolic Stress (g/cm²)	92 ± 24	117 ± 12*	163 ± 93*	96±23 [§]	94±24 [§]	90±14 [§]
Myocardial Stiffness	0.030±0.005	0.062±0.014*	0.075±0.015*#	0.061±0.054*	0.048±0.017*§	0.041±0.004*§

Data = Mean ± St.Dev

2.2 Effects of TAC and unTAC on Fibrillar Collagen Content

Histological analysis of Picrosirius Red (PSR) stained myocardial tissue sections demonstrated an increase in collagen volume fraction (CVF) at 2wk TAC and 4wk TAC compared to control (Fig. 5A-C, G). After alleviation of LVPO, CVF levels at 2wk unTAC were similar to CVF levels at 4wk TAC (Fig. 5C-D, G). CVF was significantly reduced at 4wk unTAC compared to 4wk TAC and 2wk unTAC (Fig. 5C-E, G). However, CVF at 4wk unTAC remained significantly increased compared to control (Fig. 5A, E, G). At 6wk unTAC, the CVF remained elevated compared to control (Fig. 5A, F-G). Although hemodynamic load was normalized by alleviation of LVPO (unTAC), regression of myocardial interstitial fibrosis was incomplete.

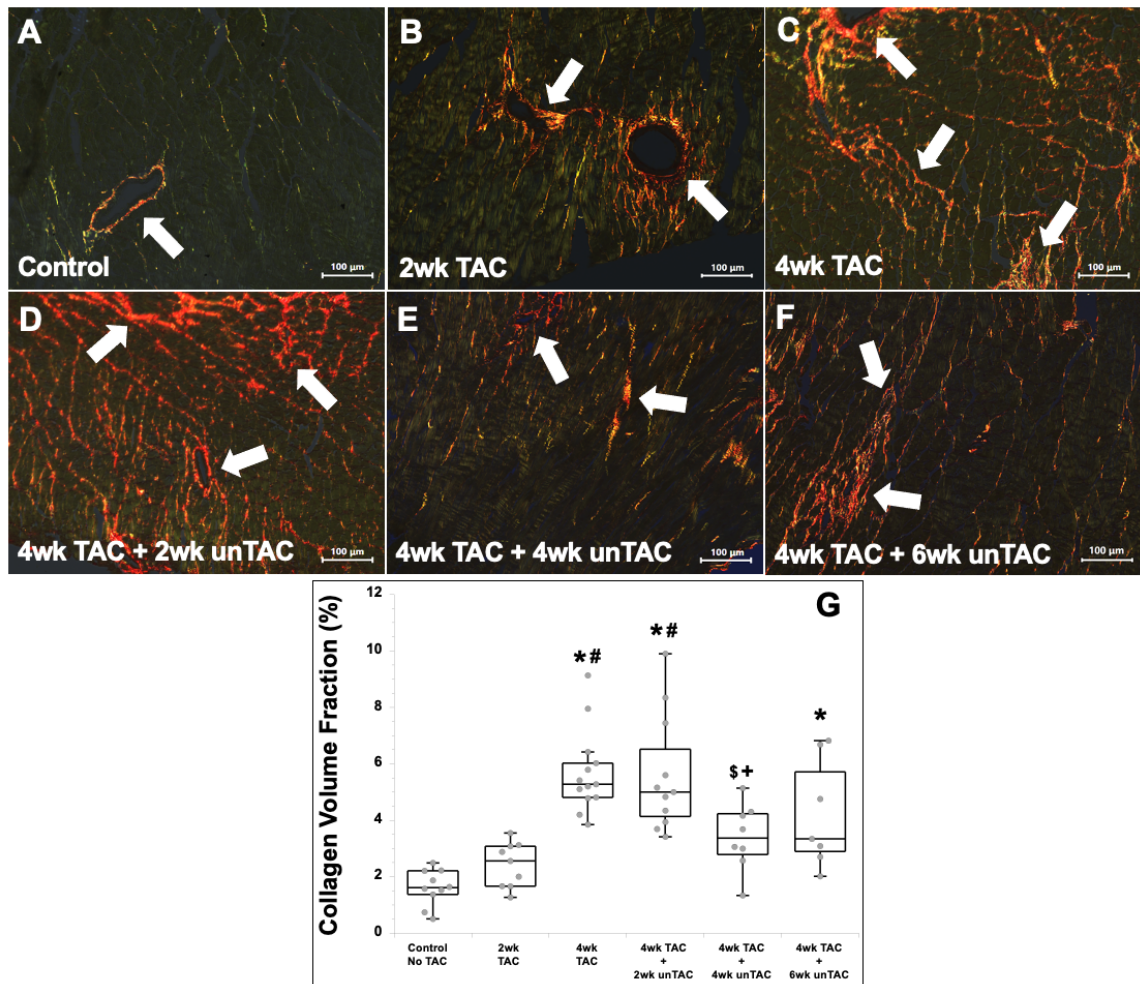


Figure 5: Characterization of Collagen Volume Fraction in TAC and unTAC Myocardium. Picosirius red staining was completed on left ventricular myocardium with transverse aortic constriction (TAC) (B and C) and following unTAC (D-F) versus control (A). Quantification of collagen volume fraction from PSR stained myocardial tissue of the TAC/unTAC time points (G). Panels A-F are represented with equivalent magnification (Scale bar = 100um). Animal sample sizes: control (n = 7), 2wk TAC (n = 7), 4wk TAC (n = 11), 2wk unTAC (n = 7), 4wk unTAC (n = 7), and 6wk unTAC (n = 7). *p<0.05 vs. Control; #p<0.05 vs. 2wk TAC; \$p<0.05 vs. 4wk TAC; +p<0.05 vs. 4wk TAC+2wk unTAC.

2.3 Effects of TAC and unTAC on Collagen Crosslinking Protein Production

Collagen cross-linking enzymes are required for incorporation of collagen fibers into insoluble ECM.⁶ Total protein extracted from TAC and unTAC LVs were assessed for levels of collagen crosslinking enzymes. The collagen cross-linking enzymes, proLysyl oxidase (proLOX) and Lysyl Oxidase like 2 (LOXL2), were significantly increased in 2wk and 4wk TAC compared to control (Fig. 6A-B, E-F). LOXL2 is implicated in both the cross-linking of fibrillar collagen and collagen IV assembly in the basement membrane.³³ The 65kDa isoform of LOXL2, implicated in collagen IV assembly in the basement membrane, demonstrated similar protein levels at 2wk unTAC compared to control (Fig. 6E-F). At 4wk unTAC, LOXL2 was increased back to TAC myocardium levels and was significantly increased compared to control (Fig. 6E-F). By 6wk unTAC, LOXL2 levels decreased again comparable to control and 2wk unTAC levels (Fig. 6E-F).

For lysyl oxidase to be enzymatically active, the propeptide domain, lysyl oxidase propeptide (LOPP) is cleaved. LOPP can be used as a surrogate marker of active protein levels of lysyl oxidase in the myocardium. LOPP protein levels were significantly increased in 2wk and 4wk TAC myocardium compared to control (Fig. 6C-D). After alleviation of LVPO, LOPP protein levels were significantly decreased at 2wk and 4wk unTAC compared to TAC myocardium. Interestingly, LOPP protein levels significantly increased in 6wk unTAC myocardium, comparable to TAC myocardium levels (Fig. 6C-D). proLOX demonstrated the same trend as LOPP in the unTAC myocardium. proLOX was decreased in 2wk and 4wk unTAC myocardium compared to TAC myocardium (Fig. 6A-B). However, proLOX was significantly increased, comparable to TAC levels, in 6wk unTAC myocardium compared to control and 2wk unTAC (Fig. 6A-B).

LILY SOON NEFF. Macrophages Promote Regression of Myocardial Fibrosis Following Alleviation of Pressure Overload. (Under the direction of AMY BRADSHAW).

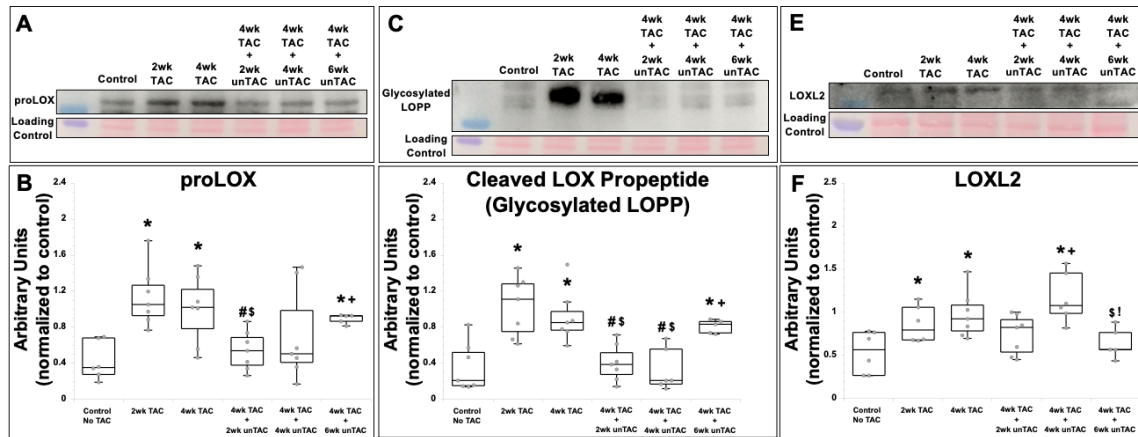


Figure 6: Characterization of Collagen Crosslinking Enzymes in TAC and unTAC

Myocardium. Levels of pro-lysyl oxidase (proLOX) was assessed by immunoblot analysis

(A). Semi-quantification of proLOX protein abundance by immunoblot analysis

normalized to levels of control protein visualized by Ponceau S staining of membranes (B).

Levels of cleaved LOX propeptide (glycosylated LOPP) was assessed by immunoblot

analysis (C). Semi-quantification cleaved LOX propeptide (glycosylated LOPP) protein

abundance by immunoblot analysis normalized to levels of control protein visualized by

Ponceau S staining of membranes (D). Levels of lysyl oxidase like 2 (LOXL2) was

assessed by immunoblot analysis (E). Semi-quantification of LOXL2 protein abundance

by immunoblot analysis normalized to levels of control protein visualized by Ponceau S

staining of membranes (F). Animal sample sizes: control (n = 6-7), 2wk TAC (n = 7), 4wk

TAC (n = 7), 2wk unTAC (n = 7), 4wk unTAC (n = 6-7), and 6wk unTAC (n = 5). *p<0.05

vs. Control; #p<0.05 vs. 2wk TAC; \$p<0.05 vs. 4wk TAC; +p<0.05 vs. 4wk TAC+2wk

unTAC.

2.4 Effects of TAC and unTAC on Initiation of Collagen Degradation

Fibrillar collagen degradation is a multistep process that begins with the cleavage of the fibrillar helical structure by collagenases to initiate unwinding.⁴ Subsequent degradation by gelatinases, such as matrix metalloproteinases, and other extracellular proteases, leads to degradation and digestion of the soluble fibrillar collagen fragments. To detect and quantify initiation of fibrillar collagen degradation, collagen hybridizing peptide (CHP) was used on myocardial tissue sections. CHP shares the internal amino acid sequence of fibrillar collagen, Gly-X-Y, and can hybridize to these collagen fibrils with unwound triple helical structures. Control and 2wk TAC myocardial tissue sections demonstrated little evidence of CHP reactivity (Fig. 7A-B, G). CHP reactivity significantly increase at 4wk TAC compared to control and 2wk TAC levels (Fig. 7A-C, G). After alleviation of LVPO, CHP reactivity significantly increased at 2wk unTAC compared to 4wk TAC (Fig. 7C-D, G). CHP reactivity significantly decreased at 4wk unTAC compared to 2wk unTAC (Fig. 7D-E, G). At 6wk unTAC, CHP reactivity was increased compared to control and 2wk TAC but was not at 2wk unTAC levels (Fig. 7A-B, D, F-G).

LILY SOON NEFF. Macrophages Promote Regression of Myocardial Fibrosis Following Alleviation of Pressure Overload. (Under the direction of AMY BRADSHAW).

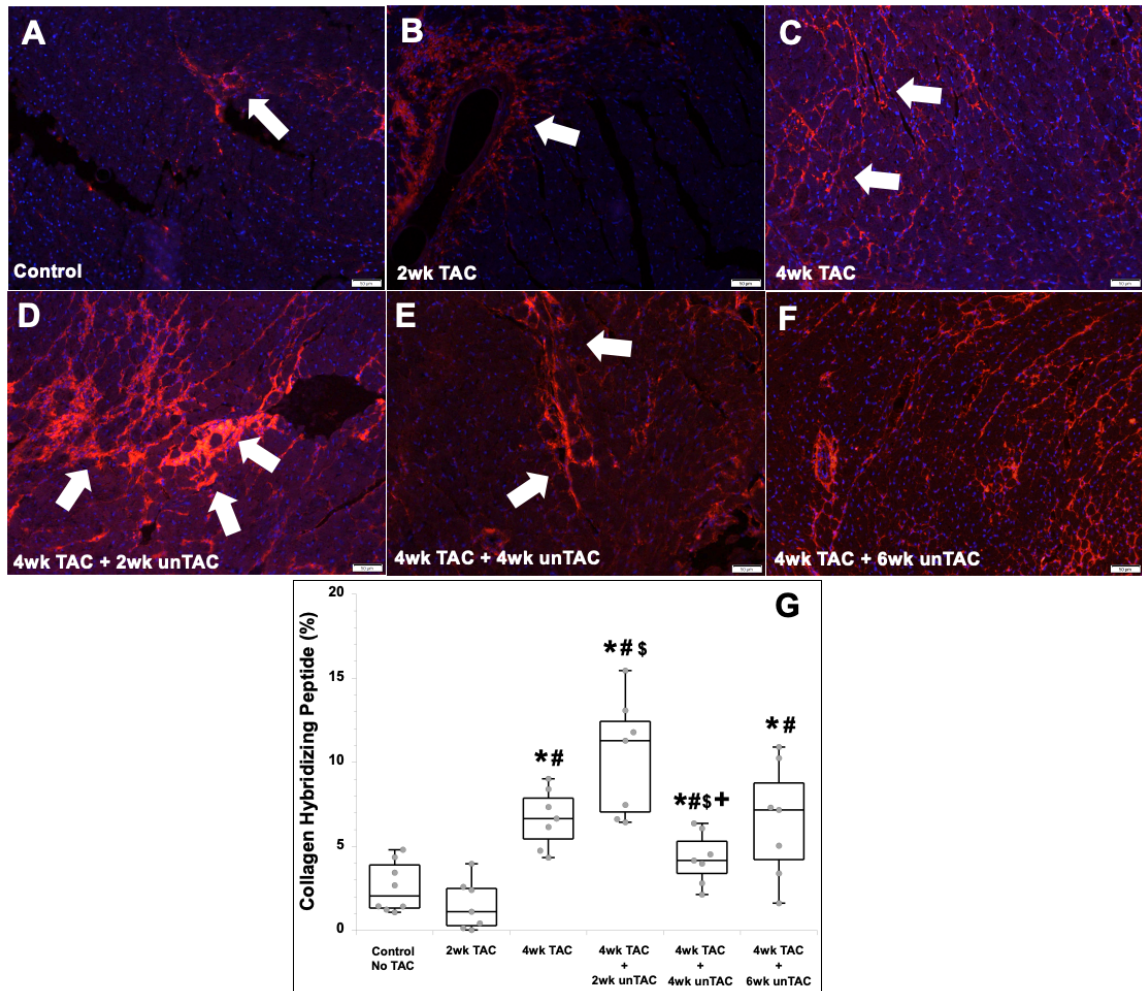


Figure 7: Characterization of Collagen Hybridizing Reactivity in TAC and unTAC Myocardium. Collagen hybridizing peptide immunoreactivity was completed on left ventricular myocardium with transverse aortic constriction (TAC) (B and C) and following unTAC (D-F) versus control (A). Quantification of CHP reactivity from the TAC/unTAC time points (G). Panels A-F are represented with equivalent magnification (Scale bar = 50um). Animal sample sizes: control (n = 8), 2wk TAC (n = 7), 4wk TAC (n = 8), 2wk unTAC (n = 7), 4wk unTAC (n = 6), and 6wk unTAC (n = 7). *p<0.05 vs. Control; #p<0.05 vs. 2wk TAC; \$p<0.05 vs. 4wk TAC; +p<0.05 vs. 4wk TAC+2wk unTAC.

Total protein extracted from TAC and unTAC LVs were assessed for levels of enzymes implicated in collagen degradation. Immunoblot analysis demonstrated an increase in Cathepsin K, a papain-like cysteine protease with collagenolytic activity, in 2wk and 4wk unTAC compared to control and TAC myocardium (Fig. 8A-B). The 2wk unTAC myocardium demonstrated an increased trend in protein production of proMMP2, the precursor form to active MMP2, and a significant increase at 4wk unTAC compared to control and 2wk TAC (Fig. 8C-D). Addressable Laser Bead Immunoassay (ALBIA) analysis demonstrated an increased trend in MMP3, MMP8, and proMMP9 in unTAC myocardium compared to control and TAC myocardium (Fig. 9). MMP3 was significantly increased in 2wk unTAC myocardium compared to control (Fig. 9A). MMP8 was significantly increased in 2wk unTAC myocardium compared to control (Fig. 9B). MMP8 significantly decreased by 4wk unTAC compared to 2wk unTAC (Fig. 9B). Although not statistically significant, unTAC myocardium demonstrated an increased trend in proMMP9 protein production at 2wk unTAC compared to control and 2wk TAC myocardium (Fig. 9C). Similar to what was observed with MMP8, proMMP9 demonstrated decreased protein production in 4wk unTAC myocardium compared to 2wk unTAC myocardium (Fig. 9C). Tissue inhibitor of matrix metalloproteinase 1 (TIMP1) binds to MMPs to inhibit their enzymatic activity on fibrillar collagen. Although not significant, TIMP1 demonstrated a modest increase in protein production in the TAC myocardium compared to control (Fig. 8E-F). Interestingly, following alleviation of LVPO, TIMP1 protein levels were significantly increased in 2wk and 4wk unTAC myocardium compared to control (Fig. 8E-F). Furthermore, TIMP1 further increased at 6wk unTAC and was significantly increased compared to both control and TAC myocardium (Fig. 8E-F).

LILY SOON NEFF. Macrophages Promote Regression of Myocardial Fibrosis Following Alleviation of Pressure Overload. (Under the direction of AMY BRADSHAW).

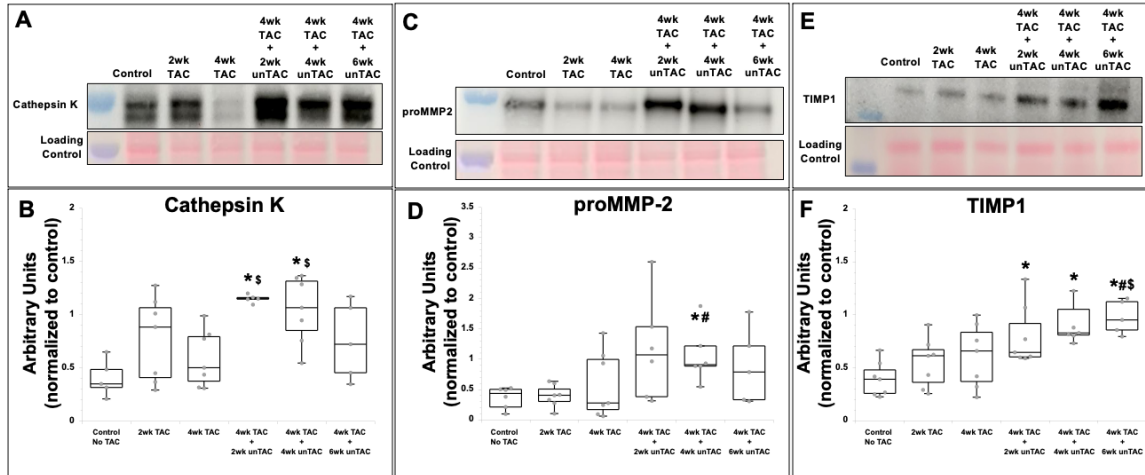


Figure 8: Characterization of Enzymes implicated in Collagen Turnover in TAC and unTAC myocardium. Levels of Cathepsin K was assessed by immunoblot analysis (A). Semi-quantification of Cathepsin K protein abundance by immunoblot analysis normalized to levels of control protein visualized by Ponceau S staining of membranes (B). Levels of pro-matrix metalloproteinase 2 (proMMP2) was assessed by immunoblot analysis (C). Semi-quantification proMMP2 protein abundance by immunoblot analysis normalized to levels of control protein visualized by Ponceau S staining of membranes (D). Tissue inhibitor of matrix metalloproteinase 1 (TIMP1) was assessed by immunoblot analysis (E). Semi-quantification of TIMP1 protein abundance by immunoblot analysis normalized to levels of control protein visualized by Ponceau S staining of membranes (F). Animal sample sizes: control (n = 6-7), 2wk TAC (n = 7), 4wk TAC (n = 7), 2wk unTAC (n = 6-7), 4wk unTAC (n = 6-7), and 6wk unTAC (n = 5). *p<0.05 vs. Control; #p<0.05 vs. 2wk TAC; \$p<0.05 vs. 4wk TAC; +p<0.05 vs. 4wk TAC+2wk unTAC.

LILY SOON NEFF. Macrophages Promote Regression of Myocardial Fibrosis Following Alleviation of Pressure Overload. (Under the direction of AMY BRADSHAW).

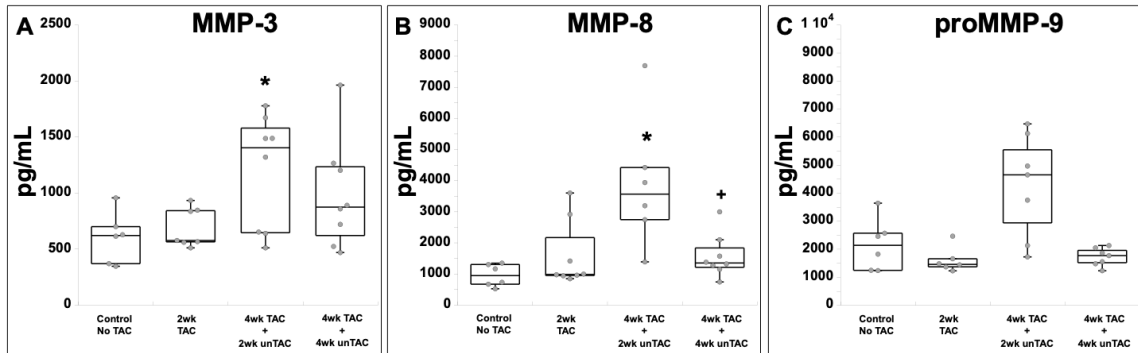


Figure 9: Characterization of Enzymes Implicated in Collagen Degradation in TAC and unTAC Myocardium. Myocardial levels of MMPs was assessed by addressable laser bead immunoassay (ALBIA) for control, 2wk TAC, 4wk TAC+2wk unTAC, and 4wk TAC+4wk unTAC. Differences in MMP3 (A), MMP8 (B), and proMMP9 (C) were observed in the unTAC myocardium compared to control and 2wk TAC. Animal sample sizes: control (n = 6), 2wk TAC (n = 8), 2wk unTAC (n = 8), 4wk unTAC (n = 8). *p<0.05 vs. Control; #p<0.05 vs. 2wk TAC; \$p<0.05 vs. 4wk TAC; +p<0.05 vs. 4wk TAC+2wk unTAC.

LILY SOON NEFF. Macrophages Promote Regression of Myocardial Fibrosis Following Alleviation of Pressure Overload. (Under the direction of AMY BRADSHAW).

2.5. Effects of TAC and unTAC on Myocardial Stiffness

At 2wk TAC, myocardial stiffness increased compared to control. A further increase was observed at 4wk TAC compared to both control and 2wk TAC. Following unloading of the myocardium, myocardial stiffness decreased at 2wk unTAC compared to 4wk TAC. A further decrease in myocardial stiffness was observed at 4wk unTAC compared to 2wk unTAC although it remained elevated to control. 6wk unTAC demonstrated a similar myocardial stiffness value compared to 4wk unTAC and remained elevated compared to control (Table 1).

2.6 Clinical Relevance

Removal of LVPO (unTAC) and normalization of LV hemodynamic load resulted in a significant but incomplete reduction of myocardial fibrosis (CVF). Removal of LVPO resulted in a complete regression of hypertrophy by CSA analysis but LV/BW remained above control levels (Table 1). The LV/BW and CVF from the TAC/unTAC murine model demonstrated a similar trend to the AS/SAVR patient paradigm demonstrating the relevance of this preclinical model to understand molecular and cellular mechanisms behind persistent fibrosis (Fig. 10).

LILY SOON NEFF. Macrophages Promote Regression of Myocardial Fibrosis Following Alleviation of Pressure Overload. (Under the direction of AMY BRADSHAW).

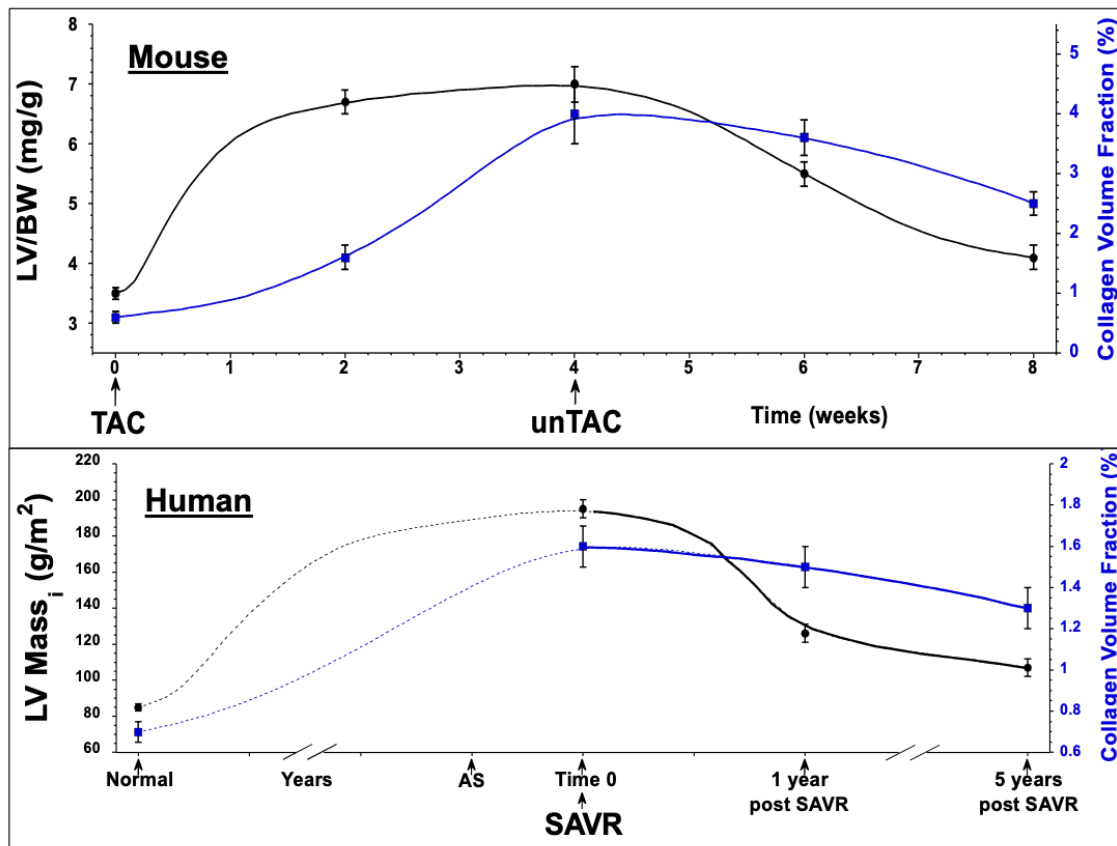


Figure 10: Comparison of TAC/unTAC Murine Model to AS/SAVR Paradigm. The TAC/unTAC model data of LV/BW (mg/g) in black and CVF in blue compared to AS/SAVR paradigm of LV mass (g/m²) in black and CVF in blue. Created by Michael Zile, M.D. and Catalin Baicu, Ph.D.

2.7 Limitations

Other models of myocardial interstitial fibrosis have been performed that utilize modulation of neurohormonal or metabolic factors.³⁴ Our current study utilized mechanical induction of LVPO through TAC to induce fibrosis. This is primarily because PO is initially and primarily sensed by resident cells. However, we appreciate that no animal model fully recapitulates the multi-factorial complexity of heart failure observed in patients and recognize this as a limitation of our current study.

LILY SOON NEFF. Macrophages Promote Regression of Myocardial Fibrosis Following Alleviation of Pressure Overload. (Under the direction of AMY BRADSHAW).

Chapter 3:

Macrophage Dependent Mechanisms of Collagen Turnover in the TAC/unTAC Preclinical Murine Model

3.1 Introduction

The role of macrophages in the progression of myocardial fibrosis is better studied than in regression of fibrosis. Previous studies of TAC induced LVPO have identified an association between myocardial macrophages and the development of myocardial interstitial fibrosis through deposition and post-translational regulation of collagen.^{29,30} In part, SPARC expression by monocyte-derived macrophages was shown to promote the deposition of interstitial fibrosis.^{28,29} Additionally, the cytokine/chemokine profile of TAC myocardium was associated with the recruitment of monocyte/macrophage populations and favored a profibrotic, alternatively activated (M2) macrophage phenotype.³⁰ Clodronate liposome mediated depletion of macrophages during TAC induced LVPO demonstrated reduced LV hypertrophy and significantly decreased fibrosis.³⁵ Pharmacologic or genetic depletion of macrophage subsets in preclinical models of LVPO demonstrated unique roles of these subsets in promoting or attenuating fibrosis and LV remodeling.^{26,31}

To date, macrophage-dependent mechanisms that regulate myocardial collagen turnover following alleviation of LVPO, have not been examined. Although macrophages are implicated in the development of myocardial interstitial fibrosis during the progression of LVPO, it is unknown what role macrophages play in regression of fibrosis following the alleviation of LVPO. We hypothesized that following alleviation of LVPO, macrophages would demonstrate a distinct, but transient, anti-fibrotic phenotype that initiates collagen degradation that is not sustained and thus contributes to the incomplete regression of LVPO-induced interstitial fibrosis.

3.2 Effects of TAC and unTAC on Myocardial Macrophage Number and

Morphology

To examine the role of macrophages, immunohistochemical analysis of IBA1⁺ macrophages in control no TAC, 2wk TAC, 4wk TAC, 4wk TAC+2wk unTAC, 4wk TAC+4wk unTAC, and 4wk TAC+6wk unTAC hearts was performed to assess the time course of changes in total myocardial macrophages in response to LVPO and alleviation of LVPO. The myocardial macrophage cell count was significantly increased at 2wk TAC and 4wk TAC compared to control (Fig. 11A-C, G). In response to alleviation of LVPO, the number of IBA1⁺ myocardial macrophages significantly increased at 2wk unTAC in comparison to control and TAC myocardium (Fig. 11A-D, G). Macrophage cell count remained elevated at 4wk unTAC and 6wk unTAC versus control (Fig. 11A, E-G).

The myocardial macrophage staining in 2wk unTAC myocardium appeared more robust than other time points. As such, quantification of IBA1⁺ percent area in stained sections and measurements of the IBA1⁺ area per cell was also evaluated and found to be significantly increased at 2wk unTAC compared to both control and TAC myocardium (Fig. 11A-D, H-I). Although the total area occupied by macrophages and macrophage size was reduced at 4wk TAC compared to 2wk TAC, it remained significantly increased compared to control (Fig. 11A-C, H-I). Peak myocardial macrophage area at 2wk unTAC was significantly decreased at 4- and 6wk unTAC but remained higher than that of control (Fig. 11A, D-F, H-I). At each time point during LVPO and following alleviation of LVPO, myocardial macrophage area remains significantly increased compared to control no TAC hearts.

LILY SOON NEFF. Macrophages Promote Regression of Myocardial Fibrosis Following Alleviation of Pressure Overload. (Under the direction of AMY BRADSHAW).

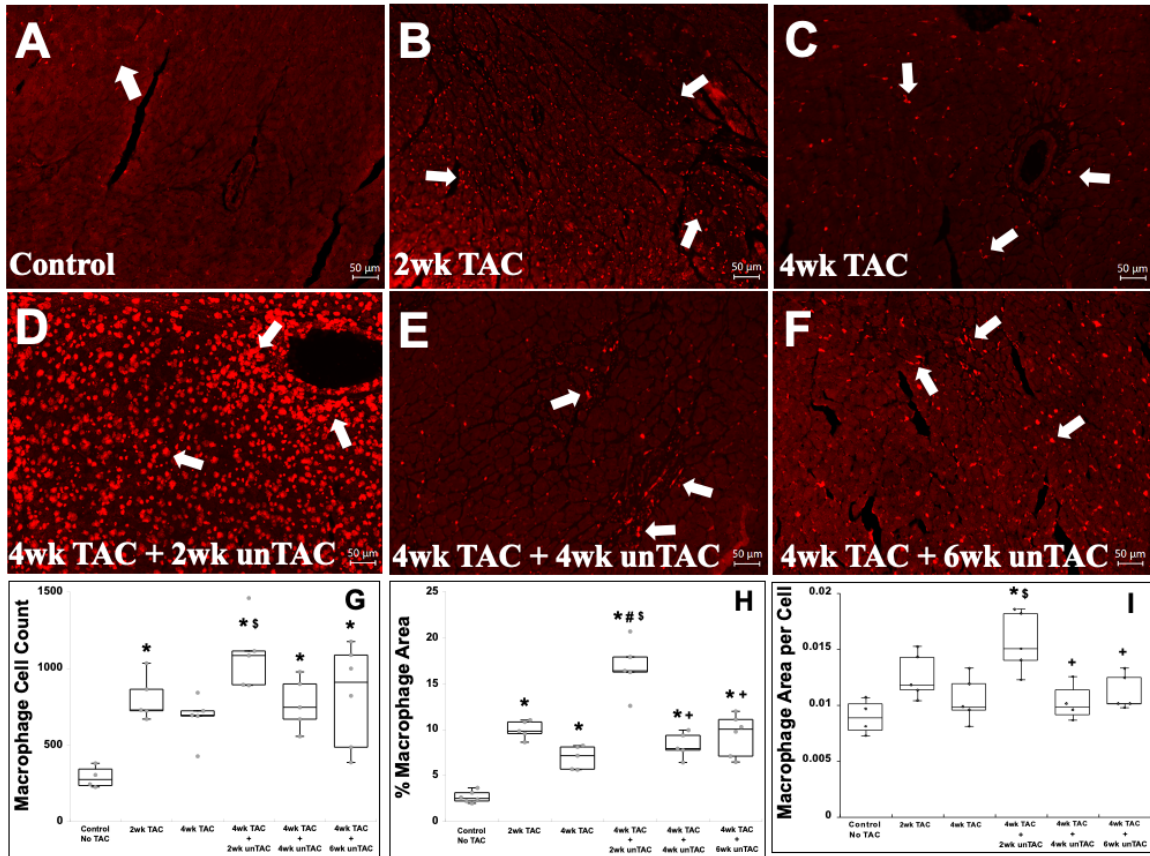


Figure 11: Characterization of IBA1+ Macrophage Number and Area in TAC and unTAC Myocardium. Macrophages stained with Ionized calcium binding adaptor molecule 1 (IBA1) in left ventricular myocardium with transverse aortic constriction (TAC) (B and C) and following unTAC (D-F) versus control (A). Quantification of IBA1+ macrophages (G). Quantification of IBA1+ macrophage area in regions of interest (%) (H). Quantification of IBA1+ macrophage area per cell (I). Panels A-F are represented with equivalent magnification (Scale bar = 50um). Animal sample sizes: control (n = 6), 2wk TAC (n = 5), 4wk TAC (n = 5), 2wk unTAC (n = 5), 4wk unTAC (n = 5), and 6wk unTAC (n = 6). *p<0.05 vs. Control; #p<0.05 vs. 2wk TAC; \$p<0.05 vs. 4wk TAC; +p<0.05 vs. 4wk TAC+2wk unTAC.

3.3 Effects of TAC and unTAC on the Myocardial Cytokine Profile

Differences in macrophage area per cell in TAC and unTAC suggested distinct macrophage populations might reside in TAC versus unTAC myocardium. To address whether these differences might be reflected in disparate cytokine production, the expression of 44 cytokines known to play a role in inflammatory cell recruitment and activation were examined in myocardial tissue from mice at the following time points: control, 2wk TAC, 4wk TAC+2wk unTAC, and 4wk TAC+4wk unTAC. Several factors were found to increase in response to both TAC and unTAC, whereas other factors were increased in unTAC only or were found to decrease in response to alleviation of LVPO. For example, proinflammatory cytokines interferon-gamma (IFN γ) and tumor necrosis factor alpha (TNF α) were not increased in 2wk TAC but were elevated in 2wk unTAC and then reached statistically significant increases at 4wk unTAC (Fig. 12A-B). Interleukin-1 beta (IL1 β) increased in both 2wk TAC and in unTAC with further increases detected in 4wk unTAC (Fig. 12C). Macrophage inflammatory protein 2 (MIP2), also known as CXCL-2, was significantly increased in the 2wk unTAC myocardium compared to both control and 2wk TAC and remained elevated at 4wk unTAC (Fig. 12D). Factors found to decrease with unbanding included vascular endothelial growth factor (VEGF) which was significantly decreased at 2wk and 4wk unTAC compared to both control and 2wk TAC (Fig. 12E) and interleukin-16 (IL-16) that was significantly increased in 2wk TAC myocardium compared to control but decreased in unTAC myocardium (Fig. 12F). Changes in cytokine production suggested that macrophage populations in TAC and unTAC myocardium exhibit distinct phenotypic differences indicative of functional properties.

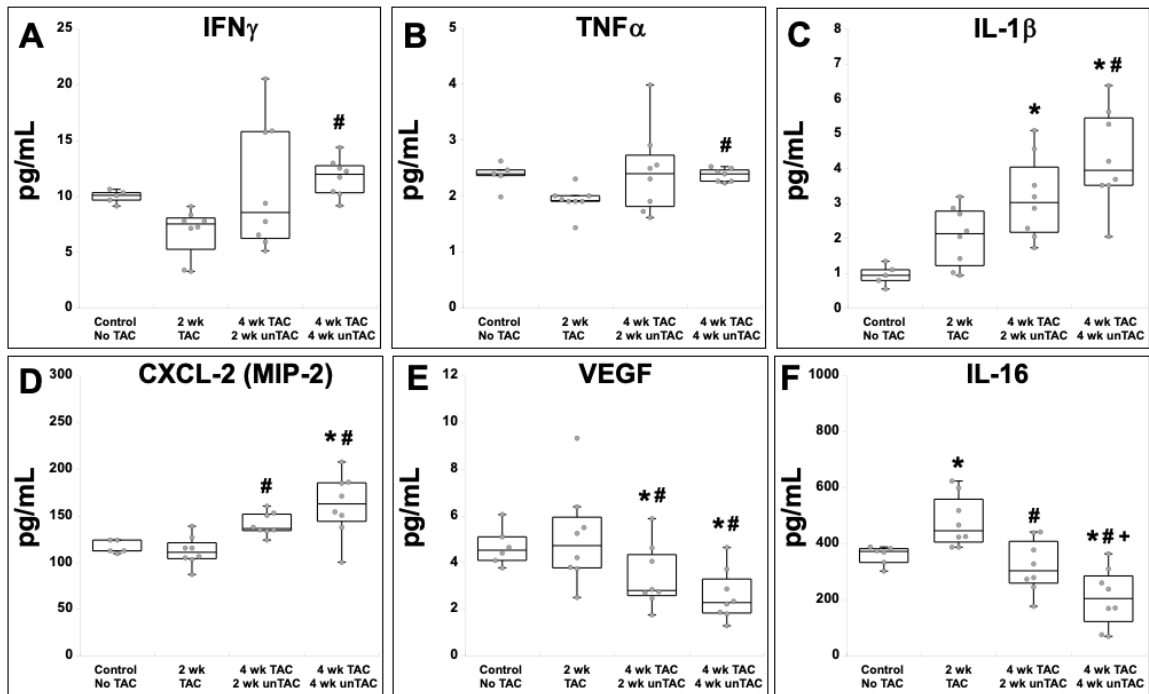


Figure 12: Differential Myocardial Cytokine Profile in TAC versus unTAC Myocardium. Levels of cytokines and chemokines in control, 2wk TAC, 4wk TAC+2wk unTAC, and 4wk TAC+4wk unTAC were assessed by ALBIA assay: Interferon gamma (IFN γ) (A), Tumor Necrosis Factor alpha (TNF α) (B), Interleukin 1 β (IL-1 β) (C), C-X-C Ligand 2 (CXCL-2) also known as Macrophage Inflammatory Protein-2 (D), Vascular Endothelial Growth Factor (E), and IL-16 (F). Animal sample sizes: control (n = 5), 2wk TAC (n = 8), 2wk unTAC (n = 8), and 4wk unTAC (n = 8). *p<0.05 vs. Control; #p<0.05 vs. 2wk TAC; §p<0.05 vs. 4wk TAC; +p<0.05 vs. 4wk TAC+2wk unTAC.

3.4 Macrophage Association with Collagen Turnover

Co-staining of IBA1⁺ macrophages with CHP was completed to determine macrophage association with collagenase activity observed in the TAC and unTAC myocardium (Fig. 13). Control and 2wk TAC myocardium demonstrated very little CHP reactivity (Fig. 13D-E). 2wk TAC myocardium demonstrated a significant increase in IBA1⁺ macrophages, but most of these cells were not associated with CHP (Fig. 13B, E; arrows: macrophages associated with CHP, arrowheads: macrophages not associated with CHP). Macrophage association with CHP in control and 2wk TAC myocardium seemed to be localized to vasculature and not the interstitium (Fig. 13D-E). At 4wk TAC, myocardium demonstrated an increase in CVF, CHP reactivity, and IBA1⁺ macrophages compared to control (Fig. 5C, 7C, 11C). Although it appeared that more IBA1⁺ macrophages were associated with sites of CHP reactivity in 4wk TAC myocardium compared to control and 2wk TAC, many were still not associated with sites of CHP reactivity (Fig. 13C, F). In 2wk unTAC myocardium, CHP reactivity and IBA1⁺ macrophages were significantly increased. Interestingly, the IBA1⁺ macrophages in 2wk unTAC myocardium appeared to be closely associated with sites of CHP reactivity compared to other time points (Fig. 13G, J). At 4wk unTAC and 6wk unTAC, CVF, CHP reactivity, and IBA1⁺ macrophages were decreased compared to 2wk unTAC (Fig. 5E-F, 7E-F, 11E-F). 4wk unTAC and 6wk unTAC myocardium demonstrated reduced association of IBA1⁺ macrophages with sites of CHP reactivity (Fig. 13K-L). This data suggests a temporal shift in macrophage phenotype and supports the observation of persistent fibrosis in unTAC.

LILY SOON NEFF. Macrophages Promote Regression of Myocardial Fibrosis Following Alleviation of Pressure Overload. (Under the direction of AMY BRADSHAW).

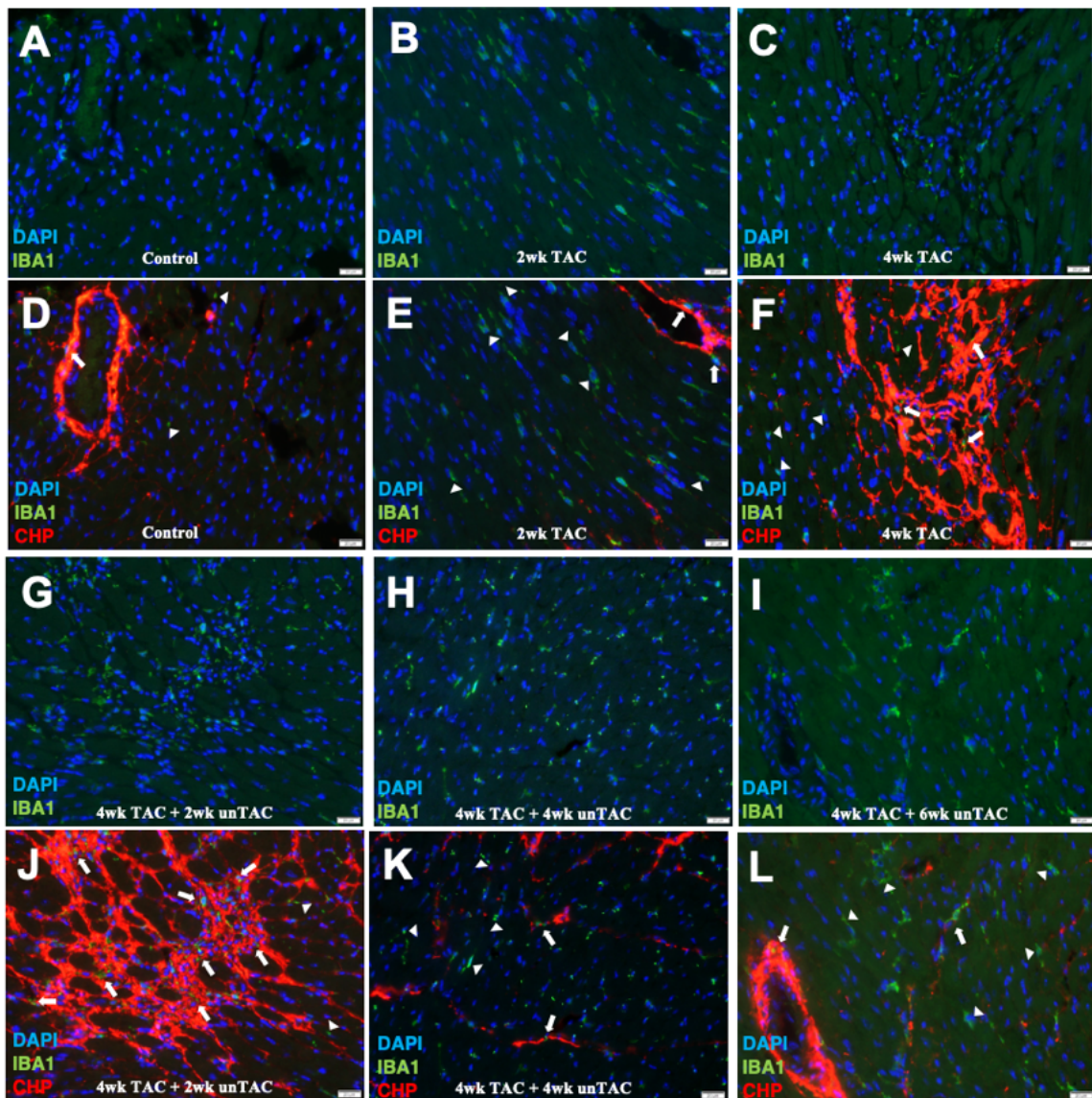


Figure 13: Macrophages Associate with Areas of Collagen Hybridizing Peptide in 2wk unTAC Myocardium. LV myocardial tissue stained with anti-IBA1 (green) and collagen hybridizing peptide (CHP), an indicator of collagenase cleaved collagen fibrils (red). A, D) Control tissue; B, E) 2wk TAC; C, F) 4wk TAC; G, J) 4wk TAC+2wk unTAC; H, K) 4wk TAC+4wk unTAC; I, L) 4wk TAC+6wk unTAC. Arrowheads: macrophages not associated with CHP. Arrows: macrophages associated with CHP activity. Panels A-L are represented with equivalent magnification (Scale bar = 20um).

3.5 Effects of TAC and unTAC on Myocardial Macrophage Phenotype

Differences in macrophage area and the cytokine milieu supported the notion that distinct macrophage phenotypes are present in the TAC versus unTAC myocardium. To address macrophage phenotype, FACS analysis using commonly published, cell surface markers was performed on control no TAC, 2wk TAC, 4wk TAC, 4wk TAC+2wk unTAC, 4wk TAC+4wk unTAC, and 4wk TAC+6wk unTAC left ventricles to assess the time course of changes in profibrotic and proinflammatory myocardial macrophage populations in response to LVPO and alleviation of LVPO. F4/80⁺ macrophages were significantly increased in 2wk TAC compared to control (Fig. 14A). Although not statistically significant, F4/80⁺ macrophages were elevated in 2wk unTAC compared to control (Fig. 14A). Cell sorting using a marker associated with a profibrotic, reparative macrophage phenotype, CD206, revealed a significant increase in F4/80⁺CD206⁺ macrophages in 2wk TAC and 4wk TAC compared to control hearts. Levels of CD206⁺ cells decreased from levels detected in TAC hearts in both 2wk, 4wk, and 6wk unTAC hearts (Fig. 14B). Furthermore, cells labeled with the profibrotic marker, CD163, were significantly increased in 2wk and 4wk TAC compared to control and were significantly decreased in 2wk-, 4wk-, and 6wk unTAC compared to 2wk TAC (Fig. 14C). Cells that sorted as Ly6C^{low}/F4/80^{high}, an expression profile also associated with profibrotic macrophages, demonstrated a similar pattern of expression to that of CD206⁺ and CD163⁺ macrophages (Fig. 14D). Interestingly, expression of the pro-inflammatory macrophage marker CD86⁺F4/80⁺ was also increased in 2wk TAC myocardium compared to control (Fig. 14E). Another indication of a pro-inflammatory macrophage phenotype, cells expressing Ly6C^{high}/F4/80^{low} profiles, were also significantly increased in 2wk TAC myocardium

LILY SOON NEFF. Macrophages Promote Regression of Myocardial Fibrosis Following Alleviation of Pressure Overload. (Under the direction of AMY BRADSHAW).

compared to control (Fig. 14F). Comparable to F4/80⁺CD86⁺ cells, Ly6C^{high}/F4/80^{low} cells were reduced in unTAC myocardium compared to 2wk TAC.

LILY SOON NEFF. Macrophages Promote Regression of Myocardial Fibrosis Following Alleviation of Pressure Overload. (Under the direction of AMY BRADSHAW).

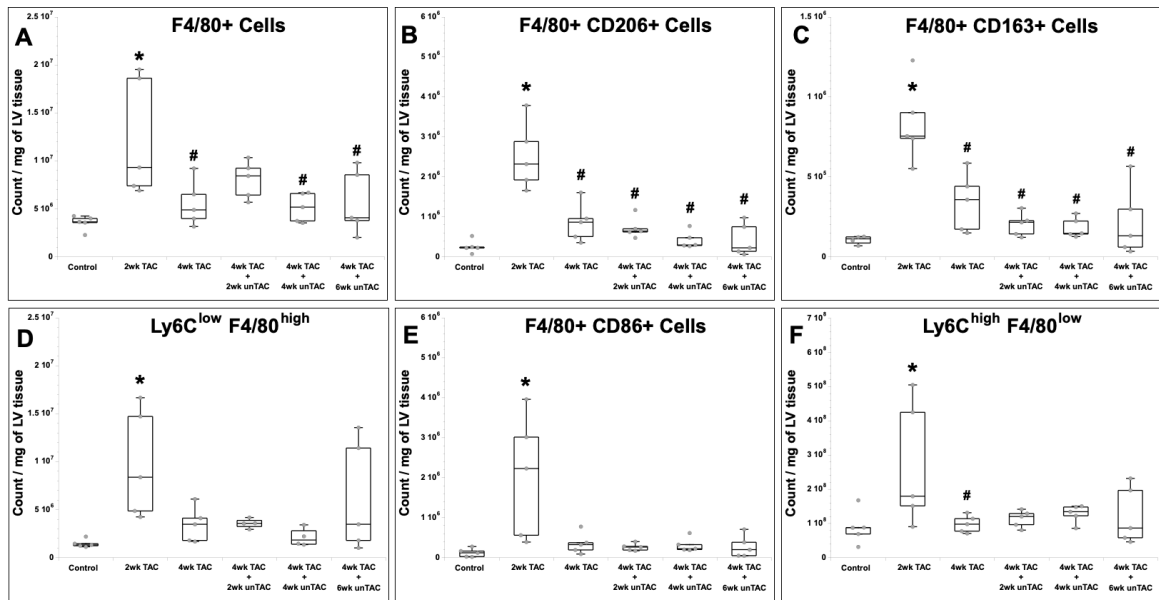


Figure 14: Macrophage Phenotype in TAC versus unTAC Myocardium. Fluorescence Activated Cell Sorting (FACS) quantitative assessment of total number of myocardial F4/80⁺ macrophages (A), Cell Differentiation (CD) 206-expressing F4/80⁺ macrophages (B), CD163-expressing F4/80⁺ macrophages (C), and Ly6C^{low}F4/80^{high}-expressing macrophages (D), CD86-expressing F4/80⁺ macrophages (E), and Ly6C^{high}F4/80^{low}-expressing macrophages (F) isolated from hearts with TAC and unTAC. Animal sample sizes: control (n = 5), 2wk TAC (n = 5), 4wk TAC (n = 4), 2wk unTAC (n = 5), 4wk unTAC (n = 5), and 6wk unTAC (n = 5). *p<0.05 vs. Control; #p<0.05 vs. 2wk TAC; \$p<0.05 vs. 4wk TAC; +p<0.05 vs. 4wk TAC+2wk unTAC.

3.6 Defining an Accurate Macrophage Phenotype for the Antifibrotic Subset

Observed in 2wk unTAC

Interestingly, all of the previously used cell surface macrophage markers used in flow cytometry were not significantly increased in 2wk unTAC myocardium compared to TAC myocardium. To try to understand this elusive, antifibrotic macrophage subset observed in 2wk unTAC myocardium identified by IBA1+ reactivity and a unique cytokine milieu, mRNA levels of enzymes implicated in collagen turnover were assessed by rt-PCR in F4/80+ macrophages isolated from control no TAC, 2wk TAC, 4wk TAC, 4wk TAC+2wk unTAC, 4wk TAC+4wk unTAC, and 4wk TAC+6wk unTAC left ventricles. F4/80+ macrophages demonstrated a 9-fold increase in *Coll1a1* mRNA levels at 2wk TAC compared to those isolated from control hearts. *Coll1a1* mRNA levels were similar in 4wk TAC and 4wk TAC+ 2wk unTAC compared to control. F4/80+ macrophages showed a shift at 4wk TAC+6wk unTAC with an increased trend in *Coll1a1* mRNA levels (Fig. 15A). F4/80+ macrophages demonstrated a 2.3-fold increase in *Sparc* mRNA levels at 2wk TAC compared to control (Fig. 15B). *Sparc* mRNA production returned to control levels in F4/80+ macrophages isolated from unTAC myocardium (Fig. 15B). *Pstn* demonstrated a 7-fold increase in mRNA levels in 2wk TAC F4/80+ macrophages compared to control (Fig. 15C). F4/80+ macrophages demonstrated a significant decrease in mRNA levels of *Pstn* at 4wk TAC, 4wk TAC+2wk unTAC, and 4wk TAC+4wk unTAC compared to 2wk TAC (Fig. 15C). However, 4wk TAC+6wk unTAC F4/80+ macrophages demonstrated an increase in *Pstn* mRNA levels compared to control (Fig. 15C). Although not statistically significant, *TGFBI* mRNA levels demonstrated an increased trend in 4wk TAC+4wk unTAC compared to control (Fig. 15D). In addition, F4/80+ macrophages in 2wk TAC

LILY SOON NEFF. Macrophages Promote Regression of Myocardial Fibrosis Following Alleviation of Pressure Overload. (Under the direction of AMY BRADSHAW).

myocardium demonstrated an increased trend in *Lox12* mRNA levels compared to control that did not reach significance (Fig. 15E). F4/80+ macrophages did not demonstrate a significant increase in *Lox* and *Timp1* mRNA levels in either TAC or unTAC myocardium compared to control (Fig. 15F-G). Also not significant, F4/80+ macrophages demonstrated a modest increase in *Mmp14* mRNA levels at 2wk TAC compared to control (Fig. 15H). *Mmp14* mRNA levels were similar between 4wk TAC and control (Fig. 15H). After unloading the myocardium, F4/80+ macrophages appeared to demonstrate a modest increase in *Mmp14* mRNA levels compared to control (Fig. 15H). In conclusion, F4/80+ macrophages demonstrate increased expression of profibrotic genes at 2wk TAC which is not sustained during 4wk TAC. 4wk TAC+ 2wk unTAC F4/80+ macrophages did not display a profibrotic phenotype by gene expression supporting the notion that these macrophages are antifibrotic in nature and do not contribute to collagen deposition at this time point.

LILY SOON NEFF. Macrophages Promote Regression of Myocardial Fibrosis Following Alleviation of Pressure Overload. (Under the direction of AMY BRADSHAW).

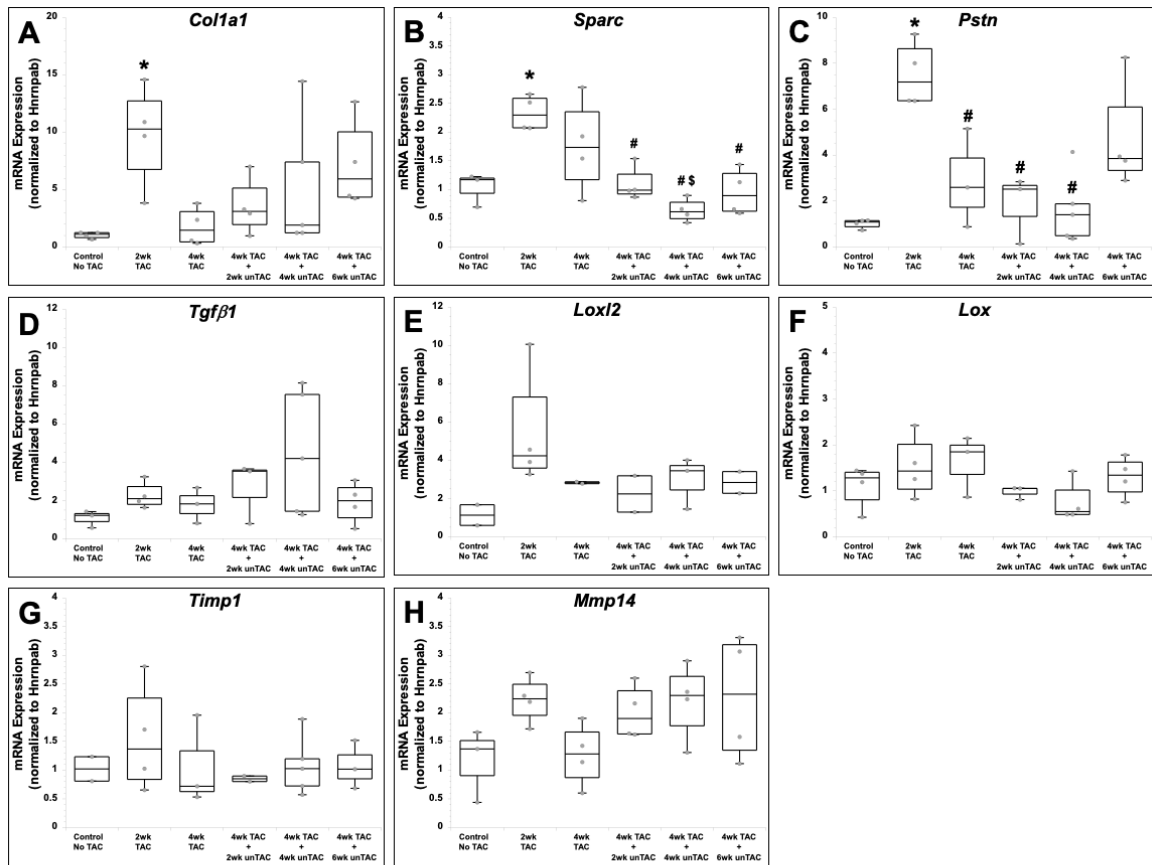


Figure 15: Differential mRNA Profiles in F4/80+ Macrophages Isolated from TAC and unTAC Myocardium. Levels of profibrotic and antifibrotic genes in control, 2wk TAC, 4wk TAC, 4wk TAC+2wk unTAC, 4wk TAC+4wk unTAC, and 4wk TAC+6wk unTAC were assessed by real-time quantitative PCR: *Col1a1* (A), *Sparc* (B), *Pstn* (C), *Tgfb1* (D), *Loxl2* (E), *Lox* (F), *Timp1* (G), *Mmp14* (H). Animal sample sizes: control (n = 2-4), 2wk TAC (n = 4), 4wk TAC (n = 2-4), 2wk unTAC (n = 2-4), 4wk unTAC (n = 3-5), and 6wk unTAC (n = 2-4). *p<0.05 vs. Control; #p<0.05 vs. 2wk TAC; \$p<0.05 vs. 4wk TAC; +p<0.05 vs. 4wk TAC+2wk unTAC.

The number of F4/80+ macrophages isolated by beads were quantified by hemocytometer and demonstrated that the lowest number of F4/80+ macrophages were isolated from 2wk unTAC myocardium in comparison to all other time points. The largest number of F4/80+ macrophages was observed at 2wk TAC in support of the flow cytometry data (Fig. 14A). *Aif1* encodes IBA1 protein used for immunohistochemistry analysis of total macrophages. F4/80+ macrophages appeared to demonstrate an increased trend in *Aif1* mRNA levels at 4wk TAC+2wk unTAC compared to 2wk TAC (Fig. 16A). *Mertk* is a cell surface receptor that mediates phagocytosis. F4/80+ macrophages at 2wk unTAC demonstrated an increased trend in *Mertk* mRNA levels compared to 2wk TAC (Fig. 16B). F4/80+ macrophages at 4wk unTAC demonstrated a significant increase in *Mertk* mRNA levels compared to 2wk TAC (Fig. 16B). *Mrc1* encodes the CD206 cell surface receptor used in our previous flow cytometry studies. F4/80+ macrophages demonstrated an increased trend in *Mrc1* mRNA levels at 4wk TAC, 4wk unTAC, and 6wk unTAC compared to 2wk TAC and 2wk unTAC, although not statistically significant (Fig. 16C). A similar trend to that of *Mrc1* was observed for *Cd163* mRNA levels (Fig. 16D).

LILY SOON NEFF. Macrophages Promote Regression of Myocardial Fibrosis Following Alleviation of Pressure Overload. (Under the direction of AMY BRADSHAW).

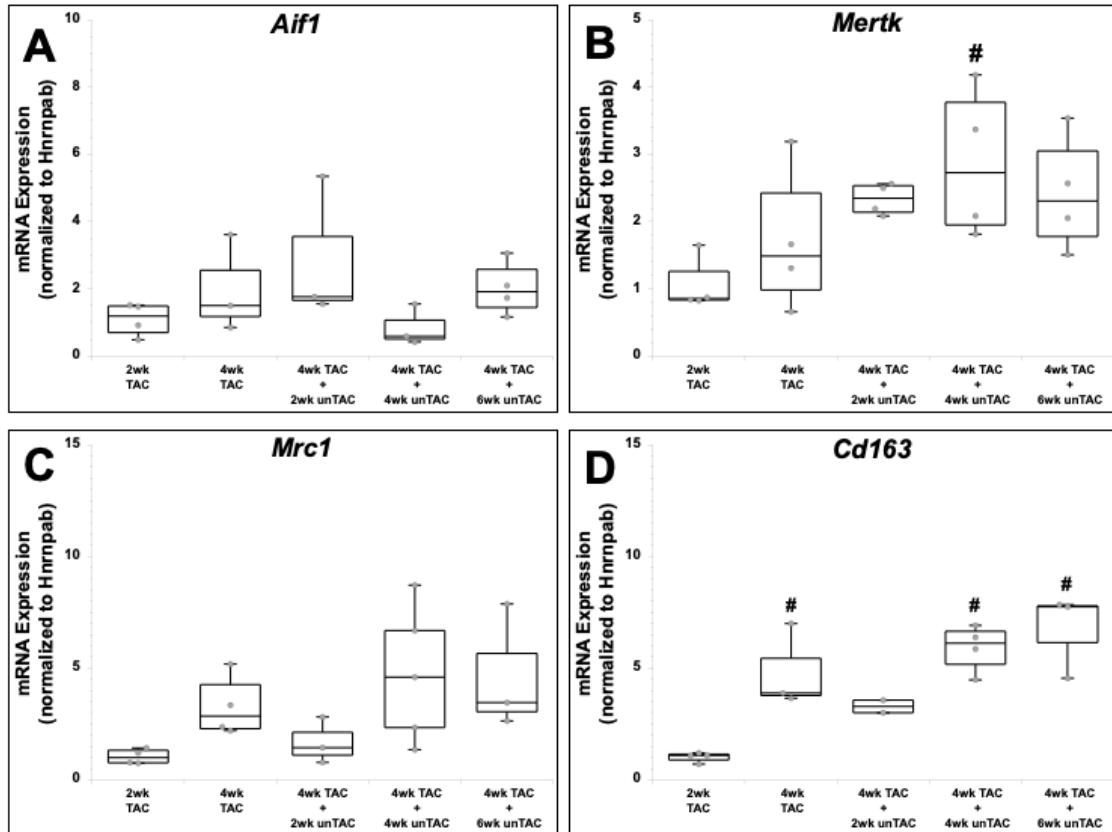


Figure 16: Differential mRNA Profiles in F4/80+ Macrophages Isolated from TAC and unTAC Myocardium. Gene levels of profibrotic and antifibrotic macrophage markers in control, 2wk TAC, 4wk TAC, 4wk TAC+2wk unTAC, 4wk TAC+4wk unTAC, and 4wk TAC+6wk unTAC were assessed by real-time quantitative PCR: *Aif1* (A), *Mertk* (B), *Mrc1* (C), *Cd163* (D). Animal sample sizes: 2wk TAC (n = 4), 4wk TAC (n = 3-4), 2wk unTAC (n = 2-4), 4wk unTAC (n = 3-5), and 6wk unTAC (n = 3-4). *p<0.05 vs. Control; #p<0.05 vs. 2wk TAC; \$p<0.05 vs. 4wk TAC; +p<0.05 vs. 4wk TAC+2wk unTAC.

3.7 Effects of Macrophage Depletion in unTAC Myocardium

To determine if macrophages play a casual role in the ECM remodeling process observed at 2wk unTAC, mice received one intraperitoneal injection of clodronate liposomes or PBS liposomes at the time of unTAC surgery and were harvested following 2wks of unTAC. No significant differences in myocardial function, assessed by echocardiography, between either clodronate liposome or PBS liposome injected mice compared to untreated 2wk unTAC mice were noted indicating liposome treatment had no adverse effects on unTAC mice (Table 2). The myocardium of mice injected with clodronate liposomes demonstrated a significant decrease in IBA1⁺ macrophages compared to PBS liposome myocardium (Fig. 17A-C). Although CVF was similar between clodronate and PBS liposome groups (Fig. 17D-F), those injected with clodronate liposomes demonstrated a significant reduction in CHP reactivity versus those receiving PBS liposomes (Fig. 17G-I).

LILY SOON NEFF. Macrophages Promote Regression of Myocardial Fibrosis Following Alleviation of Pressure Overload. (Under the direction of AMY BRADSHAW).

Table 2. Echocardiographic Measurements of C57Bl/6 Mice Treated with PBS Liposome or Clodronate Liposome and Harvested at 4wk TAC+2wk unTAC. LV mass/Body Weight (mg/g), LV mass/Tibia Length (mg/mm), LV Ejection Fraction (EF), LV End diastolic volume (mL) (EDV), Peak Aortic Velocity (m/sec), and Myocardial Stiffness parameters were measured and compared to no liposome control no TAC and no liposome 4wk TAC+2wk unTAC. *p<0.05 vs. Control.

	Control No TAC	4wk TAC + 2wk unTAC		
	No liposome	No liposome	PBS liposome	Clodronate liposome
LVmass/BW (mg/g)	3.5±0.3	4.6±0.3*	4.8±0.8*	4.4±0.3*
LVmass/TL (mg/mm)	4.3±0.8	6.0±1.0*	6.5±1.1*	5.8±1.3*
LV EF (%)	55±5	52±7	49±5	55±5
LV EDV (mL)	55±9	64±13	69±16	69±15
Peak Aortic Velocity (m/sec)	0.64 ± 0.07	0.64 ± 0.31	0.86 ± 0.15	0.85 ± 0.29
Myocardial Stiffness	0.030±0.005	0.061±0.054*	0.047±0.023 *	0.048±0.018 *

Data = Mean ± St.Dev

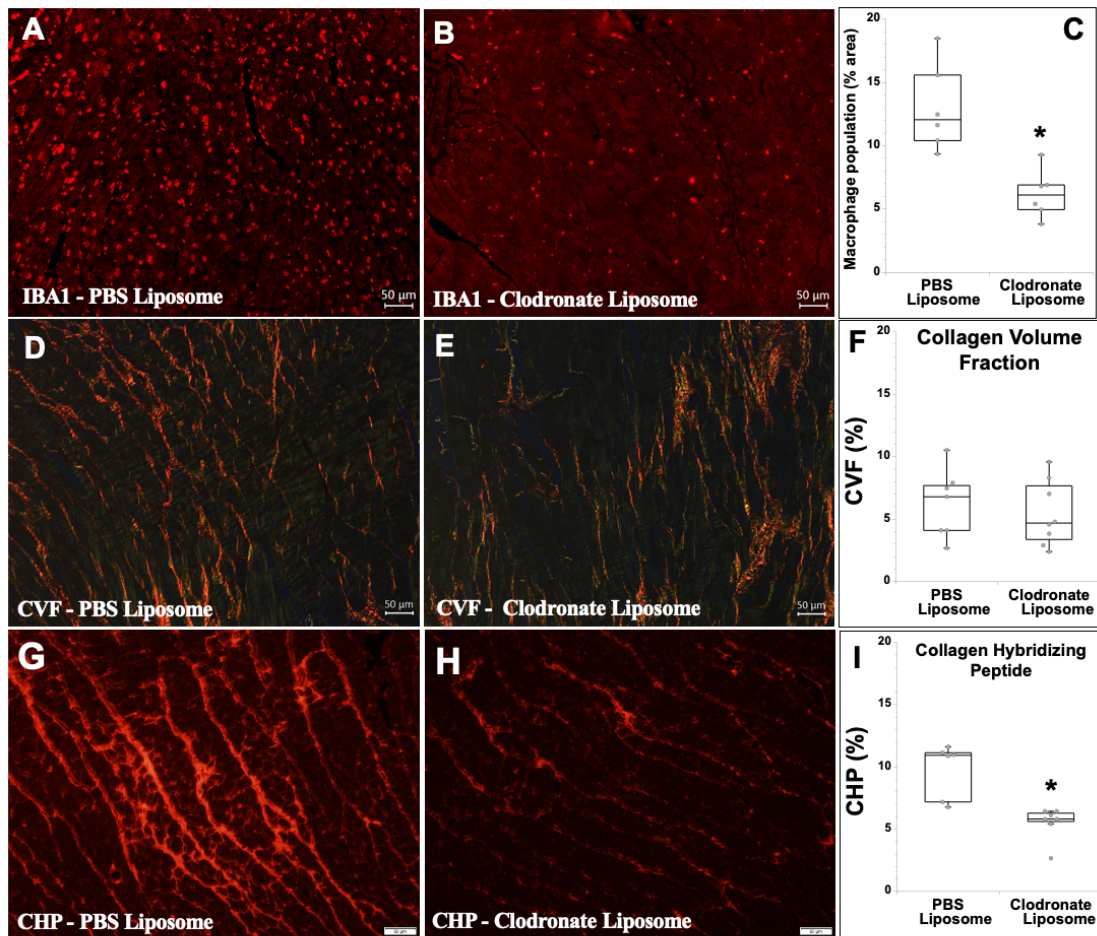


Figure 17: Decreased Macrophage Area and CHP Reactivity in unTAC Myocardium Treated with Clodronate Liposomes. Representative anti-IBA1-stained region of interest of 4wk TAC+2wk unTAC LV myocardium from mice injected with PBS liposomes (A) or clodronate liposomes (B) at the time of unTAC surgery. Quantification of total macrophage area (C). No significant changes in collagen volume fraction (CVF) were observed in unTAC myocardium treated with either clodronate (E) or PBS (D) liposomes. Quantification of CVF is shown in (F). Reduced CHP intensity in clodronate (H) versus PBS (G) liposome injected myocardium. Quantification of CHP staining is shown in (I). Animal sample sizes: PBS liposome 2wk unTAC (n = 7) and clodronate liposomes 2wk unTAC (n = 8). *p<0.05 vs. PBS liposome.

Total protein extracted from the LVs of PBS and clodronate liposome treated mice was assessed for levels of proteins associated with collagen turnover. Protein levels of Cathepsin K, a papain-like cysteine protease capable of collagenolytic activity, was significantly reduced in the clodronate liposome myocardium compared to PBS liposome myocardium (Fig. 18A). Similarly, protein levels of pro-matrix metalloproteinase 2 (proMMP2), a gelatinase, was also significantly decreased in clodronate liposome myocardium versus PBS liposome myocardium (Fig. 18B). In contrast, matrix metalloproteinase 9 (MMP9) exhibited similar protein levels in clodronate liposome compared to PBS liposome myocardium (Fig. 18C). Likewise, levels of TIMP1, an inhibitor of MMP family members, were unchanged in the clodronate liposome myocardium compared to PBS liposome myocardium (Fig. 18D).

LILY SOON NEFF. Macrophages Promote Regression of Myocardial Fibrosis Following Alleviation of Pressure Overload. (Under the direction of AMY BRADSHAW).

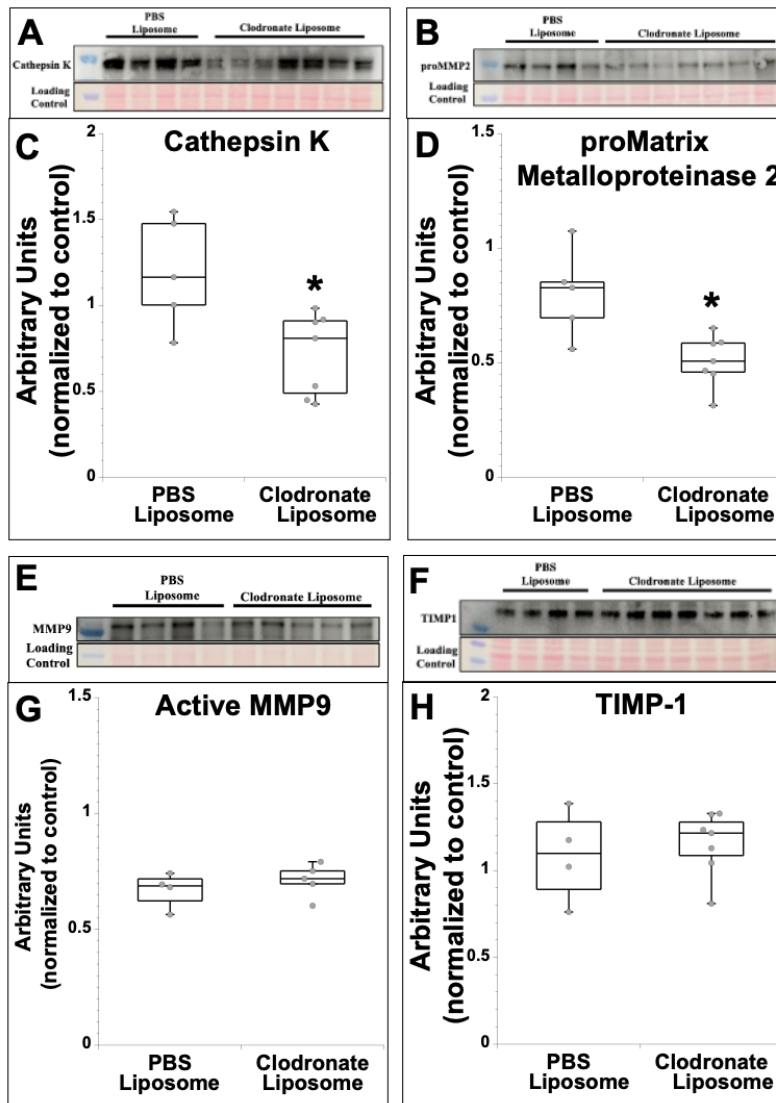


Figure 18: Reduction in Select ECM Degradatory Enzymes in Response to Clodronate Liposome Injection. Levels of Cathepsin K (A), pro-matrix metalloproteinase 2 (proMMP2) (B), MMP9 (E), and TIMP1 (F) were assessed by immunoblot analysis. Semi-quantification of Cathepsin K (C), proMMP2 (D), MMP9 (G), TIMP1 (H) protein abundance by immunoblot analysis normalized to levels of control protein visualized by Ponceau S staining of membranes. Animal sample sizes: PBS liposome 2wk unTAC (n = 4) and clodronate liposomes 2wk unTAC (n = 6). *p<0.05 vs. PBS liposome.

LILY SOON NEFF. Macrophages Promote Regression of Myocardial Fibrosis Following Alleviation of Pressure Overload. (Under the direction of AMY BRADSHAW).

In addition, vascular cell adhesion molecule 1 (VCAM1) immunoreactivity, an indicator of activated endothelium, was significantly decreased in myocardium of mice treated with clodronate liposomes versus those injected with PBS liposomes (Fig. 19A-C). Plasma levels of IL-5 were significantly decreased in clodronate liposome mice versus PBS liposome mice (Fig. 19D). The plasma and tissue cytokine profile of clodronate liposome mice did not demonstrate any further alterations of statistical significance compared to PBS liposome mice suggesting that an increase in myocardial inflammatory mediators to compensate for depletion of macrophages did not occur.

LILY SOON NEFF. Macrophages Promote Regression of Myocardial Fibrosis Following Alleviation of Pressure Overload. (Under the direction of AMY BRADSHAW).

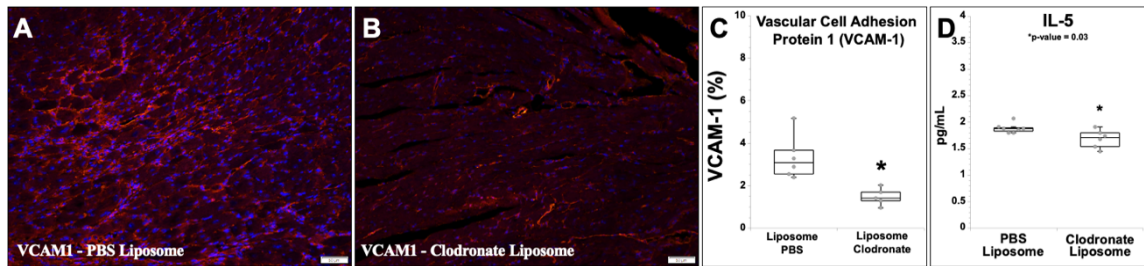


Figure 19: Differential VCAM and Cytokine Expression in Liposome Depleted

Myocardium. Representation image of anti-Vascular Cell Adhesion Molecule (VCAM)

1 stained myocardium in PBS (A) versus clodronate liposome (B) injected mice.

Quantification of VCAM1 expression (C). Level of IL-5 expression assessed by ALBIA

assay (D). Animal sample sizes: PBS liposome 2wk unTAC (n = 6) and clodronate

liposomes 2wk unTAC (n = 5). *p<0.05 vs. PBS liposome.

3.8 Discussion

Studies that support the outcomes reported here utilize Ly6C, a cell surface glycoprotein, as a marker to differentiate monocyte/macrophage phenotype as Ly6C^{high} pro-inflammatory monocytes and Ly6C^{low}F4/80^{high} profibrotic macrophages.³⁶ Weisheit et. al. also demonstrated that Ly6C^{low} macrophages are increased in response to TAC consistent with the presence of pro-fibrotic macrophage populations with LVPO.³⁷ Consistent with a function in collagen deposition, Ramachandran et. al. demonstrated that Ly6C^{low} macrophages exhibited significantly increased mRNA levels of genes encoding the collagen cross-linking enzymes, *LOX* (Lysyl oxidase) and *LOXL3* (Lysyl oxidase like 3), as well as *TIMP2* (Tissue Inhibitor of Matrix Metalloproteinase 2) an inhibitor of collagen degrading activity.³⁶ We too observed a significant increase in Ly6C^{low}F4/80^{high} macrophages in TAC myocardium, that we show decrease in unTAC hearts, consistent with enhanced collagen crosslinking and MMP inhibition in TAC that declines in unTAC.

As stated above, single cell sequencing analysis also supported an increase in pro-inflammatory macrophages in TAC myocardium. Weishert et al. also demonstrated an increase in Ly6C^{high} monocytes 3- and 6-days following TAC but not 21 days after TAC.³⁷ In our studies, we found that Ly6C^{high}F4/80^{low} monocyte derived macrophages were significantly increased at both 2wk TAC and 4wk TAC versus control, no TAC hearts similar to the single cell sequencing data. The discrepancy between our data and that of Weishert *et al.* at later time points, might be due to differences in several factors including severity of LVPO (e.g. different gauge of needle used to induce LVPO), conditions used for cell isolation and flow cytometry, or gating strategies used in the analysis. Nonetheless, that Ly6C^{high}F4/80^{low} monocytes derived macrophages and CD86⁺ macrophages, two

LILY SOON NEFF. Macrophages Promote Regression of Myocardial Fibrosis Following Alleviation of Pressure Overload. (Under the direction of AMY BRADSHAW).

markers associated with a pro-inflammatory phenotype, were not found to be increased in unTAC hearts was surprising.^{3,26,38} One possible explanation is that the macrophage population in unTAC myocardium represents a unique macrophage population that does not express traditional “M1” markers. Certainly, one characteristic of macrophages in unTAC myocardium is robust expression of IBA1, a protein implicated in phagocytic activity, a function consistent with abundant turnover of ECM.

Although the proinflammatory markers CD86 and Ly6C^{high} were not significantly increased in unTAC myocardium compared to TAC myocardium, the increased proinflammatory cytokine expression of IL-1 β , TNF α , and IFN γ in 2wk unTAC myocardium supported a pro-inflammatory milieu that is predicted to favor an antifibrotic macrophage phenotype.³⁰ Furthermore, the profibrotic macrophage markers used in these studies demonstrated a significant decrease in the unTAC myocardium compared to 2wk TAC. For example, VEGF and the TGF β -inducing cytokine IL-16 are associated with profibrotic, M2 macrophage polarization and were significantly reduced in unTAC myocardium compared to TAC myocardium.³⁰ Altogether, these data support fundamental differences in the myocardial milieu that is predicted to influence macrophage phenotype in unTAC versus TAC myocardium and studies to better characterize functional markers of macrophages in unTAC hearts are in progress. Depletion of IL-6 levels results in decreased recruitment of monocyte-derived macrophages. 4wk TAC+2wk unTAC demonstrated increased plasma levels of IL-6 supporting the notion that the robust increase in IBA1+ macrophages observed were monocyte-derived and recruited from the bone marrow. Furthermore, IFN γ induces hematopoiesis which supports the hypothesis that the recruited, monocyte-derived macrophages play an antifibrotic role at 2wk unTAC.¹¹

LILY SOON NEFF. Macrophages Promote Regression of Myocardial Fibrosis Following Alleviation of Pressure Overload. (Under the direction of AMY BRADSHAW).

VEGF is associated with angiogenesis, endothelial activation, and permeability.³⁰ IBA1⁺ macrophages remained significantly increased at 4wk unTAC and 6wk unTAC although reduction in VEGF levels was observed. Ly6C^{high}F4/80^{low} monocytes in the unTAC myocardium returned to levels similar to control. Together, these observations suggest that persistent recruitment of monocyte-derived macrophages are not largely responsible for sustained increases in macrophage populations observed in 4wk and 6wk unTAC hearts. It is unknown the role of recruited versus resident macrophages in persistent levels of macrophages observed in the 4wk and 6wk unTAC hearts. With the decrease in Ly6C-recruited monocytes and VEGF cytokine expression in the unTAC myocardium compared to the TAC myocardium, it is hypothesized that resident macrophages are largely responsible for the macrophage population in the myocardium at 4wk and 6wk unTAC. However, this sustained elevation in macrophages does not lead to complete regression of fibrosis suggesting cellular mechanisms that maintain elevated levels of myocardial collagen persist in unTAC myocardium over time.

Interestingly, with the depletion of macrophages by clodronate liposome, a robust difference in cytokine milieu was not observed at 4wk TAC+2wk unTAC compared to PBS liposome. The only significant difference observed was a significant decrease in IL-5 plasma levels in clodronate liposome mice compared to PBS liposome mice. IL-5 plays a key role in atherosclerosis plaque development, specifically, reduced levels of IL-5 lead to increased plaque size.³⁹ However, it is unknown if the decrease in IL-5 observed in clodronate liposome mice plays a detrimental or beneficial role. Along with this, cytokines should be examined 4 to 7 days following liposome injection to determine a more immediate response and change in cytokines in response to reduced macrophages.

LILY SOON NEFF. Macrophages Promote Regression of Myocardial Fibrosis Following Alleviation of Pressure Overload. (Under the direction of AMY BRADSHAW).

Analyzing the cytokine profile 2 weeks following liposome injection may be too long to determine critical differences.

3.9 Limitations

Preclinical models of myocardial interstitial fibrosis that utilize modulation of neurohormonal or metabolic factors are available. Our preclinical model utilizes a mechanical induction of LVPO, by TAC, to induce myocardial interstitial fibrosis. We utilize this preclinical model because it does not activate confounding processes which could alter, for example, immune cell activation, proliferation, and activity. Nonetheless, we appreciate that no preclinical model fully recapitulates the multi-factorial complexity of clinical heart failure.

Two macrophage markers, Ly6C^{high} and CD86, were used to try to identify antifibrotic macrophages in the unTAC myocardium. Interestingly, both markers were observed to be increased in 2wk TAC but not in the 2wk unTAC myocardium. Previous literature has demonstrated the use of Ly6C^{high} and CD86 to characterize pro-inflammatory (M1) macrophages in response to myocardial infarction. Taken together, based off macrophage phenotype markers and the cytokine milieu, the 2wk TAC myocardium is both profibrotic and pro-inflammatory. Instead of these commonly published pro-inflammatory markers, other markers could be utilized that are known to play a functional role in phagocytosis and/or collagen proteolysis to accurately characterize this unique macrophage population observed in 2wk unTAC.

3.10 Clinical Relevance

Both in response to PO and after alleviation of PO, macrophage populations expand in the myocardium. In both cases, these increases in macrophage populations are not sustained. Despite fewer macrophages at 4wk TAC, fibrosis continues to accumulate in the myocardium. Fewer macrophages are observed at 4wk unTAC from the initial peak observed at 2wk unTAC. Macrophages at 2wk unTAC were associated with collagen degradation. We hypothesize that the persistent fibrosis observed at 4wk and 6wk unTAC, is at least in part due to the decrease in macrophages. One limitation to studying persistent fibrosis post-SAVR is the lack of biopsies available from patients undergoing this procedure and years following the procedure. Although there are limitations to our murine model of LVPO and alleviation of LVPO, it is useful to clarify mechanistic roles of specific cell types in collagen turnover and persistent fibrosis. Although macrophages have been implicated in contributing to fibrosis in animal models of LVPO and in HFpEF patients, our data demonstrates a potential benefit of macrophages in contributing to collagen degradation following normalization of hemodynamic load.^{27,40} Future strategies to augment specific phenotypic macrophage activities might provide new therapeutic strategies to further regress fibrosis and alleviate symptoms of Heart Failure.

3.11 Conclusion

Our novel findings highlight the dynamic changes in myocardial macrophage populations that occur during LVPO and following alleviation of LVPO. Our findings indicate the following: 1) macrophage cell count is significantly increased in both TAC and unTAC hearts, peaking in both cases at 2wk TAC and 2wk unTAC, respectively. In

LILY SOON NEFF. Macrophages Promote Regression of Myocardial Fibrosis Following Alleviation of Pressure Overload. (Under the direction of AMY BRADSHAW).

both cases, the number of macrophages decrease with time, e.g. at 4wk TAC and 4wk unTAC, although elevated levels persisted over control, 2) evidence that macrophages in 2wk unTAC myocardium are distinct from those in 2wk TAC myocardium are: a pro-inflammatory cytokine profile in 2wk unTAC that is distinct from the profibrotic cytokine profile in 2wk TAC, a significant decrease in profibrotic macrophage markers in unTAC myocardium, a significant decrease in profibrotic gene expression in 2wk unTAC F4/80+ macrophages, a significant increase in macrophage area in unTAC hearts, and an association of macrophages with CHP reactivity in 2wk unTAC, 3) depletion of macrophages following alleviation of LVPO resulted in a significant reduction in CHP and protein production of enzymes implicated in collagen degradation. Overall, these findings support the hypothesis that macrophages favor a profibrotic phenotype in TAC myocardium but an anti-fibrotic phenotype in 2wk unTAC. Furthermore, the decreased number of macrophages observed at 4wk unTAC and 6wk unTAC compared to 2wk unTAC might be one mechanism contributing to the loss of sustained collagen degradation that is predicted to exacerbate the observed persistent fibrosis.

The functional role of macrophages in contributing to fibrosis in PO has been addressed in several studies. For example, in an angiotensin II infusion model of PO, clodronate mediated depletion of infiltrating monocytes led to reduced levels of myocardial fibrosis as did blocking CCR2+ cell recruitment after 4 weeks of PO in a TAC model.^{26,41} However, very little is known regarding the functional role of macrophages in regression of myocardial interstitial fibrosis. We have demonstrated that macrophage depletion at the time of unTAC surgery resulted in significantly decreased CHP reactivity in 2wk unTAC versus control emphasizing an important function of macrophages in initiation of collagen

LILY SOON NEFF. Macrophages Promote Regression of Myocardial Fibrosis Following Alleviation of Pressure Overload. (Under the direction of AMY BRADSHAW).

degradation. In Chapter 2, we demonstrated significantly increased CHP reactivity at 2wk unTAC with no changes detected in CVF until 4wks of unTAC.⁴² In addition, levels of Cathepsin K and proMMP2 were also decreased in macrophage depleted unTAC myocardium suggesting overall reductions in collagen degradation activity. Although differences in CVF were not detected in clodronate-treated 2wk unTAC hearts, we also did not detect differences in CVF at this time point in untreated mice. We hypothesize that decreases in CVF in untreated mice at 4wk unTAC, would not be as great in macrophage-depleted hearts due to the decrease observed in CHP reactivity at 2wks of unTAC. At what point after unTAC macrophage depletion might influence further collagen degradation is speculated to be a critical factor with implications for translational studies and the subject of ongoing experiments.

LILY SOON NEFF. Macrophages Promote Regression of Myocardial Fibrosis Following Alleviation of Pressure Overload. (Under the direction of AMY BRADSHAW).

Chapter 4:

Future Directions and Conclusions

4.1 Introduction

The murine preclinical model established in our lab demonstrates that normalization of hemodynamic load regresses cardiomyocyte hypertrophy and leads to the partial, but incomplete regression of interstitial fibrosis which recapitulates important aspects of human heart pathologies. Unloading the myocardium leads to the initiation of collagen degradation, demonstrated by increased CHP reactivity, at 2wk unTAC followed by reduction in CVF at 4wk unTAC. However, CVF remains significantly increased at 4wk unTAC and 6wk unTAC compared to control. Furthermore, preliminary data demonstrates that CVF remains significantly increased out to 8wk unTAC compared to control (LN, unpublished). Hence, unloading the myocardium, either by unTAC in mice or SAVR in humans, does not appear to be sufficient to drive full regression of fibrosis after prolonged LVPO. Future work should focus on further elucidating the cellular mechanisms limiting this regression of fibrosis that might lead to new therapies to target persistent cardiac fibrosis.

4.2 The Complexity of Total Macrophage Markers

For flow cytometry and rt-PCR methodologies, macrophages were identified and/or isolated by their expression of F4/80. Isolation of F4/80+ macrophages for rt-PCR demonstrated the lowest number of macrophages in the myocardium was present at 4wk TAC+2wk unTAC compared to other TAC and unTAC time points. A similar trend was observed in flow cytometry when gating macrophages by F4/80 expression (Fig. 14). This low expression of F4/80+ macrophages in the 4wk TAC+2wk unTAC myocardium does not support the robust amount of IBA1+ macrophages observed by IHC (Fig. 11). Ionized

LILY SOON NEFF. Macrophages Promote Regression of Myocardial Fibrosis Following Alleviation of Pressure Overload. (Under the direction of AMY BRADSHAW).

calcium binding adaptor molecule 1 (IBA1) plays a role in actin-bundling activity and supports membrane ruffling and phagocytosis.⁴³ This supports the notion that the increased number and size of IBA1+ macrophages at 2wk unTAC is necessary for phagocytosis of collagen for reduction of CVF in 4wk unTAC. F4/80 is a 160-kDa glycoprotein encoded by *Emr1*.⁴⁴ Previous research in lymphoid and hemopoietic tissues has demonstrated that IBA1 stains more macrophages than the F4/80 macrophage marker.⁴⁵ Furthermore, recent literature supports the notion that resident macrophages, which seed the heart during embryogenesis are considered F4/80^{high}. F4/80^{low} macrophages express monocyte markers demonstrating a potential difference in resident versus recruited macrophages in the expression level of F4/80.¹¹ However, another potential reason for this disparity in total macrophage numbers in 4wk TAC+2wk unTAC myocardium based on the utilization of IBA1 or F4/80 is that IBA1 can be expressed by other immune cell types. Single cell sequencing of CD45+ immune cells in 1wk TAC and 4wk TAC demonstrated that the gene which encodes IBA1, Allograft Inflammatory Factor 1 (*Aif1*), is expressed in neutrophils and dendritic cells as well.³ Overall, the data presented supports that both F4/80 and IBA1 may not be ideal total macrophage markers to utilize in the unTAC myocardium on their own. Instead, in the TAC and unTAC myocardium, the addition of another macrophage marker, in conjunction with IBA1, may be beneficial. CyTOF analysis of TAC and sham myocardium demonstrated that from the commonly used immune cells markers studied, CD64 appears to be the most specific to macrophages without being expressed by neutrophils and dendritic cells.³¹ Altogether, a future method for properly identify macrophages in the TAC and unTAC myocardium would utilize more than one marker, such as IBA1+CD64+ macrophages instead of IBA1+ macrophages. This would delineate

LILY SOON NEFF. Macrophages Promote Regression of Myocardial Fibrosis Following Alleviation of Pressure Overload. (Under the direction of AMY BRADSHAW).

between IBA1⁺ immune cells which are possibly neutrophils or dendritic cells versus IBA1⁺CD64⁺ which are macrophages.

4.3 Parsing the Causal Role of Recruited Macrophages versus Resident Macrophages

Altogether, macrophages are innate immune cells whose primary role are to detect and phagocytose foreign objects and microorganisms that enter the body to attenuate injury or infection.⁴⁶ In the steady-state heart, the macrophage population is made of resident macrophages that patrol the heart. These resident macrophages are derived from yolk-sac progenitors and proliferate locally rather than population maintenance through monocyte recruitment.⁴⁶⁻⁴⁸ Resident macrophages express markers such as TIMD4, CD206, and CX3CR1 but do not express Ly6C.^{36,41,46} Recruited monocyte-derived macrophages express markers such as CCR2, Ly6C, CD11b, and MHC-II^{hi} but do not express TIMD4.^{26,36,46}

In response to LVPO, monocyte-derived macrophages are recruited from the bone marrow to the heart. Previous research from our lab and others have demonstrated the role of recruited monocyte-derived macrophages and resident macrophages in promoting or attenuating fibrosis in LVPO.^{28,29,31,37} We have incorporated Ly6C into our flow cytometry panel to characterize the macrophage subsets in our TAC and unTAC myocardium. However, this is a characterization that can support correlation only. To determine the causal role of recruited monocyte-derived macrophages or resident macrophages in promoting regression of fibrosis in unTAC myocardium, we must utilize pharmacological or genetic based depletions of these specific populations. A potential future application for the TAC/unTAC model in the Bradshaw laboratory.

LILY SOON NEFF. Macrophages Promote Regression of Myocardial Fibrosis Following Alleviation of Pressure Overload. (Under the direction of AMY BRADSHAW).

Several mouse models for the genetic depletion of macrophage subsets are currently available.⁴⁹ We chose to utilize an inducible toxin receptor-mediated cell depletion mouse model to target macrophages after unTAC while allowing for the development of hypertrophy and fibrosis during TAC.⁴⁹ B6.FVB-Tg(ITGAM-DTR/EGFP)³⁴Lan/J mice (Jackson Laboratory, Strain #006000) is a CD11b-diphtheria toxin receptor (DTR) transgenic mice available from Jackson Laboratory. This CD11b-DTR transgenic model utilizes the higher sensitivity to diphtheria toxin of human DTR, as compared to the endogenous mouse DTR, through expression of the human DTR driven by the monocyte-specific CD11b promoter.⁴⁹ Previous research has demonstrated that CD11b preferentially depletes monocytes and macrophages although CD11b can be expressed by multiple myeloid lineage cell populations like neutrophils.⁵⁰ A preclinical model of liver fibrosis demonstrated that, in the injury phase, depletion of CD11b⁺ macrophages by diphtheria toxin resulted in reduced levels of fibrosis compared to control. However, in the recovery phase, depletion of CD11b⁺ macrophages by diphtheria toxin resulted in persistent fibrosis compared to control PBS demonstrating that recruited macrophage can play distinct roles dependent on the tissue conditions and time after injury.⁵⁰

To determine whether CD11b⁺ recruited macrophages play a casual role in the ECM remodeling process observed at 2wk unTAC, CD11b-DTR mice underwent TAC surgery induced LVPO for 4 weeks. At the time of unTAC surgery, mice received one intraperitoneal injection of diphtheria toxin (25ng/g) or vehicle (water) and then one intraperitoneal injection 48 hours after the initial dose. Unfortunately, these mice became sick with the 25ng/g diphtheria toxin injections and over 50% of the mice died. The remaining mice were harvested at 1wk unTAC instead of the desired 2wk unTAC time

LILY SOON NEFF. Macrophages Promote Regression of Myocardial Fibrosis Following Alleviation of Pressure Overload. (Under the direction of AMY BRADSHAW).

point. For histological and immunohistochemical analysis, the following biological samples sizes were used: Diphtheria toxin 1wk unTAC (n = 3) and Vehicle 1wk unTAC (n = 5). The myocardium of mice that received diphtheria toxin demonstrated reduced levels of IBA1+ macrophages compared to vehicle control (Figure 20A-B). CVF was similar between diphtheria toxin and vehicle myocardium (Fig. 20C-E). Furthermore, CHP reactivity was not significantly different between diphtheria toxin and vehicle myocardium (Fig. 20F-H). Interestingly, CVF and CHP levels, for both diphtheria toxin and vehicle myocardium, demonstrated lower levels compared to 4wk TAC+2wk unTAC myocardium of C57/Bl6 mice suggesting potentially strain-specific responses to TAC/unTAC in these mice.

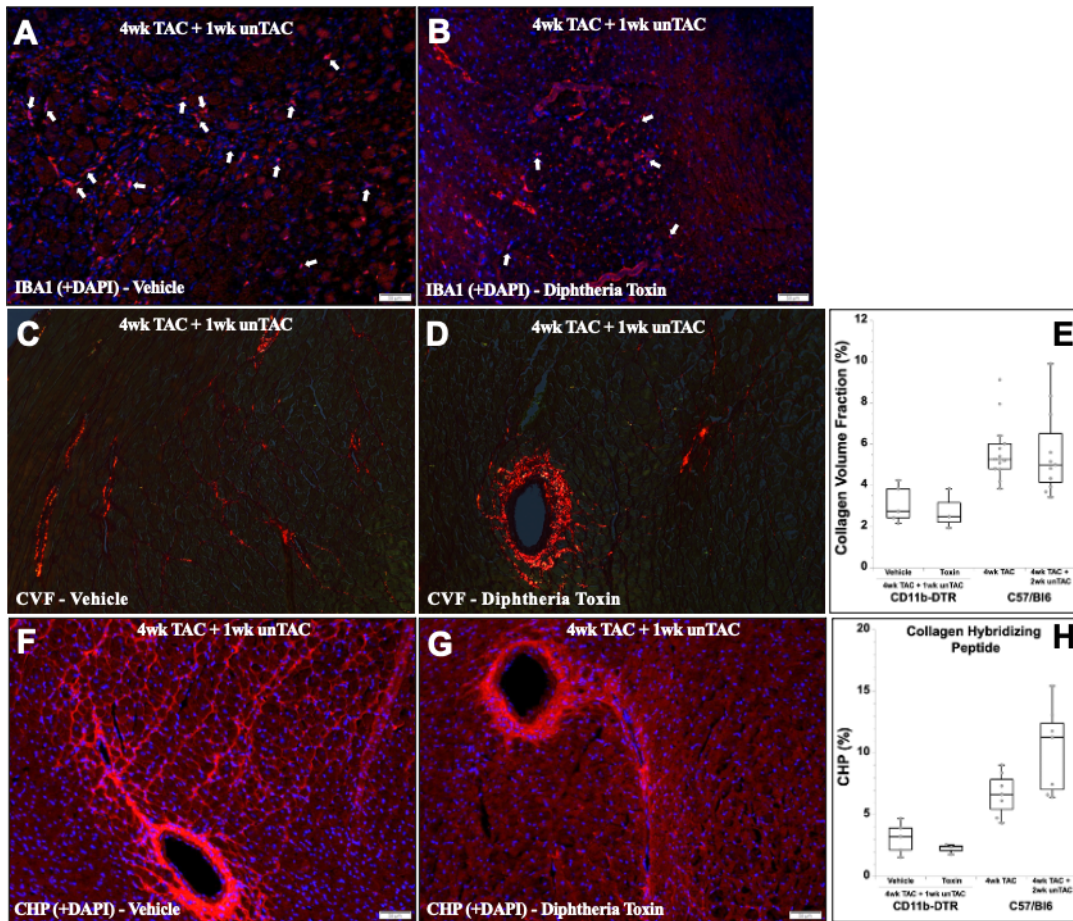


Figure 20: Depletion of CD11b+ Cells by Diphtheria Toxin in unTAC Myocardium.

Representative anti-IBA1-stained region of interest of 4wk TAC+1wk unTAC LV myocardium from CD11b-DTR mice injected with diphtheria toxin (B) or vehicle (A) at the time of unTAC surgery. No significant changes in collagen volume fraction (CVF) were observed in CD11b-DTR mice treated with diphtheria toxin (D) or vehicle (C). Quantification of CVF is shown in (E). No significant changes in collagen hybridizing peptide (CHP) reactivity were observed in CD11b-DTR mice treated with diphtheria toxin (G) or vehicle (F). Quantification of CHP reactivity is shown in (H). Animal sample sizes: CD11b-DTR mice; 1wk unTAC vehicle (n = 4-5), 1wk unTAC diphtheria toxin (n = 3), C57Bl/6 4wk TAC (n = 6-10), and 2wk unTAC (n = 6-11).

LILY SOON NEFF. Macrophages Promote Regression of Myocardial Fibrosis Following Alleviation of Pressure Overload. (Under the direction of AMY BRADSHAW).

Upon inspection, this transgenic mouse model was developed on an FVB/N background. Using fertilized FVB/N donor eggs, the transgenic construct containing DTR under the control of the human ITGAM promoter was introduced, and then mice were backcrossed to the C57BL/6 strain for six generations. Breeding this strain in-house, we have noticed an overall slower growth rate so pups are weaned at 4 weeks instead of 3 weeks. Because of the results from this pilot study and these observations from breeding, we determined it was necessary to evaluate whether this transgenic mouse strain develops hypertrophy and fibrosis after induction of LVPO similar to our C57/Bl6 mice from the TAC/unTAC time course.

CD11b-DTR mice were randomized and were either assigned to control no TAC or TAC surgery. The following samples sizes were analyzed: control no TAC (n = 4), 4wk TAC (n = 5), and 6wk TAC (n = 5). Histological analysis of PSR stained myocardial tissue sections demonstrated an average CVF of $2.01\% \pm 0.32\%$ in control CD11b-DTR which is similar to the average CVF of control C57Bl6 mice ($1.58\% \pm 0.19\%$). However, the average CVF of 4wk TAC CD11b-DTR mice was only $3.54\% \pm 1.18\%$ compared to $5.71\% \pm 0.44\%$ in C57Bl6 4wk TAC mice. Furthermore, average CVF of 6wk TAC CD11b-DTR myocardium was $3.18\% \pm 0.57\%$ (Fig. 21). Interestingly, the CD11b-DTR mice do not exhibit the same level of cardiac fibrosis as our C57Bl6 colony. Hence, it was determined that the CD11b-DTR mouse model might not be ideal to test our hypothesis of the role of recruited macrophages in collagen turnover following alleviation of LVPO as these mice did not demonstrate the same extent of cardiac fibrosis with LVPO. Alternative methodologies to test our hypothesis would be to focus on utilizing a neutralizing antibody

LILY SOON NEFF. Macrophages Promote Regression of Myocardial Fibrosis Following Alleviation of Pressure Overload. (Under the direction of AMY BRADSHAW).

against, for example, CCR2, to limit recruited macrophages expressing this cell surface receptor in our C57Bl6 TAC/unTAC mice.

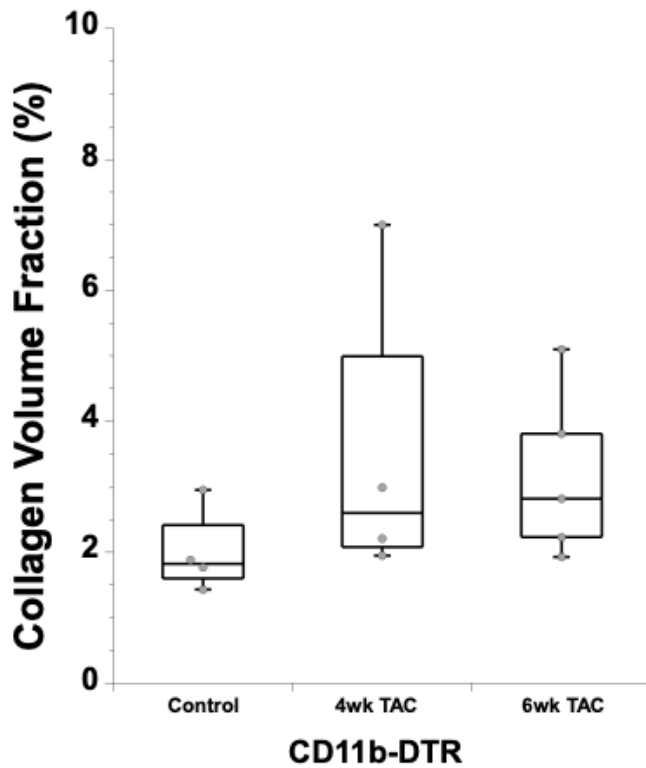


Figure 21: Quantification of Fibrosis in CD11b-DTR TAC Mice. Myocardium isolated from CD11b-DTR control mice and CD11b-DTR mice receiving TAC for 4 or 6 weeks were stained with picrosirius red. Quantification of CVF for control, 4wk TAC, and 6wk TAC. Animal sample sizes: control (n = 4), 4wk TAC (n = 4), and 6wk TAC (n = 5).

4.4 Immune Cell Profiling of the unTAC Myocardium

4.4.1 Introduction

The data presented herein focused primarily on the different roles of macrophages in collagen deposition and turnover in LVPO and after alleviation of LVPO. Clearly, other immune cells likely play important roles in regulating collagen turnover in myocardial tissues as has been demonstrated in progression of fibrosis after induction of LVPO. For example, two neutrophil clusters were observed following induction of LVPO and expanded after 4wks.³ The two clusters identified expressed distinct chemokine receptors, CCR2 versus CXCR2 and CCR1, and unique gene profiles, *CD69* versus *Mmp9* and *Arg2*.³ Depletion of neutrophils using a Ly6G antibody resulted in a reduction in posterior wall thickness and hypertrophy with improved fractional shortening.⁵¹ Interestingly, Ly6G-mediated depletion of neutrophils also resulted in a reduction in infiltrating monocytes and macrophages in the myocardium.⁵¹

In response to TAC, increased myocardial levels of CCL17, CXCL9, and CXCL10, implicated in the recruitment of T-cells were reported. Following 4 weeks of TAC, specific CD4⁺ and CD8⁺ T-cell subpopulations were shown to expand.^{30,52} However, the CD4⁺ Treg subpopulation did not expand in response to TAC compared to sham.³ RAG2^{-/-} mice lack functional B- and T-cells, and upon induction of LVPO by TAC, fibrosis was reduced compared to WT TAC mice.⁵² When RAG2^{-/-} mice were reconstituted with CD3 T-cells along with receiving TAC surgery, fibrosis levels were comparable to WT TAC mice. Furthermore, T-cells have previously been reported to produce and secrete the collagen crosslinking enzyme, LOX.⁵² Interestingly, RAG2^{-/-} TAC mice demonstrate reduced levels of CD68⁺ macrophages compared to WT TAC and RAG2^{-/-} CD3 T-cell with TAC mice.⁵²

LILY SOON NEFF. Macrophages Promote Regression of Myocardial Fibrosis Following Alleviation of Pressure Overload. (Under the direction of AMY BRADSHAW).

This suggests the role of lymphocytes, specifically CD4⁺ and CD8⁺ T-cells, in recruiting macrophages to the myocardium and promoting fibrosis in response to TAC.

To date, immune cell profiling of the myocardium, following alleviation of LVPO, has not been examined. To begin to address this, the expression of 44 cytokines known to play a role in immune cell recruitment and activation were examined from plasma and myocardial tissue homogenate from mice at the following time points: control, 2wk TAC, 4wk TAC+2wk unTAC, and 4wk TAC+4wk unTAC. As discussed below, temporal changes in distinct cytokines implicated in recruitment and activation of different immune cells were identified.

4.4.2 Neutrophils

Macrophages and monocytes are a primary source for secretion of MIP2 which promotes neutrophil recruitment through transepithelial migration into the myocardium.⁵³ MIP2 was significantly increased in 2wk and 4wk unTAC myocardium compared to 2wk TAC (Fig. 12D). Plasma from 2wk unTAC mice demonstrated significant increase in MIP2 expression compared to 2wk TAC plasma (Fig. 22A). Furthermore, plasma from 4wk unTAC mice demonstrated a significant increase in MIP2 expression compared to both control and 2wk TAC. Lipopolysaccharide-induced CXC chemokine (LIX) is an additional cytokine implicated in neutrophil migration and activation. LIX was significantly increased in both 2wk unTAC and 4wk unTAC myocardium compared to 2wk TAC myocardium (Fig. 22B). Previous research has demonstrated that neutrophils are a primary source of MMP9 in LVPO.³ Although Cathepsin K and proMMP2 protein levels were decreased after clodronate-mediated macrophage depletion, MMP9 did not demonstrate the same

LILY SOON NEFF. Macrophages Promote Regression of Myocardial Fibrosis Following Alleviation of Pressure Overload. (Under the direction of AMY BRADSHAW).

trend. MMP9 protein levels remain similar in clodronate liposome and PBS liposome myocardium. As CHP reactivity was significantly reduced with the depletion of macrophages, but not absent, a lower level of collagen degradation persisted. The muted level of collagen turnover might therefore derive, at least in part, from secretion of MMPs by neutrophils among other potential sources. Furthermore, MMP8, known as neutrophil collagenase, and proMMP9 were increased in 2wk unTAC myocardium compared to 2wk TAC and 4wk unTAC myocardium (Fig. 9B-C). Taken together, recruitment of neutrophils to the myocardium following alleviation of LVPO may play an important role in production and secretion of MMPs that promotes the initial, although incomplete, regression of fibrosis. Whereas, it is hypothesized during the progression of LVPO, neutrophils may be dispensable for the development of fibrosis from the muted production of cytokines implicated in neutrophil recruitment and activation at 2wk TAC compared to 2wk unTAC.

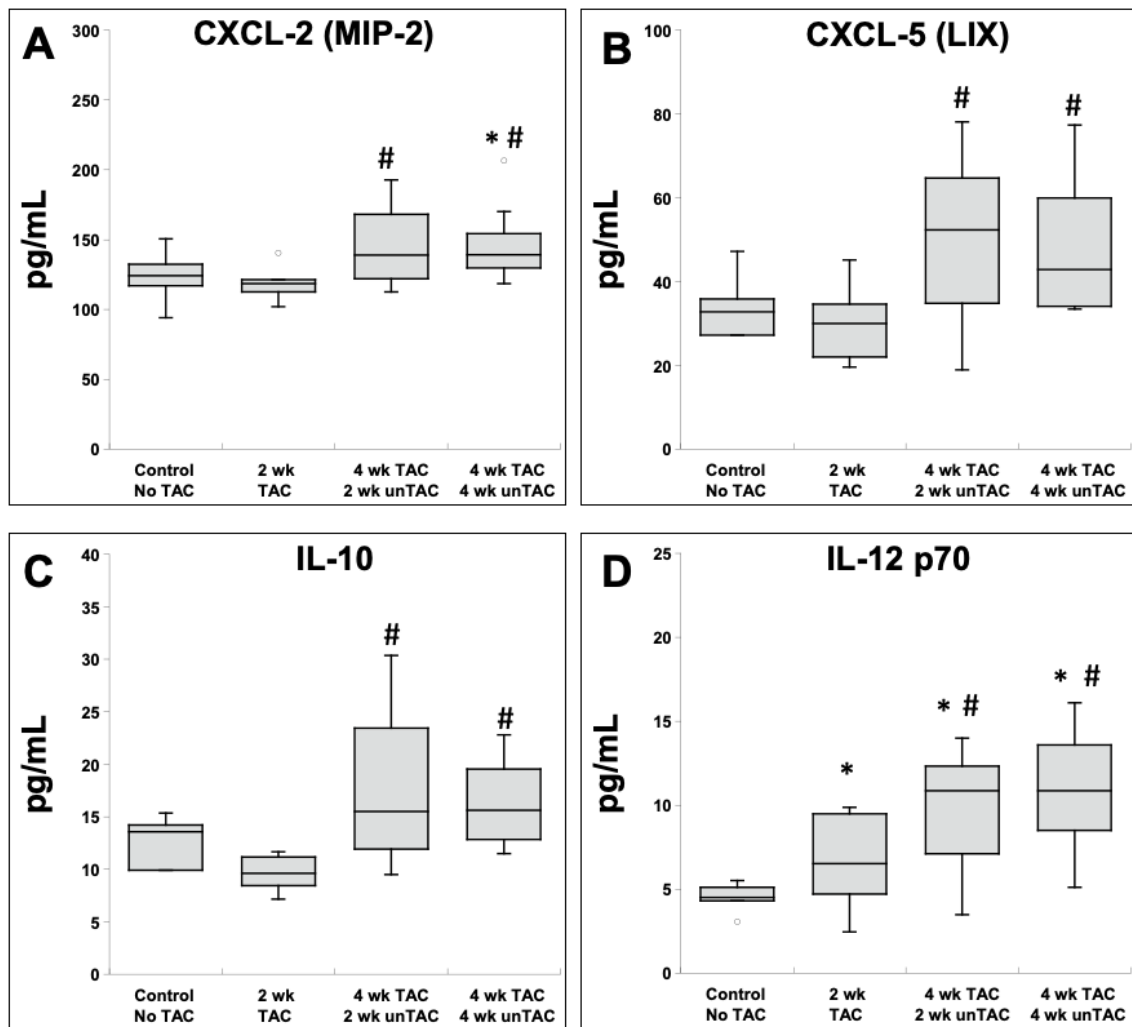


Figure 22: Differential Cytokine Profile in TAC versus unTAC Myocardium. Levels of cytokines and chemokines in control, 2wk TAC, 4wk TAC+2wk unTAC, and 4wk TAC+4wk unTAC were assessed by ALBIA assay: Plasma C-X-C Ligand 2 (CXCL-2) also known as Macrophage Inflammatory Protein-2 (A), Myocardial C-X-C Ligand 5 (CXCL5) also known as Lipopolysaccharide-induced CXC chemokine (LIX) (B), Interleukin 10 (C), Interleukin 12 (D). Animal sample sizes: control (n = 5), 2wk TAC (n = 8), 2wk unTAC (n = 8), and 4wk unTAC (n = 8). *p<0.05 vs. Control; #p<0.05 vs. 2wk TAC; \$p<0.05 vs. 4wk TAC; +p<0.05 vs. 4wk TAC+2wk unTAC.

4.4.3 T-cells

Interleukin-2 (IL-2) promotes the proliferation and differentiation of T-cells. 2wk unTAC myocardial protein homogenate demonstrated an increased trend in IL-2 protein production compared to 2wk TAC. 4wk unTAC demonstrated a significant increase in IL-2 compared to 2wk TAC. IL-10 and IL-12 are implicated in development of Th2 T-cells and inhibiting Th1 T-cell development. IL-10 demonstrated a significant increase in 2wk unTAC and 4wk unTAC compared to 2wk TAC (Fig. 22C). IL12 displayed a significant increase in 2wk TAC compared to control (Fig. 22D). Following alleviation of LVPO, IL12 was significantly increased in 2wk unTAC compared to 2wk TAC and control. IL12 remained significantly increased in 4wk unTAC myocardium compared to 2wk TAC and control (Fig. 22D). In conclusion, cytokines implicated in the activation and differentiation of T-cells are increased in response to alleviation of LVPO. Previous research has demonstrated that T-cells produce LOX to support collagen deposition and fibrosis.⁵² It is possible that T-cells, in late unTAC, may be supporting the persistent fibrosis observed by producing profibrotic proteins, such as LOX. Future research could focus on elucidating if T-cells promote persistent fibrosis in unTAC by inducible, genetic or pharmaceutical methodologies.

4.4.4 Conclusion

Although our preliminary cytokine data support the notion that specific immune cells and subsets inhabit the myocardium at different time points following alleviation of LVPO, future research should focus on properly characterizing the immune cell profile in the unTAC myocardium and assessing the role of cytokine production in either promoting

LILY SOON NEFF. Macrophages Promote Regression of Myocardial Fibrosis Following Alleviation of Pressure Overload. (Under the direction of AMY BRADSHAW).

or attenuating the regression of fibrosis. Isolation of CD45⁺ immune cells in the unTAC myocardium by FACS or microbeads to allow for single cell sequencing is one approach that might provide information as to which immune cell types produce important factors/enzymes that play functional roles in collagen turnover. Pharmacological or genetic depletion of immune cell populations would identify causal roles of specific cell types in collagen turnover following alleviation of LVPO. For example, neutrophils could be depleted during unTAC using a Ly6G antibody to inhibit their recruitment to the myocardium.

4.5 Fibroblasts in the TAC/unTAC Myocardium

Previous research has identified several key markers that can be used to identify cardiac fibroblasts and their activation state. Platelet derived growth factor receptor alpha (PDGFR α), discoidin domain receptor 2 (DDR2), periostin, vimentin, and alpha-smooth muscle actin (α SMA) have all been used to identify total and activate myocardial fibroblasts.⁵⁴ During embryonic development, fibroblasts populate the heart from two primary sources: epicardial cells that undergo epithelial-to-mesenchymal transformation and differentiation, and endothelial cells that undergo endothelial-to-mesenchymal transformation and differentiation. At steady state, cardiac fibroblasts play an important role in maintaining cardiac structure, function, and biochemical features of the heart. In response to disease, quiescent fibroblasts become activated and the fibroblast population expands primarily by proliferation of resident cardiac fibroblasts. Evidence for other sources of cardiac fibroblasts such as, endothelial-to-mesenchymal transformation and recruitment of bone marrow progenitor cells are reported, however, these sources likely

LILY SOON NEFF. Macrophages Promote Regression of Myocardial Fibrosis Following Alleviation of Pressure Overload. (Under the direction of AMY BRADSHAW).

contribute to a small percentage of activated fibroblasts.⁵⁵ In response to mechanical stress, activated fibroblasts demonstrate enhanced mobility, contractility, and excessive production of ECM proteins.²

To determine the role of fibroblasts in collagen turnover during LVPO and following alleviation of LVPO, PDGFR α ⁺ fibroblasts were isolated from the LV at control, 2wk TAC, 4wk TAC, 4wk TAC+2wk unTAC, 4wk TAC+4wk unTAC, and 4wk TAC+6wk unTAC. The profibrotic gene, *Colla1*, demonstrated an 11-fold increase in 2wk TAC myocardial fibroblasts compared to control. An 8-fold increase in *Colla1* was observed in PDGFR α ⁺ fibroblasts isolated from 4wk TAC myocardium compared to control (Fig. 23A). Interestingly, *Colla1* mRNA levels were similar in 4wk TAC+2wk unTAC to that of control myocardium. However, PDGFR α ⁺ fibroblasts displayed an increased trend in mRNA levels of *Colla1* at 4wk TAC+6wk unTAC compared to control (Fig. 23A). PDGFR α ⁺ fibroblasts demonstrated a significant increase, approximately 4-fold, of *Sparc* mRNA levels in 2wk TAC and 4wk TAC myocardium compared to control (Fig. 23B). A significant reduction in *Sparc* mRNA levels in the unTAC myocardium compared to TAC myocardium was observed in PDGFR α ⁺ fibroblasts (Fig. 23B). PDGFR α ⁺ fibroblasts exhibited a 14-fold increase at 2wk TAC and 11-fold increase at 4wk TAC in *Timp1* mRNA levels compared to control (Fig. 23C). Interestingly, PDGFR α ⁺ fibroblast *Timp1* levels were significantly decreased at 4wk TAC+2wk unTAC compared to TAC. However, PDGFR α ⁺ fibroblasts displayed increased levels of *Timp1* mRNA levels in 4wk TAC+4wk unTAC and 4wk TAC+6wk unTAC, 13-fold and 9-fold, respectively. A significant increase in *Lox* mRNA levels in TAC PDGFR α ⁺ fibroblasts was observed compared to control PDGFR α ⁺ fibroblasts (Fig. 23D). *Lox* mRNA levels returned to control levels at 4wk TAC+2wk

LILY SOON NEFF. Macrophages Promote Regression of Myocardial Fibrosis Following Alleviation of Pressure Overload. (Under the direction of AMY BRADSHAW).

unTAC compared to control (Fig. 23D). However, PDGFR α ⁺ fibroblasts revealed a 4-fold increase in *Lox* mRNA at 4wk TAC+4wk unTAC and 4wk TAC+6wk unTAC compared to control (Fig. 23D). Although not statistically significant, PDGFra⁺ fibroblasts demonstrated an increased trend in *Loxl2* mRNA levels in TAC myocardium compared to control (Fig. 23E). *Loxl2* mRNA levels in PDGFra⁺ fibroblasts isolated from the unTAC myocardium were comparable to control (Fig. 23E). A significant increase in *Pstn* at 2wk TAC and 4wk TAC was observed compared to control (Fig. 23F). After alleviating pressure overload, PDGFra⁺ fibroblasts from the unTAC myocardium exhibited similar levels of *Pstn* compared to control (Fig. 23F). PDGFR α ⁺ fibroblasts did not demonstrate a significant difference in *TGF β 1* mRNA levels in the TAC and unTAC myocardium compared to control (Fig. 23G). Although not statistically significant, *Mmp14* mRNA levels displayed an increased trend at 2wk TAC and 4wk TAC compared to control (Fig. 23H). Similar levels of *Mmp14* mRNA were observed between control and 4wk TAC+2wk unTAC. However, an increased trend in *Mmp14* mRNA levels was observed in 4wk TAC+6wk unTAC compared to control (Fig. 23H).

In conclusion, these quantitative rt-PCR results show that profibrotic genes implicated in collagen deposition and crosslinking were increased in PDGFR α ⁺ fibroblasts isolated from TAC myocardium. Interestingly, a shift was observed in 4wk TAC+2wk unTAC where mRNA levels of these profibrotic genes returned to control levels. However, a reinitiation in the mRNA production of certain profibrotic genes, such as *Timp1*, *Coll1a1*, and *Lox*, was observed at 4wk and 6wk unTAC. Levels of gene expression for these proteins were similar to that seen in TAC fibroblasts suggesting that fibroblasts might reactivate their profibrotic phenotype in the 4wk TAC+4wk unTAC and 4wk TAC+6wk

LILY SOON NEFF. Macrophages Promote Regression of Myocardial Fibrosis Following Alleviation of Pressure Overload. (Under the direction of AMY BRADSHAW).

unTAC myocardium. In conclusion, this data provides cellular mechanistic insight into the persistent fibrosis observed by picrosirius red staining of myocardium at 4wk TAC+4wk unTAC and 4wk TAC+6wk unTAC.

LILY SOON NEFF. Macrophages Promote Regression of Myocardial Fibrosis Following Alleviation of Pressure Overload. (Under the direction of AMY BRADSHAW).

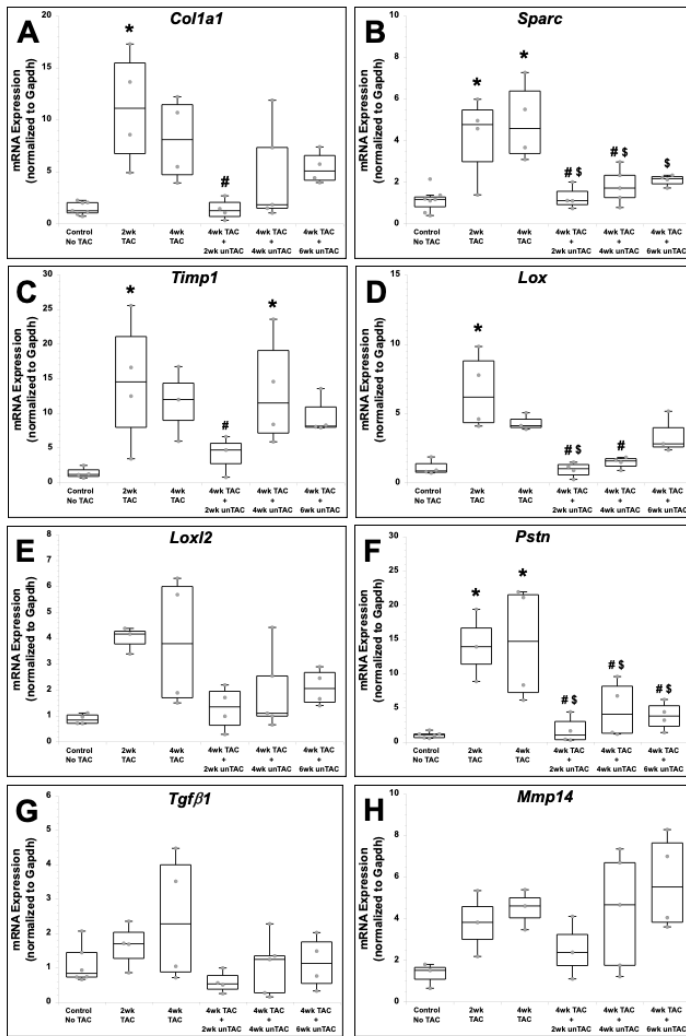


Figure 23: Differential mRNA Profiles in PDGFra+ Fibroblasts Isolated from TAC and unTAC Myocardium. Levels of profibrotic and antifibrotic genes in control, 2wk TAC, 4wk TAC, 4wk TAC+2wk unTAC, 4wk TAC+4wk unTAC, and 4wk TAC+6wk unTAC were assessed by real-time quantitative PCR: *Col1a1* (A), *Sparc* (B), *Timp1* (C), *Lox* (D), *Loxl2* (E), *Pstn* (F), *Tgfβ1* (G), *Mmp14* (H). Animal sample sizes: control (n = 3-7), 2wk TAC (n = 3-4), 4wk TAC (n = 3-4), 2wk unTAC (n = 3-4), 4wk unTAC (n = 4-5), and 6wk unTAC (n = 3-4). *p<0.05 vs. Control; #p<0.05 vs. 2wk TAC; \$p<0.05 vs. 4wk TAC; +p<0.05 vs. 4wk TAC+2wk unTAC.

4.6 Targeting the Persistent Fibrosis Observed in the unTAC Myocardium

4.6.1 Earlier Alleviation of LVPO

Previous literature and the characterization of our TAC/unTAC murine model has demonstrated that proteins which favor the development and persistence of fibrosis, such as TIMP1 and LOX, are significantly increased in the TAC myocardium.^{6,42} Although a partial regression of fibrillar collagen is observed at 4wk unTAC, it is incomplete and does not return to control levels. Data from AS/SAVR patients was shown to exhibit the same trend of persistent fibrosis (Fig. 10). We hypothesize that unloading the myocardium earlier, at 2wk TAC instead of 4wk TAC, would demonstrate a complete regression of fibrillar collagen that returned to levels of control. Furthermore, we hypothesize that unloading at 2wk TAC will reduce the amount of collagen crosslinking leading to a reduction in insoluble collagen that is resistant to degradation.

To test this hypothesis, 12-15wk old C57/Bl6 mice underwent TAC surgery. Following 2 weeks of TAC, mice were randomized to be harvested at 2wk TAC or undergo unTAC surgery. After unTAC surgery, mice were randomized to be harvested at 2wk TAC+2wk unTAC or 2wk TAC+4wk unTAC. The following sample sizes were utilized: control (n = 5), 2wk TAC (n = 7), 2wk TAC+2wk unTAC (n = 5), and 2wk TAC+4wk unTAC (n = 3). Histological analysis of PSR stained myocardial tissue sections demonstrated an increase in CVF at 2wk TAC compared to control. After alleviation of LVPO at 2wk TAC, unexpectedly, CVF at 2wk TAC+2wk unTAC demonstrated an increased trend compared to 2wk TAC and was significantly increased compared to control (Fig. 24A). 2wk TAC+4wk unTAC demonstrated a decreased trend in CVF compared to 2wk TAC+2wk unTAC. However, 2wk TAC+4wk unTAC CVF levels were not

LILY SOON NEFF. Macrophages Promote Regression of Myocardial Fibrosis Following Alleviation of Pressure Overload. (Under the direction of AMY BRADSHAW).

statistically different from 2wk TAC or control levels. CHP reactivity was significantly increased in 2wk TAC+2wk unTAC myocardium compared to control and 2wk TAC (Fig. 24B). This increased CHP reactivity in the 2wk TAC+2wk unTAC myocardium with reduction in CVF at 2wk TAC+4wk unTAC mimics the CVF and CHP trends observed at 4wk TAC+2wk unTAC and 4wk TAC+4wk unTAC. To determine if the CVF at 2wk TAC+4wk unTAC is detrimental to cardiac function, myocardial stiffness should be measured and compared to control.

Continuation of this research project might focus on determining the myocardial CVF at 2wk TAC+6wk unTAC to assess if CVF eventually returns to control levels. If CVF regresses to control levels by 2wk TAC+6wk unTAC, this might support the necessity of an earlier intervention in patients for SAVR surgery to regress fibrosis. However, if CVF does not regress to control levels by 2wk TAC+6wk unTAC, it would be important to understand why persistent fibrosis is still observed even after only 2wks of TAC. For example, is the same trend in macrophage area, CHP reactivity, and increase in collagenolytic enzymes observed as the 4wk TAC+unTAC time course? If persistent fibrosis is observed, these cellular and molecular components could be significantly increased at 2wk TAC+2wk unTAC but dampened by 2wk TAC+4wk unTAC. If CVF did return to control levels by 2wk TAC+6wk unTAC, cellular mechanisms contributing to complete regression could be deactivated fibroblasts and antifibrotic macrophages. Second harmonic generation imaging could be utilized to determine if there is a difference in the compositional structure of fibrillar collagen that allows for complete or incomplete regression following alleviation of LVPO at 2wk TAC and 2wk TAC+unTAC when compared to 4wk TAC and 4wk TAC+unTAC.

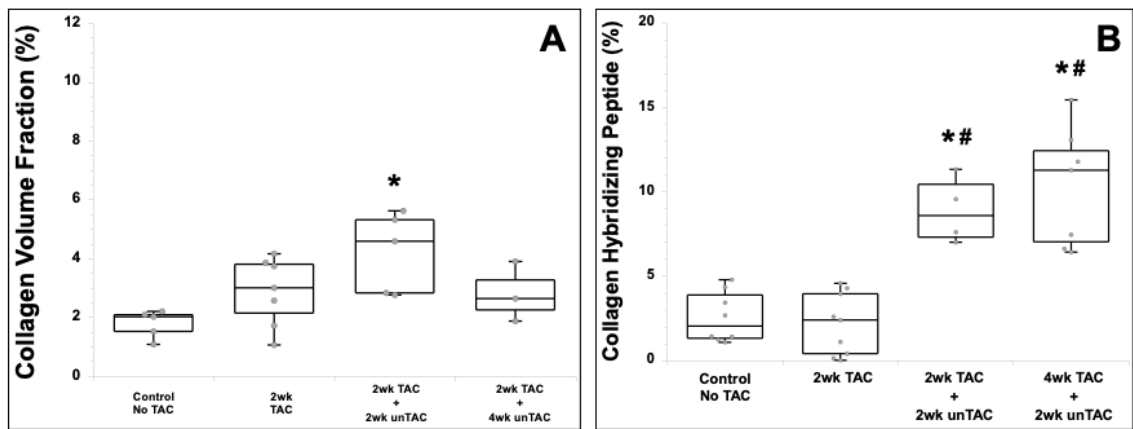


Figure 24: Characterization of Unloading the Myocardium at 2wk TAC. Myocardial tissue sections were stained with picrosirius red and analyzed for collagen volume fraction (CVF) at the following time points: control, 2wk TAC, 2wk TAC+2wk unTAC, and 2wk TAC+4wk unTAC (A). Myocardial tissue sections were stained with collagen hybridizing peptide and analyzed for CHP reactivity at the following time points: control, 2wk TAC, 2wk TAC+2wk unTAC, and 4wk TAC+2wk unTAC (B). Animal sample sizes: control no TAC (n = 5), 2wk TAC (n = 7), 2wk TAC + 2wk unTAC (n = 5), and 2wk TAC + 4wk unTAC (n = 3) (A). Animal sample sizes: control (n = 8), 2wk TAC (n = 9), 2wk TAC + 2wk unTAC (n = 4), and 4wk TAC + 2wk unTAC (n = 7) (B). *p<0.05 vs. Control; #p<0.05 vs. 2wk TAC.

LILY SOON NEFF. Macrophages Promote Regression of Myocardial Fibrosis Following Alleviation of Pressure Overload. (Under the direction of AMY BRADSHAW).

4.6.2 Combination Therapy of LOX Inhibition and Unloading the Myocardium for Regression of Myocardial Fibrosis

Fibrillar collagen cross-linking is an important factor that dictates cardiac tissue properties. Preclinical models of heart failure (HF) demonstrate increased levels of collagen crosslinking enzymes, such as LOX and LOXL2.^{42,56} Serum and myocardial biopsies isolated from HF patients demonstrate increased production of LOXL2.^{6,56} Furthermore, increased levels of collagen cross-linking enzymes were correlated with restrictive diastolic filling pressure and risk of hospitalization.⁵⁶

Genetic manipulation of preclinical models to knockout collagen cross-linking enzymes were not viable and resulted in perinatal fetal death.⁵⁷ Pharmacological or neutralizing antibody based inhibition of LOX family members in preclinical models of HF demonstrated decreased fibrosis and improved cardiac function.^{6,56,58-60} Although these preclinical models of targeting collagen cross-linking enzymes to reduce fibrosis were largely successful, pharmacological depletion of these enzymes in clinical trials have not been as promising. Although unknown the specific amount needed, some level of collagen cross-linking is necessary for maintenance of normal cardiac function. Because of this, a combination therapy that utilizes a lower concentration of collagen cross-linking inhibition with alleviation of LVPO may result in better outcomes.

Our data demonstrated a significant increase in proLysyl oxidase (proLOX) and Lysyl oxidase like 2 (LOXL2) at 2wk and 4wk TAC that decreased in 2wk unTAC hearts.⁴² Interestingly, proLOX protein levels significantly increased at 6wk unTAC back to TAC levels. Klepfish et. al. demonstrated that a functional blocking antibody against LOXL2 enhanced the regression of liver fibrosis by hindering the tightly packed, linear morphology

LILY SOON NEFF. Macrophages Promote Regression of Myocardial Fibrosis Following Alleviation of Pressure Overload. (Under the direction of AMY BRADSHAW).

of collagen fibrils, consistent with LOXL2 collagen cross-linking activity.¹⁴ Inhibition of LOXL2 rendered the collagen matrix more accessible to macrophages and allowed for further degradation by the membrane-bound collagenase, MMP14.¹⁴ One might speculate that increases in LOXL2 leads to increases in collagen crosslinking and thus contributes to a denser matrix that is more resistant to degradation. One might speculate the same is possible due to LOX as well.

The incomplete regression of interstitial fibrosis after alleviation of LVPO, mediated at least in part by macrophages, might be due to increases in collagen cross-linking generated in response to LVPO. Because an increase in proLOX levels were observed again at 6wk unTAC, comparable to TAC levels, targeting LOX instead of LOXL2 may be more useful in regressing myocardial interstitial fibrosis. To test this hypothesis, 12-15wk old C57/Bl6 mice would undergo TAC or sham surgery. Following this, mice would be randomized to receive either an antibody generated against LOX or an IgG control antibody creating four groups: 1) TAC surgery + LOX antibody, 2) TAC surgery + IgG control antibody, 3) Sham surgery + LOX antibody, 4) Sham surgery + IgG control antibody. Furthermore, one might speculate the length of the antibody regimen would affect if complete regression will be observed. To test this hypothesis, mice in the four groups will be further randomized and grouped to start receiving antibody injections 1 week following TAC/sham surgery or to start receiving antibody injections 3 weeks after TAC/sham surgery. Following 4 weeks of TAC, mice will undergo unTAC surgery and will be harvested at either 2wk unTAC, 4wk unTAC, or 6wk unTAC. To determine if fibrosis regresses to control levels, myocardial tissue sections will be stained with PSR and quantified for CVF.

4.6.3 Combination Therapy of Unloading the Myocardium and Inhibition of TIMP1

Previously published data from our lab and other laboratories support the notion that TIMP1 protein production is increased in LVPO myocardium to promote the deposition of fibrillar collagen and persistent fibrosis.^{30,42} As shown in Fig. 5, a sustained rise in TIMP1 was observed in the unTAC myocardium and remained significantly elevated at 6wk unTAC despite normalization of hemodynamic load and cardiomyocyte cross-sectional area. Elevated levels of TIMP1 levels in unTAC myocardium has important clinical applications because increased TIMP1 levels has been observed in clinical studies. In clinical studies using sacubitril/valsartan (Paradigm, Paramount) and spironolactone (TOP-CAT), the circulating biomarker with the most prognostic significance was TIMP1.⁶¹⁻⁶³ TIMP1 levels correlated with HF hospitalization and cardiovascular mortality rates in these patients. An increase in TIMP1 levels demonstrated an increase in HF hospitalization and cardiovascular mortality rates, whereas a decrease in TIMP1 levels predicted a decrease in these event rates.

PDGFR α + fibroblasts isolated from the myocardium at each time point during the TAC/unTAC time course demonstrated a significant increase in *Timp1* mRNA levels at 2wk TAC and demonstrated an increased trend at 4wk TAC compared to control (Fig. 23C). Although *Timp1* mRNA levels returned to control levels at 4wk TAC+2wk unTAC in PDGFR α + fibroblasts, a significant increase compared to control was observed at 4wk TAC+4wk unTAC. *Timp1* mRNA levels remained elevated in 4wk TAC+6wk unTAC compared to control. F4/80+ macrophages isolated from the myocardium at each time point during the TAC/unTAC time course did not demonstrate significant increase in *Timp1* mRNA levels compared to control.

LILY SOON NEFF. Macrophages Promote Regression of Myocardial Fibrosis Following Alleviation of Pressure Overload. (Under the direction of AMY BRADSHAW).

Interestingly, research has demonstrated that TIMP1 activates cardiac fibroblasts by binding to the cell surface receptor, CD63, which amplifies fibroblast integrin attachment to the ECM.⁶⁴ This enhanced integrin engagement to the ECM, mediated by TIMP1, has been shown to promote TGF β signaling and increase the production of collagen I.⁶⁴ Furthermore, it has been previously shown that TIMP1 can enhance fibroblast proliferation.^{65,66} The current literature plus our data supports the notion that the persistent fibrosis observed may be in-part due to a TIMP1 autocrine-mediated activation of fibroblasts in the unTAC myocardium.

Based off our data, TIMP1 may be a therapeutic target following alleviation of pressure overload to inhibit the persistent fibrosis observed. To test this hypothesis, we could utilize a TIMP1 monoclonal blocking antibody. A previously published study from another laboratory utilized subcutaneous injections of a TIMP1 monoclonal blocking antibody at 5 μ g/mL in C57Bl/6 mice to study dermal fibroblast migration and angiogenesis of microvascular endothelial cells.⁶⁷ 12-15wk old C57/Bl6 mice will undergo TAC surgery. After 4wks of TAC, mice will be randomized to receive unTAC surgery or sham surgery. Following this, mice will be randomized to receive either a TIMP1 monoclonal blocking antibody or an IgG control antibody creating four groups: 1) TAC and unTAC surgery + TIMP1 antibody, 2) TAC and unTAC surgery + IgG control antibody, 3) TAC and sham surgery + TIMP1 antibody, 4) TAC and sham surgery + IgG control antibody. To eliminate the stress of daily injections, mice will receive a subcutaneous implantation of an Alzet Osmotic Pump. PDGFR α + fibroblasts isolated from 4wk TAC+2wk unTAC myocardium did not demonstrate the same profibrotic profile as TAC myocardium. Because a specific subset of profibrotic genes were elevated again at 4wk TAC+4wk unTAC, the Alzet

LILY SOON NEFF. Macrophages Promote Regression of Myocardial Fibrosis Following Alleviation of Pressure Overload. (Under the direction of AMY BRADSHAW).

Osmotic pumps will be implanted at 4wk TAC+2wk unTAC to inhibit the activated fibroblast phenotype observed in the later unTAC myocardium. Mice will be harvested at 4wk TAC+4wk unTAC and 4wk TAC+6wk unTAC. To determine if fibrosis regresses to control levels, myocardial tissue sections will be stained with PSR and quantified for CVF. PDGFR α ⁺ fibroblasts will be isolated from 4wk TAC+4wk unTAC and 4wk TAC+6wk unTAC myocardium and profibrotic genes will be analyzed to determine if Timp1 inhibition prevents the re-initiation of the profibrotic, activated fibroblast phenotype.

4.6.4 Combination Therapy of Unloading the Myocardium and Pirfenidone

Pirfenidone is a small molecule, orally active drug that has been approved for treatment of idiopathic pulmonary fibrosis. *In vitro* and *in vivo* models have demonstrated that pirfenidone has anti-fibrotic properties and is useful for the regression of fibrosis.⁶⁸⁻⁷⁰ Alveolar macrophages treated with pirfenidone demonstrated a reduction in expression of pro-fibrotic, M2 marker such as CD206 and reduced secretion of TGF β 1. Rat lung fibroblasts treated with pirfenidone demonstrated a reduction collagen type 1 and α SMA production.^{69,71} 10-week-old mice underwent TAC or sham surgery and were randomized to receive either pirfenidone or vehicle until harvest following 8 weeks. The TAC with pirfenidone group demonstrated a reduction in HW, fibrosis, fibroblast proliferation, and protein production of TGF β 1 compared to the TAC with vehicle group. Although not back to sham levels, the pirfenidone increased EF and fractional shortening compared to the TAC with vehicle group.⁷⁰ Interestingly, FACS analysis demonstrated a shift in the immune cell profile in the TAC with pirfenidone compared to TAC with vehicle group. In

LILY SOON NEFF. Macrophages Promote Regression of Myocardial Fibrosis Following Alleviation of Pressure Overload. (Under the direction of AMY BRADSHAW).

the TAC with pirfenidone group, Th1 T-cells and M1 macrophages were increased, whereas Th2 T-cells, Th-17 cells, and M2 macrophages were decreased.⁷⁰

A randomized phase 2 clinical trial for Heart failure with preserved ejection fraction (HFpEF) utilized 80 patients with an ejection fraction greater than 45%.⁷² Patients were randomized to receive placebo or pirfenidone for 52 weeks before completing final efficacy analysis. Patients underwent cardiovascular magnetic resonance imaging to determine extracellular volume (ECV), a non-invasive measurement used to determine myocardial fibrosis. Patients with an ECV below 27% were excluded from the clinical trial. Following 52 weeks, patients who received pirfenidone demonstrated a 0.7% reduction in ECV whereas the placebo cohort demonstrated a 0.5% increase in ECV. The -1.21 between group difference observed in ECV was significantly different. Patients who received pirfenidone demonstrated small improvements in ejection fraction (EF), 6-minute walk distance, and clinical KCCQ scores. These results are promising because no other interventions were used in the treatment of these HFpEF patients and yet a reduction in ECV with an increase in EF was observed.

Taken together, this preclinical and clinical data demonstrates that pirfenidone has antifibrotic properties in the myocardium. The decrease in collagen production by fibroblasts while inhibiting profibrotic immune cell populations are two key mechanisms in which pirfenidone reduces fibrosis. Although echocardiographic measurements and fibrosis were attenuated in TAC mice that received pirfenidone, it was still increased compared to sham mice. Using pirfenidone in a combinational therapy, such as with unTAC surgery, may reduce fibrosis back to control levels.

LILY SOON NEFF. Macrophages Promote Regression of Myocardial Fibrosis Following Alleviation of Pressure Overload. (Under the direction of AMY BRADSHAW).

To test this hypothesis, 12-15wk old mice would receive TAC surgery and LVPO would be induced for 4 weeks. Following 4 weeks of TAC, mice would undergo unTAC surgery. To eliminate the stress of daily injections, mice will receive a subcutaneous implantation of an Alzet Osmotic Pump containing either pirfenidone or vehicle creating four groups: 1) TAC and unTAC surgery + pirfenidone, 2) TAC and unTAC surgery + vehicle, 3) TAC and sham surgery + pirfenidone, 4) TAC and sham surgery + vehicle. Mice will be harvested at 4wk TAC+4wk unTAC and 4wk TAC+6wk unTAC. Key outputs would be CVF and myocardial stiffness to determine if fibrosis returns to control levels. Protein tissue homogenate will be analyzed for differences in proLOX, LOX, and TIMP1 protein production. If CVF and myocardial stiffness do not return to control levels, utilizing pirfenidone during TAC may promote the regression of CVF to control levels following unTAC surgery.

Research has not been conducted to determine if pirfenidone reduces the production of TIMP1 and LOX which might promote the persistent fibrosis observed in unTAC. It is hypothesized that fibroblasts will demonstrate decreased protein production of TIMP1 and LOX when cultured with pirfenidone. Previous studies from our laboratory demonstrate that a substrate stiffness of 2kPa is equivalent to referent control myocardium while a substrate stiffness of 8kPa is equivalent to the stiffness of a fibrotic myocardium. Previous data from our lab has shown that fibroblasts cultured on 8kPa demonstrate increased proliferation and production of collagen I compared to fibroblasts cultured on 2kPa. These physiologically relevant Cytosoft culture plates could be utilized for fibroblast cultures. Fibroblasts isolated from control mouse hearts plated on 2kPa and 8kPa cell culture plates, could be treated with either pirfenidone or vehicle control and allowed to grow for 48 hours

LILY SOON NEFF. Macrophages Promote Regression of Myocardial Fibrosis Following Alleviation of Pressure Overload. (Under the direction of AMY BRADSHAW).

before harvest. Western blots of cell lysate and media will be conducted to look at protein levels of proLOX, LOX, and TIMP1.

4.7 CHP reactivity in referent control, LVH, and HFpEF patients

Our preclinical model of heart failure demonstrated low levels of CHP reactivity in control and 2wk TAC myocardium. CHP reactivity increased in 4wk TAC mice compared to control and 2wk TAC mice. Interestingly, myocardial biopsies isolated from referent control, hypertension, and HFpEF patients demonstrated the opposite trend. Tissues from referent control and hypertensive patients demonstrated strong CHP reactivity (Fig. 25). However, CHP reactivity was significantly decreased in biopsies from HFpEF patients (Fig. 25). Although MMP2 and MMP13 levels were decreased in hypertensive patients, an increase in TIMP1 was not observed until development of HF.⁷³ These shifts in ECM protease activity support our CHP data in biopsies because the decrease in collagen degradatory enzymes (MMP2 and MMP13) accompanied by an increase in TIMP1 is predicted to shift the balance toward reduced collagen degradation as observed in HFpEF patients (Fig. 25).

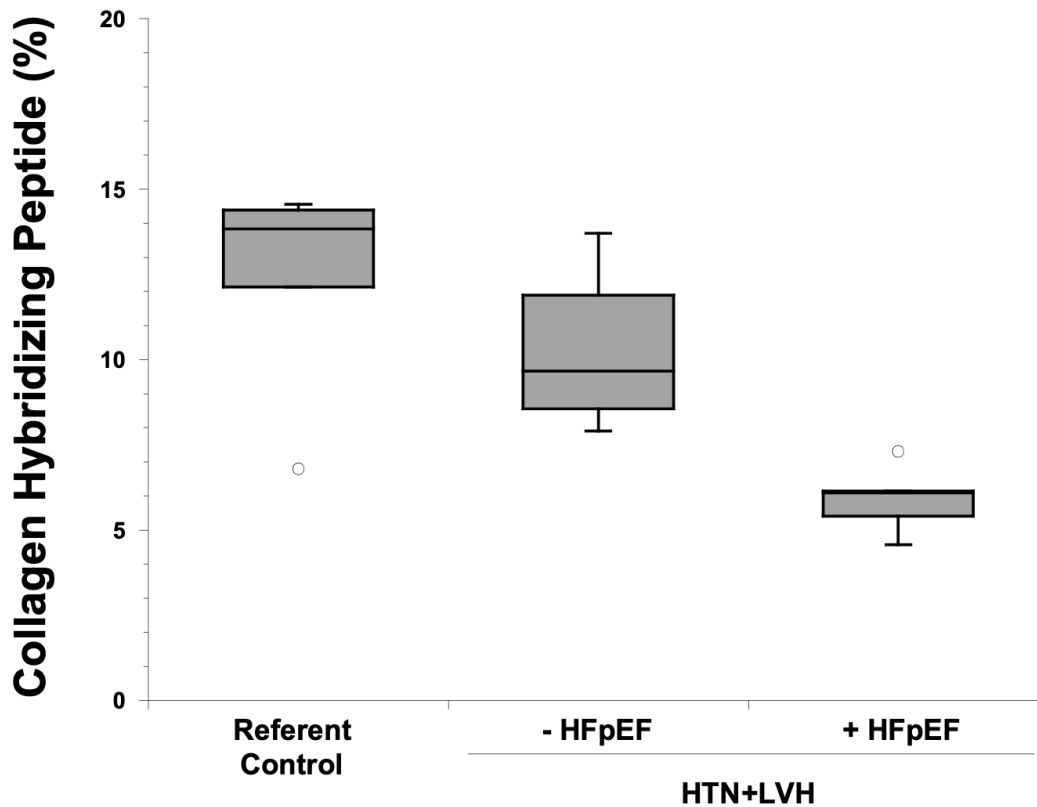


Figure 25: Decreased CHP Reactivity in Biopsies Isolated from HFpEF patients.

Myocardial tissue sections of biopsies isolated from referent control, Hypertension (HTN) plus Left Ventricular Hypertrophy (LVH), and HTN+LVH with Heart Failure Preserved Ejection Fraction (HFpEF) were stained with CHP. CHP reactivity was decreased in HFpEF patients compared to referent control and HTN+LVH patients.

4.8 Conclusions

In response to LVPO, induced by TAC, myocytes undergo concentric hypertrophy, which is the addition of sarcomeres in parallel rather than series, demonstrated by increased cardiomyocyte CSA, LV/BW, and LV/TL (Fig. 25). At the tissue level, production of profibrotic proteins such as LOX, LOXL2, and TIMP1 were increased in TAC myocardium. PDGFra⁺ fibroblasts isolated from 2wk TAC and 4wk TAC displayed increased mRNA expression of profibrotic genes such as *Colla1*, *Pstn*, *Timp1*, *Lox*, *Loxl2*, and *Sparc*. Although not an all-inclusive list of profibrotic genes, it could be hypothesized that other profibrotic genes demonstrate increased expression in PDGFra⁺ fibroblasts. The increased *Timp1* mRNA expression observed in PDGFra⁺ fibroblasts supports the notion that fibroblasts are a main producer of TIMP1 which enhances fibrosis by two key mechanisms: 1) reducing collagen degradation by inhibiting MMPs and 2) activating fibroblasts through CD63 interactions and downstream signaling. Along with this, although not looked at specifically in our TAC model, cardiomyocytes could be a potential source of TIMP1. Our data demonstrates that F4/80⁺ macrophages are most likely not a main contributor to TIMP1 protein production. However, although our data is at the gene level, F4/80⁺ macrophages in 2wk TAC myocardium most likely promote fibrosis through production of proteins like SPARC and periostin which facilitate the deposition of collagen. Interesting, these profibrotic macrophages are necessary for the initial profibrotic response to LVPO but it is not sustained by 4wk TAC. Taken together, both fibroblasts and macrophages promote the initial response to the pathological stimulus at 2wk TAC, but fibroblasts, not macrophages, demonstrate a sustained profibrotic phenotype at 4wk TAC

LILY SOON NEFF. Macrophages Promote Regression of Myocardial Fibrosis Following Alleviation of Pressure Overload. (Under the direction of AMY BRADSHAW).

which results in the increased CVF and myocardial stiffness observed in TAC myocardium (Fig. 25).

In response to alleviation of LVPO, induced by removal of the TAC suture, myocytes regress back to control size demonstrated by cardiomyocyte CSA. However, gravimetric and echocardiographic measurements demonstrated a sustained increase in myocardial mass. It is proposed that the main source for this elevated myocardial mass is from the increased ECM proteins and fibrillar collagen. At the tissue level, production of MMPs and Cathepsin K increase in 2wk unTAC leading to enhanced CHP staining which results in a partial regression of CVF in 4wk unTAC. The fall in MMPs and Cathepsin K, while TIMP1 and proLOX increase in protein production leads to persistent fibrosis in 6wk unTAC. PDGFra⁺ fibroblasts and F4/80⁺ macrophages isolated from 2wk unTAC displayed reduced mRNA expression of profibrotic genes, such as *Colla1*, *Pstn*, *Timpl*, *Lox*, *Loxl2*, and *Sparc*, compared to TAC which promotes the partial regression of fibrosis observed in 4wk unTAC by CVF. Depletion of macrophages, at time of unTAC surgery, resulted in reduced CHP reactivity and decreased protein levels of enzymes implicated in collagen degradation supporting the role of antifibrotic macrophages at 2wk unTAC which play an important role in phagocytosing collagen. One method that macrophages may be phagocytosing collagen is through an MMP14-mediated mechanism. Fibroblasts in 4wk unTAC and 6wk unTAC demonstrate a significant increase in profibrotic genes demonstrating an activated phenotype compared to 2wk unTAC which supports the persistent fibrosis and elevated myocardial stiffness observed. Along with this, the antifibrotic macrophages observed at 2wk unTAC is a transient population. The macrophages observed in late unTAC (6wk unTAC) display a profibrotic phenotype and

LILY SOON NEFF. Macrophages Promote Regression of Myocardial Fibrosis Following Alleviation of Pressure Overload. (Under the direction of AMY BRADSHAW).

may promote the persistent fibrosis observed by an increase in mRNA expression of specific profibrotic genes, such as *Colla1* and *Pstn*. Taken together, the data presented herein demonstrates that macrophages display a distinct, but transient, anti-fibrotic phenotype that leads to the incomplete, partial regression of fibrosis (Fig. 26). Furthermore, activated fibroblasts are a key cellular mechanism behind persistent fibrosis (Fig. 26).

LILY SOON NEFF. Macrophages Promote Regression of Myocardial Fibrosis Following Alleviation of Pressure Overload. (Under the direction of AMY BRADSHAW).

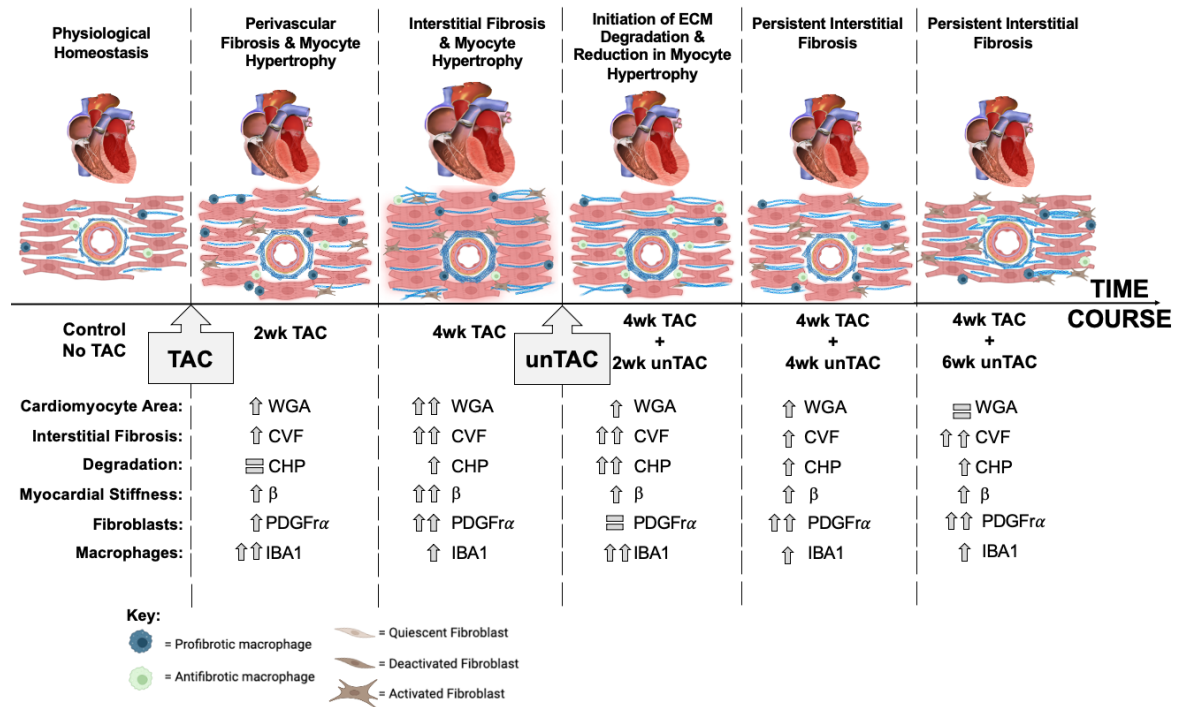


Figure 26: TAC/unTAC Schematic Summary. Schematic summary of data highlighting the biochemical and structural changes associated with the partial, but incomplete regression of fibrosis following alleviation of LVPO. Both perivascular and interstitial fibrosis are demonstrated in the schematic. Dark blue macrophages indicate profibrotic macrophages, light green macrophages denote antifibrotic macrophages, light brown fibroblasts refer to quiescent fibroblasts, dark brown elongated fibroblasts indicate deactivated fibroblasts, and dark brown fibroblasts with protrusions denotes activated fibroblasts (Refer to Key). Arrows and equal signs for each time point are in comparison to Control No TAC. Created with Biorender.com.

LILY SOON NEFF. Macrophages Promote Regression of Myocardial Fibrosis Following Alleviation of Pressure Overload. (Under the direction of AMY BRADSHAW).

Chapter 5:
Materials and Methods

5.1 Murine Model of LVPO and Alleviation of LVPO

C57Bl6 male and female mice (bred in house, stock no. 002014, Jackson Laboratories, Bar Harbor, ME), 12-15 weeks of age, were randomized into a control (no TAC) group or transverse aortic constriction (TAC) group. LVPO was induced by TAC as previously described.^{8,42} Briefly, mice were anesthetized using inhalation of 5% isoflurane vapors in a chamber then transferred to a thermostatically controlled surgical platform under a dissecting microscope. Nair hair removal and alcohol sterilization were treated on the surgical area. During surgery, a modified mask assembly was utilized on the mice to provide a continuous flow of anesthesia (1.5-2% isoflurane). After making a 5-mm skin incision in the neck region, the trachea was visualized to complete an orotracheal intubation. Analgesia (0.05mg/kg buprenorphine) by intraperitoneal injection was administered. A 5-mm horizontal incision was created at the suprasternal notch with blunt dissection completed to visualize the transverse aorta. Transverse aorta arch banding was performed by placing a 7.0 silk suture over a 26-gauge needle, cause complete occlusion of the aorta. Then, the needle was removed, restoring the aortic lumen but leaving a stenotic aortic orifice. The 5-mm horizontal incision was closed after air was removed through a drainage tube. Mice were extubated and recovered from anesthesia on a warming blanket within an oxygen supplemented container. After TAC, mice were randomized for harvest at 2wk TAC or 4wk TAC or to receive unTAC surgery to alleviate LVPO after 4wks of TAC. For unTAC, mice were anesthetized using inhalation of 5% isoflurane vapors in a chamber then transferred to a thermostatically controlled surgical platform under a dissecting microscope. Nair hair removal and alcohol sterilization were treated on the surgical area. During surgery, a modified mask assembly was utilized on the mice to

LILY SOON NEFF. Macrophages Promote Regression of Myocardial Fibrosis Following Alleviation of Pressure Overload. (Under the direction of AMY BRADSHAW).

provide a continuous flow of anesthesia (1.5-2% isoflurane). After making a 5-mm skin incision in the neck region, the trachea was visualized to complete an orotracheal intubation. Analgesia (0.05mg/kg buprenorphine) by intraperitoneal injection was administered. A 5-mm horizontal incision was created at the suprasternal notch to visualize the transverse aorta. The suture around the transverse aorta was visualized, cut, and removed to reverse the occlusion of the aorta. The 5-mm horizontal incision was closed after air was removed through a drainage tube. Mice were extubated and recovered from anesthesia on a warming blanket within an oxygen supplemented container. 4wk TAC mice which underwent surgical removal of the transverse aortic constriction (unTAC), to alleviate LVPO, were randomized to be harvested at 2wks, 4wks, or 6wks after unTAC (4wk TAC+2wk unTAC, 4wk TAC+4wk unTAC, 4wk TAC+6wk unTAC)⁴². All animal procedures were reviewed and approved by the Ralph H. Johnson Veterans Affairs Institutional Animal Care and Use Committee.

5.2 Liposome Mediated Depletion of Macrophages

At the time of unTAC surgery, mice were randomized and received one intraperitoneal injection of either PBS Liposome or Clodronate Liposome (both 10uL/g). Mice were harvested at 2wk unTAC. Forty-three mice underwent TAC surgery to induce LVPO, and thirty-seven mice survived to 4wk TAC. Thirty-two mice of the thirty-seven mice that underwent unTAC surgery survived. Nine mice received one PBS liposome injection whereas twenty-three mice received one clodronate liposome injection. Of the twenty-three mice that received one clodronate liposome injection, nine survived to 2wk

LILY SOON NEFF. Macrophages Promote Regression of Myocardial Fibrosis Following Alleviation of Pressure Overload. (Under the direction of AMY BRADSHAW).

unTAC and were used as an endpoint. Of the nine mice receiving PBS liposomes, seven survived to 2wk unTAC and were used as an endpoint.

5.3 Echocardiography

To obtain echocardiographic measurements, a Vevo 3100 echocardiography system and 40-MHz transducer were used. LV dimension and wall thickness were measured at end-diastole and end-systole using standard American Society of Echocardiography criteria. Normalization of LV mass was conducted using body weight (LV-to-BW) and tibial length (LV-to-TL). Ejection fraction (EF, %) was calculated as $EF = 100 \times (LVEDV - LVESV)/LVEDV$. Echocardiographic measurements were obtained for control, 2wk TAC, 4wk TAC, 4wk TAC+2wk unTAC, 4wk TAC+4wk unTAC, and 4wk TAC+6wk unTAC (Table 1). For echocardiograph data presented in Table 2, the following sample sizes were used: No Liposomes: no TAC (n = 5), 4wk TAC+2wk unTAC (n = 11), PBS Liposomes: 4wk TAC+2wk unTAC (n = 7), Clodronate Liposomes: 4wk TAC+2wk unTAC (n = 6).

5.4 Histological Quantification of Cardiomyocyte Cross-Sectional Area (CSA)

LV myocardium from each mouse were fixed in zinc formalin for 24 hours, paraffin embedded, and sectioned into 5-micron sections. LV myocardial tissue sections were preheated on a slide warmer at 45°C for one hour prior to deparaffinization and rehydration. Following rehydration, tissue sections were incubated in antigen retrieval buffer in a steamer for 20 minutes. After antigen retrieval, tissue sections were incubated in 1% BSA blocking buffer for one hour. To visualize cardiomyocyte borders, tissue sections were

LILY SOON NEFF. Macrophages Promote Regression of Myocardial Fibrosis Following Alleviation of Pressure Overload. (Under the direction of AMY BRADSHAW).

incubated with horse radish peroxidase conjugated wheat germ agglutinin (WGA) (1:200, Vector Laboratories, No. PL-1026) overnight at 4°C. Following washes with 1X PBS, Tyramide 488 fluorophore amplification was performed (1:500, Biotium, No. 92171). Tissue samples were mounted and cover slipped with ProLong Gold Antifade reagent with DAPI (Invitrogen, cat. no. P36931). WGA fluorescent images were captured on a BZ-X800 Keyence microscope. Cardiomyocyte cross-sectional area (CSA) was quantified using the Hybrid Cell Count function in the BZ-X800 Analyzer Software. For CSA, the following biological sample sizes were used: control (n = 8), 2wk TAC (n = 5), 4wk TAC (n = 3), 4wk TAC+2w unTAC (n = 5), 4wk TAC+4wk unTAC (n = 5), and 4wk TAC+6wk unTAC (n = 6).

5.5 Histological Quantification of Collagen Volume Fraction (CVF)

To quantify myocardial collagen content, as collagen volume fraction, LV myocardial tissue sections were stained with picrosirius red (PSR) then imaged using polarized light microscopy on a BZ-800 Keyence microscope, as previously described⁴². The entire LV PSR-stained tissue section was imaged and stitched together to generate a complete representative image for CVF analysis. Using the BZ-X800 Analyzer, CVF was quantified for the entire stitched tissue section as birefringent fibrillar collagen positive pixels to total area of pixels in the tissue section. For CVF, the following samples sizes were used: control (n = 10), 2wk TAC (n = 9), 4wk TAC (n = 13), 2wk unTAC (n = 11), 4wk unTAC (n = 8), 6wk unTAC (n = 7), PBS Liposome 2wk unTAC (n = 7) and Clodronate Liposome 2wk unTAC (n = 8).

LILY SOON NEFF. Macrophages Promote Regression of Myocardial Fibrosis Following Alleviation of Pressure Overload. (Under the direction of AMY BRADSHAW).

5.6 Histological Quantification of Collagen Hybridizing Peptide Reactivity (CHP)

One hundred micromolar biotinylated collagen hybridizing peptide stock (b-CHP, Advanced Biomatrix, #5265) was diluted in 1X PBS to create a three micromolar b-CHP working solution. To denature self-hybridizations, three micromolar b-CHP was heated for 5 minutes at 80°C then cooled to room temperature prior to tissue application. LV myocardial tissue sections were preheated on a slide warmer at 45°C for one hour prior to deparaffinization and rehydration. Following rehydration, tissue sections were incubated overnight at 4°C with 3µM b-CHP. Following three washes with 1X PBS, tissue sections were incubated for one hour with streptavidin horseradish peroxidase secondary antibody (Jackson ImmunoResearch, cat. no. 016-030-084). Following three washes with 1X PBS, tissue sections were incubated with 594 Tyramide working solution for 10 minutes. 594 Tyramide working solution was created by diluting 594 Tyramide (1:500, Biotium, cat. no. 99827) in a 0.0015% hydrogen peroxide amplification buffer solution (Biotium, cat. no. 99832). Tissue sections were washed three times with 1X PBS followed by a 30 second incubation in Trueblack Autofluorescence Quencher diluted in 70% ethanol (Biotium, cat. no. 23007). Tissue samples were mounted and cover slipped with ProLong Gold Antifade reagent with DAPI (Invitrogen, cat. no. P36931). At least five regions of interest which were positive for b-CHP reactivity were imaged on an Olympus BX53 microscope. Quantification and analysis of these regions of interest was performed using Sigma scan software with the following biological sample sizes were used: control (n = 8), 2wk TAC (n = 7), 4wk TAC (n = 8), 4wk TAC+2wk unTAC (n = 7), 4wk TAC+4wk unTAC (n = 6), 4wk TAC+6wk unTAC (n = 7), PBS Liposome 2wk unTAC (n = 6) and Clodronate Liposome 2wk unTAC (n = 7).

LILY SOON NEFF. Macrophages Promote Regression of Myocardial Fibrosis Following Alleviation of Pressure Overload. (Under the direction of AMY BRADSHAW).

5.7 Immunohistochemical Analysis of Macrophages

LV myocardial tissue sections were preheated on a slide warmer at 45°C for one hour prior to deparaffinization and rehydration. Following rehydration, tissue sections were incubated in antigen retrieval buffer in a steamer for 20 minutes. After antigen retrieval, tissue sections were incubated in 1% BSA blocking buffer for one hour. Tissue sections were incubated overnight at 4°C with a primary antibody against the total macrophage marker, Ionized calcium binding adaptor molecule 1 (IBA1) (1:500, Wako cat. no. 019-19741). Following washes with 1X PBS, tissue sections were incubated with a 594-fluorophore donkey anti-rabbit secondary (1:500, Invitrogen cat. no. A21207). Sections were incubated for 30 seconds with Trueblack Autofluorescence Quencher in 70% ethanol (Biotium cat. no. 23007). Samples were mounted and cover slipped with ProLong Gold Antifade reagent with DAPI (Invitrogen cat. no. P36931). Sections were imaged using fluorescence microscopy on a BZ-X800 Keyence microscope. The entire LV section was imaged and $n \geq 5$ regions of interest for each biological replicate was analyzed on a BZ-X800 Analyzer to determine macrophage population (% area) and macrophage cell count. The following biological sample sizes were used: control ($n = 6$), 2wk TAC ($n = 5$), 4wk TAC ($n = 5$), 4wk TAC+2wk unTAC ($n = 5$), 4wk TAC+4wk unTAC ($n = 5$), and 4wk TAC+6wk unTAC ($n = 6$).

5.8 Immunoblotting to Measure Protein Levels in TAC and unTAC Myocardium

Total protein was homogenized and extracted from LV tissue in 2% SDS and quantified using a Bradford assay. 30ug of total protein from each sample was separated by SDS-PAGE. Proteins were transferred to nitrocellulose membranes overnight in a wet

LILY SOON NEFF. Macrophages Promote Regression of Myocardial Fibrosis Following Alleviation of Pressure Overload. (Under the direction of AMY BRADSHAW).

transfer system at 20V. As a loading control, membranes were stained with Ponceau S to visualize total protein. Following washes and two hours of blocking in 3% BSA in TBST, membranes were probed with pro- and active MMP2 (1:1000, Novus Biologicals no. NB200-114SS), mouse anti-Cathepsin K (1:1000, Santa Cruz no. sc-48353), rabbit anti-MMP9 (1:1000), rabbit anti-proLOX (1:1000, Novus Biologicals no. NB110-41568), rabbit anti-Lysyl oxidase-like 2 (1:1000, Abcam no. ab96233) and goat anti-TIMP1 (1:1000, R&D Systems no. AF980). Secondary antibodies conjugated to horseradish peroxidase (1:10000, Vector Laboratories) were detected with Western Lightning Plus-ECL (PerkinElmer cat. no. NEL104001). To visualize chemiluminescence, an Amersham ImageQuant 800 instrument was used. Relative protein expression was determined using ImageJ software. For immunoblot analysis of TAC and unTAC myocardium, the following sample sizes were used: control no TAC (n = 6), 2wk TAC (n = 7), 4wk TAC (n = 7), 4wk TAC+2wk unTAC (n = 7), 4wk TAC+4wk unTAC (n = 6), and 4wk TAC+6wk unTAC (n = 5). For immunoblot analysis of PBS Liposome or Clodronate Liposome myocardium, the following sample sizes were used: PBS Liposome 2wk unTAC (n = 4-5) and Clodronate Liposome 2wk unTAC (n = 5-7).

5.9 Addressable Laser Bead Immunoassay (ALBIA) to Measure Cytokine Profiles in TAC and unTAC Myocardium

LV tissue from each harvest time point was homogenized and incubated in 20mM Tris HCl, pH 7.5, 150mM NaCl with protease inhibitors, 0.05% Tween 20 for one hour. Following this, centrifugation was performed to removed insoluble material. 120uL of individual protein homogenates were aliquoted and flash-frozen in liquid nitrogen for

LILY SOON NEFF. Macrophages Promote Regression of Myocardial Fibrosis Following Alleviation of Pressure Overload. (Under the direction of AMY BRADSHAW).

-80°C storage. ALBIA MMP 5-plex and Cytokine 44-plex bead-based multiplexing technology which allows quantitative protein analysis for up to 100 targets in a single assay well was used (Eve Technologies Corp., Calgary, Canada). Biological sample sizes were as follows: Control (n = 5), 2wk TAC (n = 8), 4wk TAC+2wk unTAC (n = 8), and 4wk TAC+4wk unTAC (n = 8).

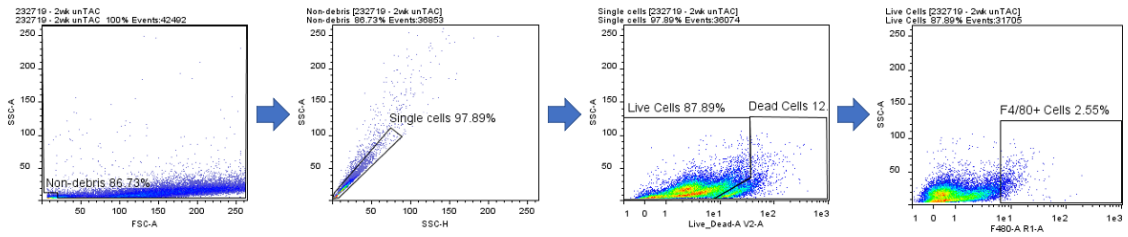
5.10 Fluorescence Activated Cell Sorting (FACS) to Assess Macrophage Phenotype in TAC and unTAC Myocardium

The heart was excised and rinsed in cold Hanks' Balanced Salt Solution (HBSS) buffer (Gibco, cat. no. 14025-134). The LV was isolated by removing the atria and RV, then digested in Collagenase working solution at 37°C with 5% CO₂ (Collagenase II, Worthington, 600U/mL, and Dnase I, Qiagen, 60U/mL, in HBSS). Following tissue digestion, the cell suspension was washed in PEB buffer and filtered through a 40-micron filter to remove cell clumps. Red blood cells were lysed from single cell suspension (RBC Lysis 10X, Miltenyi Biotec cat. no. 130094183) and cell number was determined using a hemacytometer. Cells from each sample were transferred to a 1.5mL Eppendorf tube and incubated in FCR blocking reagent for 20 minutes (Miltenyi Biotec). After subsequent washes in PEB buffer, cells were stained with live/dead fix yellow (1:1000, ThermoFisher cat. no. L34968) for thirty minutes. After subsequent washes, cells were incubated with primary antibodies against the following cell surface markers: F4/80 (1:30, Invitrogen, cat. no. MF48005), Ly6C (1:40, Miltenyi Biotec, cat. no. 130-111-918), CD86 (1:50, Miltenyi Biotec, cat. no. 130-123-279), CD206 (1:40, ThermoFisher Scientific, cat. no. 12-2061-82), and CD163 (1:30, Invitrogen, cat. no. 11-1631-82). Subsequent washes in PEB buffer

LILY SOON NEFF. Macrophages Promote Regression of Myocardial Fibrosis Following Alleviation of Pressure Overload. (Under the direction of AMY BRADSHAW).

were performed, and prior to analysis, cells were resuspended in fresh PEB buffer and filtered through 35-micron cell strainer caps into 5mL tubes. Samples were assayed on a cell analyzer (MACS Quant 10 Analyzer, Miltenyi Biotec) and analyzed using Flowlogic software (Miltenyi Biotec). Prior to macrophage phenotyping of the samples, sequential gating was performed to eliminate debris, non-single cells, and dead cells from analysis (Supplemental Figure 1). The following biological sample sizes were used: control (n = 5), 2wk TAC (n = 5), 4wk TAC (n = 4), 4wk TAC+2wk unTAC (n = 5), 4wk TAC+4wk unTAC (n = 5), and 4wk TAC+6wk unTAC (n = 5).

LILY SOON NEFF. Macrophages Promote Regression of Myocardial Fibrosis Following Alleviation of Pressure Overload. (Under the direction of AMY BRADSHAW).



Supplemental Figure 1. Gating Strategy used for Macrophage Phenotyping. For FACS analysis to determine macrophage phenotyping of TAC and unTAC samples began with sequential gating to eliminate debris, non-single cells, and dead cells, and to positively select F4/80 cells.

LILY SOON NEFF. Macrophages Promote Regression of Myocardial Fibrosis Following Alleviation of Pressure Overload. (Under the direction of AMY BRADSHAW).

5.11 Rt-qPCR of Macrophage and Fibroblast Populations in the TAC and unTAC Myocardium

The heart was excised and rinsed in cold Hanks' Balanced Salt Solution (HBSS) buffer (Gibco, cat. no. 14025-134). The LV was isolated by removing the atria and RV, then digested in Collagenase working solution at 37°C with 5% CO₂ (Collagenase II, Worthington, 600U/mL, and Dnase I, Qiagen, 60U/mL, in HBSS). Following tissue digestion, the cell suspension was washed in PEB buffer and filtered through a 40-micron filter to remove cell clumps. Red blood cells were lysed from single cell suspension (RBC Lysis 10X, Miltenyi Biotec cat. no. 130094183). All cells were transferred to a 1.5mL Eppendorf and incubated for 15 minutes in PEB buffer with 10uL of anti-F4/80 Microbeads Ultrapure (Miltenyi Biotec cat. no. 130-119-443). MS columns were placed in the magnetic field of the MACS Separator (Miltenyi Biotec cat. no. 130-042-108) and columns were rinsed with PEB buffer. Cell suspension was placed in the columns and the flow-through, containing unlabeled cells, was collected for additional magnetic separation of cell types. The columns, containing F4/80+ cells, were removed from the magnet and placed on a 1.5mL Eppendorf tube. PEB buffer was placed in the column and the plunger was used in the column to flush out F4/80+ magnetically labeled cells. F4/80+ cell number was counted using a hemacytometer. Previous flow-through was incubated for 15 minutes at 4°C with 10uL of CD140a (PDGFR α) Microbeads (Miltenyi Biotec cat. no. 130-101-502). MS columns were placed in the magnetic field of the MACS Separator and columns were rinsed with PEB buffer. Cell suspension was placed in the columns and the flow-through was discarded. The columns, containing PDGFR α + cells, were removed from the magnet and placed on a 1.5mL Eppendorf tube. PEB buffer was placed in the column and the

LILY SOON NEFF. Macrophages Promote Regression of Myocardial Fibrosis Following Alleviation of Pressure Overload. (Under the direction of AMY BRADSHAW).

plunger was used in the column to flush out PDGFR α ⁺ magnetically labeled cells. PDGFR α ⁺ cell number was counted using a hemacytometer. Samples were frozen in dry ice ethanol bath and stored at -80°C. RNA was isolated from F4/80⁺ and PDGFR α ⁺ cell populations using the RNeasy Mini Kit (Qiagen cat. no. 74104). RNA concentration was measured on a NanoDrop 2000. cDNA was synthesized from RNA using the high-capacity RNA-to-cDNA kit (ThermoFisher cat. no. 4387406). cDNA concentrations were measured on a NanoDrop 2000. Real time quantitative PCR was run on a Quant Studio 5 Real-Time PCR System using a 96-well 0.2mL plate with the following components: TaqMan Fast Advance Master Mix (ThermoFisher cat. no. 4444556), FAMdye primers (ThermoFisher cat. no. 4448892), cDNA, and RNase free H₂O. The FAMdye primers used were *Coll1a1* (Mm00801666_g1), *Sparc* (Mm05915229_s1), *Lox* (Mm00495386_m1), *Loxl2* (Mm00804740_m1), *Pstn* (Mm01284919_m1), *Timp1* (Mm01341361_m1), *TGF β 1* (Mm01178820_m1), *Mmp14* (Mm00485054_m1), *Aif1* (Mm00520165_m1), *Mrc1* (Mm01329359_m1), *Cd163* (Mm00474091_m1), *Mertk* (Mm00434920_m1). *Gapdh* (Mm99999915_g1) was used as a housekeeping gene for PDGFR α ⁺ cells, and *Hnrnpab* (Mm01288699_m1) was used as a housekeeping gene for F4/80⁺ cells. The following instrument conditions were used: Experiment Type: Standard Curve, run mode: Fast, 20uL volume, hold stage: step 1 at 50°C for 2 minutes followed by step 2 at 95°C for 20 seconds, PCR stage: 40 cycles of step 1 at 95°C for 1 second followed by step 2 at 60°C for 20 seconds. An NFQ-MGB quencher was used and the Ct threshold was set to 0.2 for all targets of interest. The following biological sample sizes were used: control (n = 2-5), 2wk TAC (n = 3-4), 4wk TAC (n = 2-4), 4wk TAC+2wk unTAC (n = 2-4), 4wk TAC+4wk unTAC (n = 2-5), and 4wk TAC+6wk unTAC (n = 2-4).

LILY SOON NEFF. Macrophages Promote Regression of Myocardial Fibrosis Following Alleviation of Pressure Overload. (Under the direction of AMY BRADSHAW).

5.12 Myocardial Stiffness

As previously described in Bradshaw et. al., LV myocardial papillary muscles were isolated at the time of harvest to determine passive stiffness⁸. To measure passive stiffness, passive tension and stretch strain were measured using an Aurora 308-B dual-mode force-length control system (Aurora Scientific Inc., Richmond Hill, ON, Canada). Tension normalized to papillary muscle cross-sectional area was used to determine stress. Stretching length normalized to resting length of papillary muscle was used to determine strain. The passive stiffness constant, β , was calculated using the following formula: stress = $Ae^{(\beta \times \text{strain})} + C$, where A and C are curve-fitting constants obtained from the stress-versus-strain relationship. Quantification of the following sample sizes were used for myocardial stiffness: control (n = 5), 2wk TAC (n = 13), 4wk TAC (n = 10), 4wk TAC+2wk unTAC (n = 11), 4wk TAC+ 4wk unTAC (n = 12), 4wk TAC+6wk unTAC (n = 7)⁴². The following sample sizes were used for the liposome mediated depletion of macrophage study: PBS Liposomes: 4wk TAC+2wk unTAC (n = 7) and Clodronate Liposomes: 4wk TAC+2wk unTAC (n = 6).

5.13 Statistical Analysis

Box and whisker plots are utilized to graphically present the locality, spread, and skewness of the data points from the semiquantitative and quantitative results. The box represents the interquartile range as the difference between the upper quartile and lower quartile. The whiskers show the minimum and maximum values. Where applicable, a two-tailed student's t-test, Kruskal-Wallis one-way ANOVA on Ranks, or one-way ANOVA followed by Holm-Sidak, Tukey, or Student-Newman-Keuls test was utilized to detect

LILY SOON NEFF. Macrophages Promote Regression of Myocardial Fibrosis Following Alleviation of Pressure Overload. (Under the direction of AMY BRADSHAW).

significant differences between experimental groups (SigmaStat 4.0; Systat Software Inc., San Jose, CA). $p < 0.05$ was defined as statistically significant. The following statistical symbols were used in figures: * $p < 0.05$ vs. Control no TAC, # $p < 0.05$ vs. 2wk TAC, \$ $p < 0.05$ versus 4wk TAC, + $p < 0.05$ vs. 4wk TAC+2wk unTAC.

LILY SOON NEFF. Macrophages Promote Regression of Myocardial Fibrosis Following Alleviation of Pressure Overload. (Under the direction of AMY BRADSHAW).

References

LILY SOON NEFF. Macrophages Promote Regression of Myocardial Fibrosis Following Alleviation of Pressure Overload. (Under the direction of AMY BRADSHAW).

- 1 Del Monte-Nieto, G., Fischer, J. W., Gorski, D. J., Harvey, R. P. & Kovacic, J. C. Basic Biology of Extracellular Matrix in the Cardiovascular System, Part 1/4: JACC Focus Seminar. *J Am Coll Cardiol* **75**, 2169-2188, doi:10.1016/j.jacc.2020.03.024 (2020).
- 2 Dong Fan, A. T., Jiwon Lee, and Zamaneh Kassiri Cardiac fibroblasts fibrosis and ECM remodeling in heart disease. *Fibrogenesis & Tissue Repair* **5** (2012).
- 3 Martini, E. *et al.* Single-Cell Sequencing of Mouse Heart Immune Infiltrate in Pressure Overload-Driven Heart Failure Reveals Extent of Immune Activation. *Circulation* **140**, 2089-2107, doi:10.1161/CIRCULATIONAHA.119.041694 (2019).
- 4 Fields, G. B. Interstitial collagen catabolism. *J Biol Chem* **288**, 8785-8793, doi:10.1074/jbc.R113.451211 (2013).
- 5 Lodish, B., Zipursky, Matsudaira, Baltimore, Darnell. *Molecular Cell Biology 4.0*. (W. H. Freeman and Company, 1999).
- 6 Neff, L. S. & Bradshaw, A. D. Cross your heart? Collagen cross-links in cardiac health and disease. *Cell Signal* **79**, 109889, doi:10.1016/j.cellsig.2020.109889 (2021).
- 7 Hannah J. Riley, A. D. B. The Influence of the Extracellular Matrix in Inflammation: Findings from the SPARC-Null Mouse. *The Anatomical Record*, doi:10.1002/ar.24133 (2019).
- 8 Bradshaw, A. D. *et al.* Pressure overload-induced alterations in fibrillar collagen content and myocardial diastolic function: role of secreted protein acidic and rich in cysteine (SPARC) in post-synthetic procollagen processing. *Circulation* **119**, 269-280, doi:10.1161/CIRCULATIONAHA.108.773424 (2009).
- 9 Marieke Rienks, A.-P. P., Nikolaos G Frangogiannis, Stephane Heymans. Myocardial extracellular matrix: an ever-changing and diverse entity. *Circulation Research Review* **114**, 860-871, doi:10.1161/CIRCRESAHA.114.302533 (2014).
- 10 Toru Oka, J. X., Robert A. Kaiser, Jaime Melendez, Michael Hambleton, Michelle A. Sargent, Angela Lorts, Eric W. Brunskill, Gerald W. Dorn, II, Simon J. Conway, Bruce J. Aronow, Jeffrey Robbins, and Jeffery D. Molkentin. Genetic manipulation of periostin expression reveals a role in cardiac hypertrophy and ventricular remodeling. *Circulation Research* **101**, 313-321 (2007).
- 11 Vanessa Frodermann, M. N. Macrophages and Cardiovascular Health. *Physiol Rev* **98**, 2523-2569, doi:doi:10.1152/physrev.00068.2017 (2018).
- 12 Marcin Dobaczewski, W. C., Nikolaos G Frangogiannis. Transforming growth factor (TGF)- β signaling in cardiac remodeling. *J Mol Cell Cardiol* **51**, doi:10.1016/j.yjmcc.2010.10.033 (2011).
- 13 Michael R. Zile, C. F. B., Robert E. Stroud, An Van Laer, Jazmine Arroyo, Rupak Mukherjee, Jeffrey A. Jones, and Francis G. Spinale. Pressure overload-dependent membrane type 1-matrix metalloproteinase induction: relationship to LV remodeling and fibrosis. *Am J Physiol Heart Circ Physiol* **302**, H1429-H1437 (2012).

LILY SOON NEFF. Macrophages Promote Regression of Myocardial Fibrosis Following Alleviation of Pressure Overload. (Under the direction of AMY BRADSHAW).

- 14 Klepfish, M. *et al.* LOXL2 Inhibition Paves the Way for Macrophage-Mediated Collagen Degradation in Liver Fibrosis. *Front Immunol* **11**, 480, doi:10.3389/fimmu.2020.00480 (2020).
- 15 Merry L. Lindsey, K. Y. D.-P., Amy D. Bradshaw, R. Amanda C. LaRue, Daniel R. Anderson, Geoffrey M. Thiele, Catalin F. Baicu, Jeffrey A. Jones, Donald R. Menick, Michael R. Zile, and Francis G. Spinale. Focusing Heart Failure Research on Myocardial Fibrosis to Prioritize Translation. *J Card Fail*, doi:10.1016/j.cardfail.2020.05.009 (2020).
- 16 Michael R. Zile, D. L. B. New Concepts in Diastolic Dysfunction and Diastolic Heart Failure: Part 1. *Clinical Cardiology: New Frontiers* **105**, 1387-1393 (2002).
- 17 Michael R. Zile, D. L. B. New Concepts in Diastolic Dysfunction and Diastolic Heart Failure: Part II Casual Mechanisms and Treatment. *Circulation* **105**, doi:<https://doi.org/10.1161/hc1202.105290> (2002).
- 18 Hessel, F. P. Overview of the socio-economic consequences of heart failure. *Cardiovasc Diagn Ther.* **11**, 254-262, doi:10.21037/cdt-20-291 (2021).
- 19 Hess, O. M. *et al.* Diastolic stiffness and myocardial structure in aortic valve disease before and after valve replacement. *Circulation* **69**, 855-865, doi:10.1161/01.cir.69.5.855 (1984).
- 20 Krayenbuehl, H. P. *et al.* Left ventricular myocardial structure in aortic valve disease before, intermediate, and late after aortic valve replacement. *Circulation* **79**, 744-755, doi:10.1161/01.cir.79.4.744 (1989).
- 21 Monrad, E. S. *et al.* Time course of regression of left ventricular hypertrophy after aortic valve replacement. *Circulation* **77**, 1345-1355, doi:10.1161/01.cir.77.6.1345 (1988).
- 22 Gao, X. M. *et al.* Regression of pressure overload-induced left ventricular hypertrophy in mice. *American journal of physiology. Heart and circulatory physiology* **288**, H2702-2707, doi:10.1152/ajpheart.00836.2004 (2005).
- 23 Dadson, K. *et al.* Cellular, structural and functional cardiac remodelling following pressure overload and unloading. *Int J Cardiol* **216**, 32-42, doi:10.1016/j.ijcard.2016.03.240 (2016).
- 24 Rodrigues, P. G. *et al.* The Degree of Cardiac Remodelling before Overload Relief Triggers Different Transcriptome and miRome Signatures during Reverse Remodelling (RR)-Molecular Signature Differ with the Extent of RR. *Int J Mol Sci* **21**, doi:10.3390/ijms21249687 (2020).
- 25 Weinheimer, C. J. *et al.* Load-Dependent Changes in Left Ventricular Structure and Function in a Pathophysiologically Relevant Murine Model of Reversible Heart Failure. *Circ Heart Fail* **11**, e004351, doi:10.1161/circheartfailure.117.004351 (2018).
- 26 Patel, B. *et al.* CCR2(+) Monocyte-Derived Infiltrating Macrophages Are Required for Adverse Cardiac Remodeling During Pressure Overload. *JACC Basic Transl Sci* **3**, 230-244, doi:10.1016/j.jacbts.2017.12.006 (2018).
- 27 Hulsmans, M. *et al.* Cardiac macrophages promote diastolic dysfunction. *J Exp Med* **215**, 423-440, doi:10.1084/jem.20171274 (2018).

LILY SOON NEFF. Macrophages Promote Regression of Myocardial Fibrosis Following Alleviation of Pressure Overload. (Under the direction of AMY BRADSHAW).

- 28 Riley, H. J. *et al.* SPARC production by bone marrow-derived cells contributes to myocardial fibrosis in pressure overload. *Am J Physiol Heart Circ Physiol* **320**, H604-H612, doi:10.1152/ajpheart.00552.2020 (2021).
- 29 McDonald, L. T. *et al.* Increased macrophage-derived SPARC precedes collagen deposition in myocardial fibrosis. *Am J Physiol Heart Circ Physiol* **315**, H92-H100, doi:10.1152/ajpheart.00719.2017 (2018).
- 30 O'Brien, M. *et al.* Pressure overload generates a cardiac-specific profile of inflammatory mediators. *Am J Physiol Heart Circ Physiol* **319**, H331-H340, doi:10.1152/ajpheart.00274.2020 (2020).
- 31 Revelo, X. S. *et al.* Cardiac Resident Macrophages Prevent Fibrosis and Stimulate Angiogenesis. *Circ Res* **129**, 1086-1101, doi:10.1161/CIRCRESAHA.121.319737 (2021).
- 32 B. Emde, A. H., A. Gödecke, and K. Bottermann. Wheat Germ Agglutinin Staining as a Suitable Method for Detection and Quantification of Fibrosis in Cardiac Tissue after Myocardial Infarction. *58*, doi:10.4081/ejh.2014.2448 (2014).
- 33 Lopez-Jimenez, A. J., Basak, T. & Vanacore, R. M. Proteolytic processing of lysyl oxidase-like-2 in the extracellular matrix is required for crosslinking of basement membrane collagen IV. *J Biol Chem* **292**, 16970-16982, doi:10.1074/jbc.M117.798603 (2017).
- 34 Bacmeister, L. *et al.* Inflammation and fibrosis in murine models of heart failure. *Basic Res Cardiol* **114**, 19, doi:10.1007/s00395-019-0722-5 (2019).
- 35 Kain, D. *et al.* Macrophages dictate the progression and manifestation of hypertensive heart disease. *Int J Cardiol* **203**, 381-395, doi:10.1016/j.ijcard.2015.10.126 (2016).
- 36 Ramachandran, P. *et al.* Differential Ly-6C expression identifies the recruited macrophage phenotype, which orchestrates the regression of murine liver fibrosis. *Proc Natl Acad Sci U S A* **109**, E3186-3195, doi:10.1073/pnas.1119964109 (2012).
- 37 Weisheit, C. *et al.* Ly6C(low) and not Ly6C(high) macrophages accumulate first in the heart in a model of murine pressure-overload. *PLoS One* **9**, e112710, doi:10.1371/journal.pone.0112710 (2014).
- 38 Mouton, A. J. *et al.* Mapping macrophage polarization over the myocardial infarction time continuum. *Basic Res Cardiol* **113**, 26, doi:10.1007/s00395-018-0686-x (2018).
- 39 Anki Knutsson, P., Harry Björkbacka, PhD, Pontus Dunér, PhD, Gunnar Engström, MD, PhD, Christoph J. Binder, MD, PhD, Anna Hultgårdh Nilsson, PhD, and Jan Nilsson, MD, PhD. Associations of Interleukin-5 With Plaque Development and Cardiovascular Events. *JACC Basic Transl Sci* **4**, 891-902, doi:10.1016/j.jacbts.2019.07.002 (2019).
- 40 Glezeva, N. *et al.* Exaggerated inflammation and monocytosis associate with diastolic dysfunction in heart failure with preserved ejection fraction: evidence of M2 macrophage activation in disease pathogenesis. *J Card Fail* **21**, 167-177, doi:10.1016/j.cardfail.2014.11.004 (2015).

LILY SOON NEFF. Macrophages Promote Regression of Myocardial Fibrosis Following Alleviation of Pressure Overload. (Under the direction of AMY BRADSHAW).

- 41 Falkenham, A. *et al.* Nonclassical resident macrophages are important determinants in the development of myocardial fibrosis. *Am J Pathol* **185**, 927-942, doi:10.1016/j.ajpath.2014.11.027 (2015).
- 42 Neff, L. S. *et al.* Mechanisms that limit regression of myocardial fibrosis following removal of left ventricular pressure overload. *Am J Physiol Heart Circ Physiol* **323**, H165-H175, doi:10.1152/ajpheart.00148.2022 (2022).
- 43 Keiko Ohsawa, Y. I., Yo Sasaki, Shinichi Kohsaka. Microglia/macrophage-specific protein Iba1 binds to fimbrin and enhances its actin-bundling activity. *Journal of Neurochemistry* **88**, 844-856, doi:10.1046/j.1471-4159.2003.02213.x (2004).
- 44 Lindsey A. Waddell, L. L., Stephen J. Bush, Anna Raper, Rachel Young, Zofia M. Lisowski, Mary E. B. McCulloch, Charity Muriuki, Kristin A. Sauter, Emily L. Clark, Katharine M. Irvine, Clare Pridans, Jayne C. Hope, and David A. Hume. ADGRE1 (EMR1, F4/80) Is a Rapidly-Evolving Gene Expressed in Mammalian Monocyte-Macrophages. *9 2246*, doi:doi: 10.3389/fimmu.2018.02246 (2018).
- 45 Hanne B. Mikkelsen, J. D. H., Jytte O. Larsen, Svend Kirkeby. Ionized Calcium-Binding Adaptor Molecule 1 Positive Macrophages and HO-1 Up-Regulation in Intestinal Muscularis Resident Macrophages. *The Anatomical Record* **300**, 1114-1122 (2017).
- 46 Corker, A., Neff, L. S., Broughton, P., Bradshaw, A. D. & DeLeon-Pennell, K. Y. Organized Chaos: Deciphering Immune Cell Heterogeneity's Role in Inflammation in the Heart. *Biomolecules* **12**, doi:10.3390/biom12010011 (2021).
- 47 Epelman, S. L., K.J.; Beaudin, A.E.; Sojka, D.K.; Carrero, J.A.; Calderon, B.; Brija, T.; Gautier, E.L.; Ivanov, S.; Satpathy, A.T. Embryonic and adult-derived resident cardiac macrophages are maintained through distinct mechanisms at steady state and during inflammation. *Immunity* **40**, 91–104 (2014).
- 48 Lavine, K. J. P., A.R.; Epelman, S.; Kopecky, B.J.; Clemente-Casares, X.; Godwin, J.; Rosenthal, N.; Kovacic, J.C. The Macrophage in Cardiac Homeostasis and Disease: JACC Macrophage in CVD Series (Part 4). *J. Am. Coll. Cardiol.* **72**, 2213–2230 (2018).
- 49 Hua, L., Shi, J., Shultz, L. D. & Ren, G. Genetic Models of Macrophage Depletion. *Methods Mol Biol* **1784**, 243-258, doi:10.1007/978-1-4939-7837-3_22 (2018).
- 50 Duffield, J. S. *et al.* Selective depletion of macrophages reveals distinct, opposing roles during liver injury and repair. *Journal of Clinical Investigation* **115**, 56-65, doi:10.1172/jci200522675 (2005).
- 51 Wang, Y. *et al.* Wnt5a-Mediated Neutrophil Recruitment Has an Obligatory Role in Pressure Overload-Induced Cardiac Dysfunction. *Circulation* **140**, 487-499, doi:10.1161/CIRCULATIONAHA.118.038820 (2019).
- 52 Laroumanie, F. *et al.* CD4+ T cells promote the transition from hypertrophy to heart failure during chronic pressure overload. *Circulation* **129**, 2111-2124, doi:10.1161/CIRCULATIONAHA.113.007101 (2014).

LILY SOON NEFF. Macrophages Promote Regression of Myocardial Fibrosis Following Alleviation of Pressure Overload. (Under the direction of AMY BRADSHAW).

- 53 Qin, C. C., Liu, Y. N., Hu, Y., Yang, Y. & Chen, Z. Macrophage inflammatory protein-2 as mediator of inflammation in acute liver injury. *World J Gastroenterol* **23**, 3043-3052, doi:10.3748/wjg.v23.i17.3043 (2017).
- 54 Frangogiannis, N. G. Cardiac fibrosis. *Cardiovasc Res* **117**, 1450-1488, doi:10.1093/cvr/cvaa324 (2021).
- 55 Tallquist, M. D. Cardiac Fibroblast Diversity. *Annual Review of Physiology* **82**, 63-78, doi:<https://doi.org/10.1146/annurev-physiol-021119-034527> (2020).
- 56 Yang, J. *et al.* Targeting LOXL2 for cardiac interstitial fibrosis and heart failure treatment. *Nat Commun* **7**, 13710, doi:10.1038/ncomms13710 (2016).
- 57 Zhang, J. Y., R.; Liu, Z.; Hou, C.; Zong, W.; Zhang, A.; Sun, X.; Gao, J. Loss of lysyl oxidase-like 3 causes cleft palate and spinal deformity in mice. *Human Molecular Genetics* **24**, 6174-6185 (2015).
- 58 E.C. El Hajj, M. C. E. H., V.K. Ninh, J.D. Gardner Cardioprotective effects of lysyl oxidase inhibition against volume overload-induced extracellular matrix remodeling. *Experimental Biology and Medicine* **241**, 539-549 (2016).
- 59 El Hajj, E. C., El Hajj, M. C., Ninh, V. K. & Gardner, J. D. Inhibitor of lysyl oxidase improves cardiac function and the collagen/MMP profile in response to volume overload. *Am J Physiol Heart Circ Physiol* **315**, H463-H473, doi:10.1152/ajpheart.00086.2018 (2018).
- 60 S. Kato, F. G. S., R. Tanaka, W. Johnson, Gt Cooper, M.R. Zile Inhibition of collagen cross-linking: effects on fibrillar collagen and ventricular diastolic function. *American Journal of Physiology* **269**, H863-H868 (1995).
- 61 Zile, M. R. *et al.* Effects of Sacubitril/Valsartan on Biomarkers of Extracellular Matrix Regulation in Patients With HFrEF. *J Am Coll Cardiol* **73**, 795-806, doi:10.1016/j.jacc.2018.11.042 (2019).
- 62 Cunningham, J. W. *et al.* Effect of Sacubitril/Valsartan on Biomarkers of Extracellular Matrix Regulation in Patients With HFpEF. *J Am Coll Cardiol* **76**, 503-514, doi:10.1016/j.jacc.2020.05.072 (2020).
- 63 De Marco, C. *et al.* Impact of diabetes on serum biomarkers in heart failure with preserved ejection fraction: insights from the TOPCAT trial. *ESC Heart Fail* **8**, 1130-1138, doi:10.1002/ehf2.13153 (2021).
- 64 Takawale, A. *et al.* Tissue Inhibitor of Matrix Metalloproteinase-1 Promotes Myocardial Fibrosis by Mediating CD63-Integrin β 1 Interaction. *Hypertension* **69**, 1092-1103, doi:10.1161/hypertensionaha.117.09045 (2017).
- 65 Gong, Y. *et al.* TIMP-1 promotes accumulation of cancer associated fibroblasts and cancer progression. *PLoS One* **8**, e77366, doi:10.1371/journal.pone.0077366 (2013).
- 66 Lu, Y. *et al.* Tissue inhibitor of metalloproteinase-1 promotes NIH3T3 fibroblast proliferation by activating p-Akt and cell cycle progression. *Mol Cells* **31**, 225-230, doi:10.1007/s10059-011-0023-9 (2011).
- 67 May J Reed, T. K., Eman Sadoun, E.Helene Sage, Pauli Puolakkainen. Inhibition of TIMP1 enhances angiogenesis in vivo and cell migration in vitro. *Microvascular Research Elsevier* **65**, 9-17 (2003).

LILY SOON NEFF. Macrophages Promote Regression of Myocardial Fibrosis Following Alleviation of Pressure Overload. (Under the direction of AMY BRADSHAW).

- 68 Korfei, M. *et al.* Comparison of the antifibrotic effects of the pan-histone deacetylase-inhibitor panobinostat versus the IPF-drug pirfenidone in fibroblasts from patients with idiopathic pulmonary fibrosis. *PLoS One* **13**, e0207915, doi:10.1371/journal.pone.0207915 (2018).
- 69 Conte, E. *et al.* Effect of pirfenidone on proliferation, TGF- β -induced myofibroblast differentiation and fibrogenic activity of primary human lung fibroblasts. *European Journal of Pharmaceutical Sciences* **58**, 13-19, doi:10.1016/j.ejps.2014.02.014 (2014).
- 70 Wang, Y., Wu, Y., Chen, J., Zhao, S. & Li, H. Pirfenidone attenuates cardiac fibrosis in a mouse model of TAC-induced left ventricular remodeling by suppressing NLRP3 inflammasome formation. *Cardiology* **126**, 1-11, doi:10.1159/000351179 (2013).
- 71 Michihito Toda, S. M., Yukiko Minamiyama, Hiroko YamamotoOka, Takanori Aota, Shoji Kubo, Noritoshi Nishiyama, Toshihiko Shibata and Shigekazu Takemura. Pirfenidone suppresses polarization to M2 phenotype macrophages and the fibrogenic activity of rat lung fibroblasts. *J. Clin. Biochem. Nutr.* **63**, 58-65, doi:10.3164/jcbtn.17 111 (2018).
- 72 Lewis, G. A. *et al.* Pirfenidone in heart failure with preserved ejection fraction: a randomized phase 2 trial. *Nat Med* **27**, 1477-1482, doi:10.1038/s41591-021-01452-0 (2021).
- 73 S. Hinaan Ahmed, L. L. C., Weems R. Pennington, Carson S. Webb, D. Dirk Bonnema, Amy H. Leonardi, Catherine D. McClure, Francis G. Spinale, Michael R. Zile. Matrix Metalloproteinases/Tissue Inhibitors of Metalloproteinases: Relationship Between Changes in Proteolytic Determinants of Matrix Composition and Structural, Functional, and Clinical Manifestations of Hypertensive Heart Disease. *AHA* **113**, doi:<https://doi.org/10.1161/CIRCULATIONAHA.105.573865> (2006).